THESIS FOR THE DEGREE OF DOCTOR OF PHILOSOPHY (PhD)

Revealing the importance of solute carrier transporters in thermogenic activity of human adipocytes

by

Rini Arianti

Supervisor: Prof. Dr. László Fésüs

UNIVERSITY OF DEBRECEN

DOCTORAL SCHOOL OF MOLECULAR CELL AND IMMUNE BIOLOGY

DEBRECEN, 2022

TABLE OF CONTENTS

List of Figures

List of Tables

1. Abbreviations

ABC:	ATP Binding Cassette
ADIP:	White-differentiated adipocytes
ADIPOQ:	Adiponectine
ADSC:	Adipose-derived stem cells
ANT1/2:	ADP/ATP Translocase-1/2
ASC-1:	Alanine-Serine-Cystein Transporter 1
B-ADIP:	Brown-differentiated adipocytes
BAT:	Brown adipose tissue
BCAA:	Branched-Chain Amino Acid
BCKDH:	Branched-Chain α-Ketoacid Dehydrogenase
cAMP:	3',5'-cyclic adenosine monophosphate
CAT:	Cationic Amino Acid Transporters
CITED1:	Cbp/P300 Interacting Transactivator With Glu/Asp Rich Carboxy Terminal Domain1
CKB:	Creatine Kinase B
CKMT1/2:	Creatine kinase, Mitochondrial 1/2
COX2/7A1:	Cytochrome C Oxidase Subunit 2/7A1
DEGs:	Differentially expressed genes
DIO2:	Deiodinase, Iodothyronine, Type II
DMEM:	Dulbecco's modified Eagle's medium
DMSO:	Dimethyl sulfoxide
DN:	Deep neck
EBF2/3:	Early B-Cell Factor 2/3
ECAR:	Extracellular acidification rate
ELOVL3:	ELOVL Fatty Acid Elongase 3
ETK:	Erythrocyte Transketolase
EVA1:	Epithelial V-like Antigen 1
FATP1/3:	Fatty Acid Transporter 1/3
FBS:	Fetal bovine serum
FBXO31:	F-Box Only Protein 31
GAMT:	Guanidinoacetate Methyltransferase
GAPDH:	Glyceraldehyde-3-Phosphate Dehydrogenase
GATM:	Glycine Amidinotransferase
GLUT4:	Glucose Transporter 4
GPDH:	Glycerol-3-Phosphate Degydrogenase
HACL1:	2-Hydroxyacyl-CoA lyase
hASC:	Human adipose stem cell
HAT:	Hetero(di)meric Amino Acid Transporter
HOXC8/9:	Homebox C8/9
iBAT:	Interscapular brown adipose tissue
IBMX:	3-Isobutyl-1-methylxantin

KCNK3: Potassium Two Pore Domain Channel Subfamily K Member 3
LAT1/2: L-type Amino Acid Transporter 1/2
LDH: Lactate Dehydrogenase
LEP: Leptin
LEPR: Leptin receptor
LHX8: LIM Homebox 1
MTUS1: Microtubule Associated Tumor Repressor 1
NAAs: N-acyl amino acids
NCKX2/3: Na/Ca/K Exchanger 2/3
NE: Norepinephrine
OCR: Oxygen consumption rate
OLETF: Otsuka Long-Evans Tokushima Fatty
PDH: Pyruvate Dehydrogenase
PDHA1: PDH E1 Subunit Alpha 1
PET-CT: Positron emission tomography-computed tomography
PGC1a: PPARγ Coactivator-1a
PKA: Protein Kinase A
PLIN1: Perilipin-1
PM20D1: Peptidase M20 Domain Containing 1
ROS: Reactive oxygen species
RyR2: Ryanodine Receptor 2
SC: Subcutaneous
SERCA: Sarco/Endoplasmic Reticulum Ca^{2+}-ATPase
SLC: Solute carrier
SLN: Sarcolipin
SNS: Sympathetic nervous system
TBX1: T-Box 1
TCA: Tricarboxilic acid
ThTr: Thiamine transporter
TMEM26: Transmembrane Protein 26
TMP: Thiamine monophosphate
TNAP: Tissue Non-specific Alkaline Phosphatase
TPC: Mitochodnrial TPP transporter
TPP: Thiamine pyrophosphate
TRMA: Thiamine-responsive megaloblastic anemia
TTP: Thiamine triphosphate
T3: Triiodithyronine
T4: Thyroxine
UCP1: Uncoupling Protein 1
WAT: White adipose tissue
ZIC1 : Zic Family Member 1

2. Keywords

Human brown/beige adipocytes, deep neck, RNA-Sequencing, differentially expressed genes, thermogenesis, oxygen consumption, adrenergic stimulation, thermogenic gene expression, uncoupling protein-1, solute carrier transporters, alanine-serine-cysteine transporter-1, BMS-466442, thiamine, thiamine transporter, thiamine pyrophosphate, fedratinib, amprolium.

3. Introduction

World Health Organization reported in 2016 that more than 1.9 billion adults aged 18 years and older were overweight and of these over 650 million adults were obese [World Health Organization, 2021]. Sedentary life style and high calories intake have become major factors that lead to obesity and other metabolic diseases including diabetes type 2, insulin resistance, and cardiovascular disease. In the last decade, a novel interest has emerged to explore pathways that regulate energy homeostasis in mammalian system, particularly focusing on adipose tissues. There are two types of adipose tissue: white adipose tissue (WAT) that functions as lipid storage and brown adipose tissue (BAT) that functions in thermogenesis. White adipocytes possessed unilocular lipid droplet and low amounts of mitochondria, whereas brown adipocytes have multilocular lipid droplet and high amount of mitochondria (**Figure 1**) [Cohen and Kajimura, 2021]. White adipocytes residing in WAT also have thermogenic potential which is referred as beige adipocytes. Beige adipocytes emerge when there are stimuli such as cold and exercise and they have thermogenic brown adipocyte-like phenotype (**Figure 1**) [Cohen and Kajimura, 2021]. In addition to its main role as energy reservoir, adipose tissue also releases hormones that regulate various biological processes, mediates the inflammatory process, act as insulator, and contribute in heat generation by brown and beige adipocytes to regulate body temperature [Rosen and Spiegelman, 2014, *Cell*; Sakers *et al*., 2022, *Cell*].

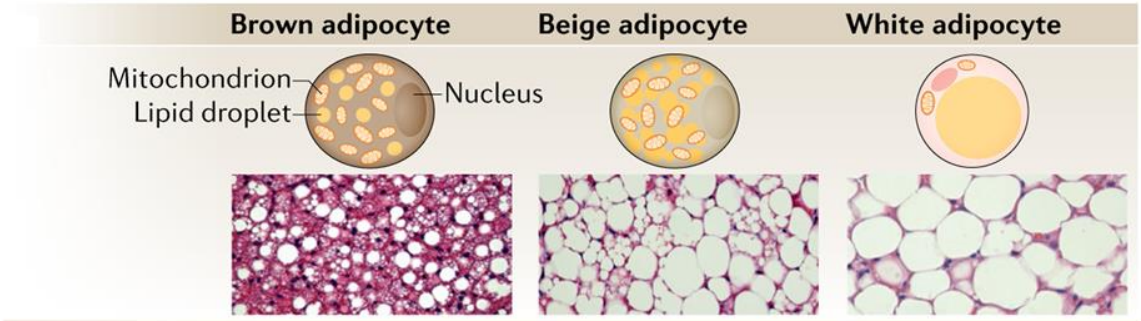

	Brown adipocyte	Beige adipocyte	White adipocyte
Function	Thermogenic	Thermogenic	Energy storage
Mitochondria	High	High	Low
Lipid droplets	Multilocular	Multilocular	Unilocular

Figure 1. *Characteristics of white and thermogenic adipocytes [Cohen and Kajimura, 2021]*

BAT has been widely studied in recent years as the potential target of obesity therapy. Brown/beige adipocytes have a special feature, uncoupling protein-1 (UCP1) which enables them to generate heat instead of ATP by non-shivering thermogenesis [Cannon and Nedergaard, 2004].

Glucose and fatty acids are main substrates for thermogenesis suggesting the important role of BAT in systemic glucose and lipid homeostasis. Recent study also reported that branched-chain amino acids (BCAAs) are oxidized by brown adipocytes during thermogenic activation by cold [Yoneshiro *et al*., 2019, *Nature*]. BAT utilize available cellular substrates for fueling the heat generation, therefore, the upregulation of transporters are required to sustain the adequate influx of substrates during thermogenic activation.

Solute carrier (SLC) transporters family members are involved in various biological processes, mainly in transporting the important molecules needed by cells. The importance of cell membrane SLCs in thermogenic activation of human brown/beige adipocytes have not been elucidated. Here we revealed the importance of amino acids and thiamine transporters in thermogenic activation of human adipocytes upon adrenergic stimulation. The inhibition of these transporters during cAMP stimulation led to the decrease of heat generation reflected by proton leak respiration. In addition, cAMP-induced upregulation of thermogenic markers were also abrogated when the activity of amino acid and thiamine transporters are blocked by their pharmacological inhibitors. Our results have raised the possibility to treat obesity by targeting the molecular elements of the regulation of amino acids and thiamine metabolism to augment heat generation by thermogenic adipocytes in obese individuals.

4. Theoretical Background

4.1. Overview of human brown/beige adipose tissue

4.1.1. Distribution of brown/beige adipose tissue in humans

BAT capacity in heat generation is essential for newborns, also for rodents and hibernating animals, to maintain their constant core body temperature [Townsend and Tseng, 2014]. The activity of BAT was found approximately up to 5% of basal metabolic rate in adult humans, which could support fat burning up to 4 kg per year [van Marken Lictenbelt and Schrauwen, 2011]. Human BAT was primarily regarded as a tissue that was only present in infants and located at anatomical sites that are difficult to reach. Several studies using positron emission tomography (PET) provided evidence that adults have significant amounts of BAT. The combination of labeled glucose uptake and PET has proven that cold exposure can activate the BAT. The most common location for brown adipose tissue in adult humans is the cervical-supraclavicular depot marked by high labeled glucose uptake in that region [Cypess *et al*., 2009; Virtanen *et al*., 2009]. Assessing the morphology of the biopsies specimen from supraclavicular depot, they found adipocytes with numerous multilocular and intracellular lipid droplets.

A more recent study had improved the PET-CT method to identify the brown/beige adipose tissue localization [Leitner *et al*., 2017]. Using a refined technique of PET-CT method, they could identify the whole-body BAT distribution and estimate its thermogenic capacity. They found that BAT and brownable adipose tissue can be found interspersed in several areas such as cervical, supraclavicular, axillary, mediastinal, paraspinal, and abdominal (**Figure 2, left panel**). Intriguingly, they also found that obese individuals possess higher amount of brownable adipose tissue than lean individuals. However, the active BAT in obese people are lower than in lean individuals (**Figure 2, right panel**). It has been well-established that cold exposure can activate thermogenesis by mediating the norepinephrin (NE) release by sympathetic nervous system (SNS). NE binds to beta-adrenergic receptor and activate cAMP-PKA signaling leading to an increase of lipolysis of cytoplasmic lipid droplets that results in the elevation of free fatty acids release [Cannon and Nedergaard, 2004]. Long-chain fatty acids anions can activate UCP1 by serving as its transport substrates [Fedorenko *et al*., 2012]. Targeting the beta-adrenergic receptor by its agonist (e.g., CL 316, 243 and mirabegron) potently stimulate the glucose uptake and thermogenic response but the negative side effect of those drugs may lead to the impairment of the cardiovascular system. The mechanism to activate the brownable adipose tissue in human is

still challenging. The transplantation of human adipose-derived stem cells (ADSCs) that was differentiated to beige adipocytes can be a promising approach to treat obesity and type 2 diabetes. ADSC obtained during liposuction in abdominal region were differentiated to beige cell, then transplanted to mice resulting in enhanced energy expenditure [Singh *et al*., 2020]. This finding raise the possibility to use obese patient's own cells for transplantation after the *ex vivo* beige differentiation.

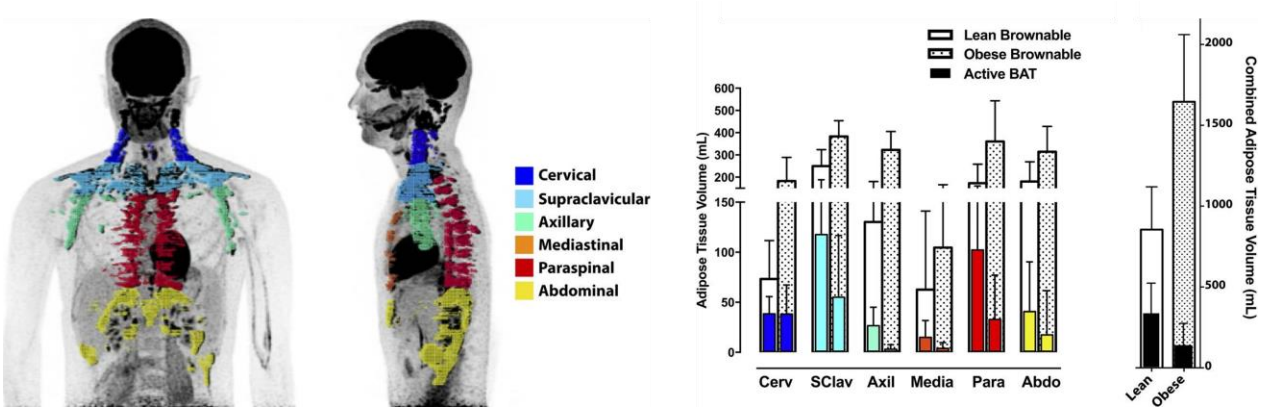

Figure 2. *The distibution of brown/beige adipose tissue in human (left panel) and the amount of brownable and active BAT in lean and obese individuals (right panel) [Leitner et al., 2017]*

4.1.2. Heat generation in brown/beige adipose tissue: UCP1-dependent and independent thermogenesis

A basic property of endothermic thermoregulation is the ability to generate heat by increasing metabolism in response to cold ambient temperatures to maintain a stable core body temperature [Brychta and Chen, 2017]. Shivering is a first defense mechanism against cold that can sharply increase heat production by contracted muscle [Haman and Blondin, 2017]. The other mechanism of heat generation in non-shivering thermogenesis by brown/beige adipose tissue. The thermogenic capacity of brown/beige adipocytes depends on fatty acids oxidation through oxidative metabolism [Gonzalez-Hurtado *et al*., 2018]. Non-shivering thermogenesis is classically activated by adrenergic signaling mediated by sympathetic neuron system, which enhances lipolysis through cAMP-PKA signaling pathway. Long-chain fatty acids released from lipolysis serve as metabolic fuel and at the same time also allosterically activate the UCP1 function [Sakers *et al*., 2022]. UCP1 catalyzes the proton leak in mitochondrial inner membrane enabling the brown/beige adipocyte to expend energy as heat instead of ATP. The accumulated

protons in the intermembrane space during respiratory chain can be brought back into the mitochondrial matrix by long-chain fatty acid that bound to UCP1 (**Figure 3a**).

The activation of UCP1 to generate heat drives a higher uptake of fuels such as glucose, fatty acids, and amino acids to sustain the metabolic substrates for TCA cycle and generate NADH and FADH that subsequently enter electron transport chain. BAT in human and mice also utilizes BCAAs during cold exposure [Yoneshiro *et al*., 2019]. Mitochondrial BCAAs transporter (encoded by *SLC25A44*) mediate the uptake of BCAAs into mitochondria that is further oxidized by branched-chain α-ketoacid dehydrogenase (BCKDH) generating NADH. Active BAT also uptakes a large amount of TCA cycle intermediate, succinate, to enhance the proton leak respiration [Mills *et al*., 2018]. The oxidation of succinate produces ROS that can promote the function of UCP1 [Chouchani *et al*., 2016]. More recent study reported that the labeled glucose consumed by mice BAT during cold exposure are converted into pyruvate, which is further converted into acetyl-CoA catalyzed by PDH [Panic *et al*., 2019]. These studies indicate that active BAT consumes the available substrates to fulfill the high energetic demand.

UCP1 has been the central/key player of non-shivering thermogenesis. The disruption of function or the deletion of UCP1 in mice result in more sensitivity to acute cold exposure but not obese [Enerback *et al.,* 1997]. However, when the temperature is gradually decreased to 4 ºC, UCP1 KO mice are still able to adapt to cold indicating that there is a compensatory mechanism in the lack of UCP1 [Ukropec *et al.,* 2006]. Cold-acclimated UCP1 KO mice expressed higher level of brown markers in inguinal WAT with more beige adipocytes as compared to wild-type indicating that more beiging occurs to compensate the UCP1 depletion. UCP1-deficient WAT exhibits elevated expression of mitochondrial creatine kinase (CKMT), DIO2, calcium-ATPase (SERCA), PGC1a, and COX2 [Kazak *et al.,* 2015]. The mechanisms of UCP1-independent thermogenesis involve futile cycles of creatine, Ca^{2+}, triacylglycerol, and uncoupling by lapidated amino acids (**Figure 3b**) [Chouchani and Kajimura, 2019; Ikeda *et al.,* 2017; Kazak *et al*., 2015; Long *et al*., 2016]. UCP1-independent thermogenesis require glycolysis and mitochondrial ATP synthesis to supply fuel for futile cycling [Sakers *et al.*, 2022].

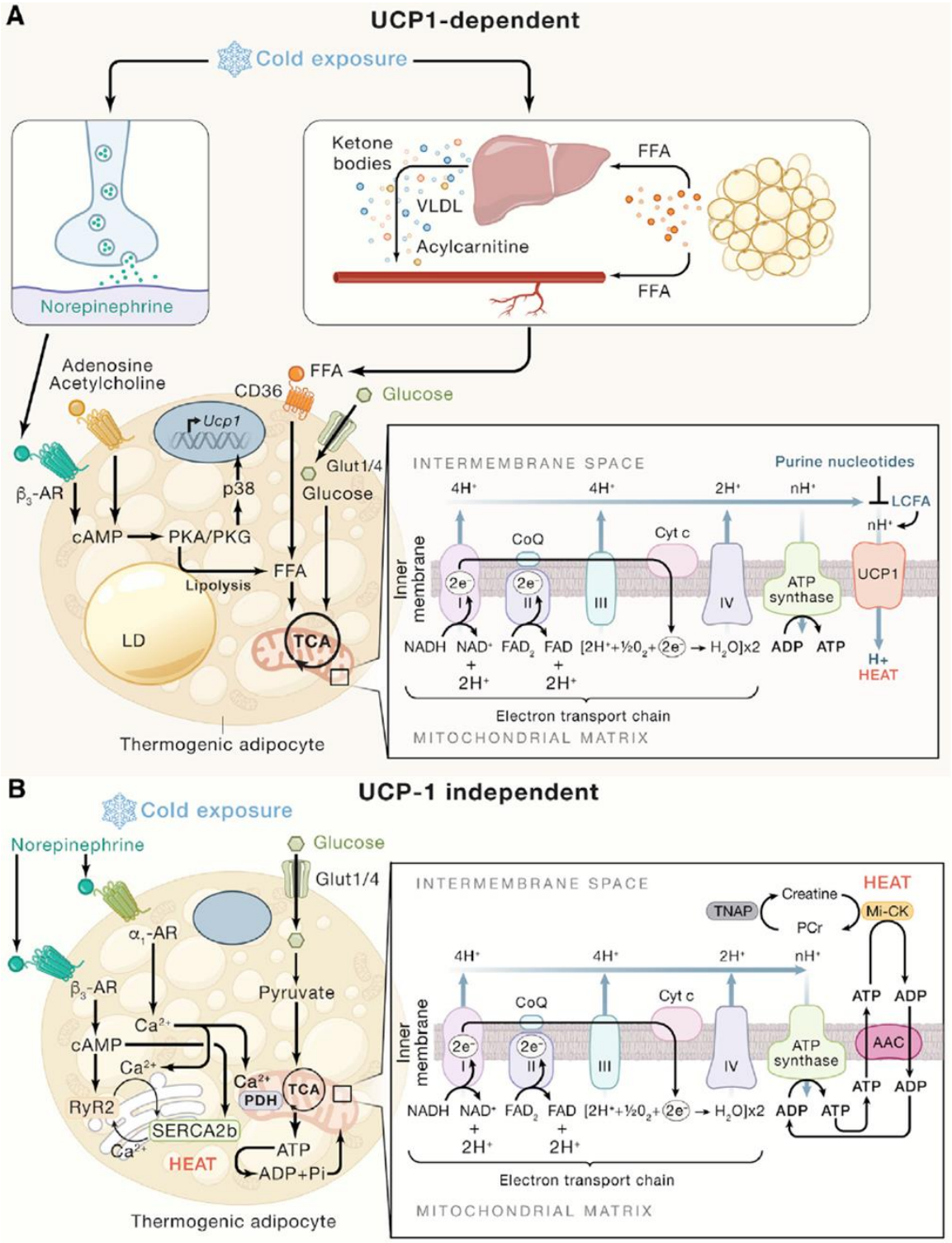

Figure 3. *Mechanism of heat generation through UCP1-dependent (top panel) and UCP1-independent (bottom panel) thermogenesis [Sakers et al., 2022]*

The creatine-driven futile substrate cycle can augment energy expenditure by releasing high-energy phosphate from phosphorylated creatine [Kazak *et al*., 2015] (**Figure 3b**). Phosphocreatine is the main energy source in skeletal muscle during high intensity exercise to support muscle contraction. The phosphocreatine/creatine cycle can generate ATP by directly phosphorylating ADP. In brown/beige adipocytes, the expression of creatine metabolism-related genes such as creatine transporter (*SLC6A8*), guanidinoacetate methyltransferase (*GAMT*), and glycine amidinotransferase (*GATM*) increase during cold exposure [Kazak *et al*., 2017]. A recent study reported that creatine kinase B (*CKB*), localized in mitochondria, play a main role in phosphorylating creatine in brown/beige adipocytes [Rahbani *et al*., 2021]. The expression of *CKB* is the highest in the human abdominal SC-derived adipocytes as compared to other creatine kinase isoform and forskolin increase its expression further [Rahbani *et al*., 2021]. Tissue non-specific alkaline phosphatase (*TNAP*), also localized in mitochondria of adipocytes, serves as phosphocreatine phosphatase in the creatine futile cycle that occurs in the adipocyte mitochondria [Sun *et al*., 2021]. The expression of both *CKB* and *TNAP* elevate in brown/beige adipocyte during cold exposure.

Muscle is the first organ that will respond to cold exposure and produce heat by shivering thermogenesis. The shivering thermogenesis will be replaced by non-shivering thermogenesis to prevent the damage in the muscles. Calcium cycling by sarco/endoplasmic reticulum Ca^{2+}-ATPase (*SERCA*) and its regulator, sarcolipin (*SLN*), has been suggested as a possible mechanism of non-shivering thermogenesis in skeletal muscle [Bal *et al*., 2012, *Nat Med*]. Sarcolipin plays role in uncoupling Ca^{2+} cycling leading to the elevation of oxidative metabolism and heat generation. Furthermore, they found that *SERCA2a*, which mediates the ATP hydrolysis in Ca^{2+} cycling, is expressed higher in WAT of cold-acclimated UCP1 KO mice. A more recent study has reported that Ca^{2+} cycling that involve SERCA2b and ryanodine receptor 2 (RyR2) control thermogenesis in beige adipose tissue and systemic energy expenditure [Ikeda *et al*., 2017].

Lipidated amino acids or N-acyl amino acids (NAAs) is synthesized by N-fatty-acyl-amino acid synthase/hydrolase (encoded by *PM20D1*). NAAs can stimulate mitochondrial respiration by serving as uncouplers even in UCP1-negative cells indicating its role as a player in UCP1-independent thermogenesis [Long *et al*., 2016]. They also revealed that the administration of exogenous NAAs elevates systemic energy expenditure resulting in weight loss

and improved glucose metabolism. ADP/ATP translocase-1 and -2 (ANT1 and ANT2), encoded by *SLC25A4* and *SLC25A5* respectively, may mediate the uncoupling activity of NAAs.

Glycerol-3-phosphate shuttles involve two enzymes: mitochondrial glycerol-3-phosphate dehydrogenase (mGPDH) and cytosolic glycerol-3-phosphate dehydrogenase (cGPDH) [Mracek *et al*., 2013]. mGPDH drives inefficient ATP synthesis through bypassing mitochondrial complex I in oxidative phosphorylation and contributes to thermogenesis [Chang *et al*., 2019]. mGPDH-deficient mice exert a decrease in oxygen consumption rate and thermogenesis [DosSantos *et al*., 2003].

4.1.3. Thermogenic gene expression in human neck tissue

Unlike in rodents, the molecular signature of human brown adipose tissue remains debatable. The gene marker for mice classical BAT has been identified such as zinc finger protein-1 (ZIC1) that can distinguish interscapular-BAT (iBAT) and beige BAT [Walden *et al.*, 2012]. Study in human adipose tissue isolated from neck area showed a higher expression of UCP1, LHX8, and ZIC1 in deep neck (DN) as compared to subcutaneous (SC) adipose tissue [Cypess *et al.,* 2013]. The mRNA expression of those classical BAT markers was also enriched in primary adipocytes derived from human fetal interscapular adipose tissue [Seiler *et al.,* 2015]. However, another study reported that the mRNA expression of ZIC1 negatively correlated to mature brown adipocytes activity such as oxygen consumption rate [Nascimento *et al.,* 2017].

Shinoda *et al.* (2015) performed RNA-sequencing analysis to identify molecular markers of clonally derived human brown adipocytes isolated from supraclavicular. They reported that the population of UCP1-positive cells displayed beige adipocyte characteristics. Moreover, they revealed that microtubule-associated tumor suppressor 1 (*MTUS1*) and potassium channel subfamily K member 3 (*KNCK3*) were essential for beige adipocyte differentiation and thermogenic activity. The knockdown of *MTUS1* and *KNCK3* decreased the expression of thermogenic genes including *UCP1*, *CIDEA* and *COX7A1*. In addition, the knockdown of *MTUS1* and *KCNK3* also decreased total and uncoupled respiration. Another study investigated the identity of the brown adipose tissue biopsies and found that BAT biopsies displayed the beige characteristic, which is marked by higher expression of beige markers including *CD137*, *TMEM26*, and *TBX1* [Wu *et al.,* 2012]. The gene markers of classical brown adipose tissue such as *EBF3*, *EVA1*, and *FBXO31* were expressed at the same level between BAT and WAT. Another study revealing the resemblance between human BAT and mice beige adipocytes was reported

by Sharp *et al*. (2012). They analyzed the mRNA expression of brown and beige markers in total RNA isolated from various anatomical locations, including subcutaneous supraclavicular areas, posterior mediastinum, retroperitoneal, intra-abdominal, mesenteric depots, and thigh tissues. Total RNA isolated from WAT and smooth muscle were used as controls. Beige-selective markers such as *HOXC8*, *HOXC9*, and *CITED1* were highly expressed in human BAT, whereas classical brown adipose tissue markers were not detectable. These studies suggested that human BAT, isolated from various anatomical locations, more resemble to mice beige adipocytes.

Other studies in human reported that there was an overlapping between classical brown and beige adipocytes in human BAT isolated from supraclavicular area [Jespersen *et al.*, 2013]. They investigated the proposed gene markers for mice classical brown, beige, and white adipocytes and compared their expression in supraclavicular BAT and SC abdominal WAT. The expression of classical brown adipocyte markers such as *LHX8* and *ZIC1* and beige adipocyte markers such as *TMEM26* and *TBX1* were enriched in human BAT. Lidell *et al.* (2013) reported that human possess two types of BAT: classical BAT in interscapular and beige BAT in supraclavicular. The expression of *ZIC1* was higher in iBAT of human infant, whereas the expression of beige adipocyte marker *TBX1* was significantly higher in supraclavicular BAT. They suggested that similarly to rodents, human also have a genuine iBAT consisting of classical brown adipocytes as thermogenic organ to protect from cold. The gene markers of brown/beige adipocyte markers in human BAT collected from various publications are listed in **Table 1**.

Computational tools had been developed to explore the characteristics and thermogenic capacity of brown/beige adipocytes samples. These web tools, which is publicly available online, were developed based on the in-depth analysis of large transcriptomic data of mice white, beige, and brown adipocytes, in case of BATLAS both mice and human adipocytes transcriptomic data were utilized. BATLAS and ProFAT web tool were developed to estimate brown adipocyte content and browning probability of heterogeneous population of adipocytes [Perdikari *et al.*, 2018; Cheng *et al.*, 2018].

Table 1. *Brown/beige adipocyte markers*

Genes	Protein	References
KCNK3	Potassium channel subfamily K member 3	Shinoda *et al*., 2015
MTUS1	Microtubule-associated tumor suppressor 1	
ZIC1	Zinc finger protein ZIC 1	Cypess *et al*., 2013
LHX8	LIM/homeobox protein Lhx8	
BMP7	Bone morphogenetic protein 7	Tseng *et al*., 2008
BMP2	Bone morphogenetic protein 2	Salisbury *et al*., 2012
CKMT1A	Creatine kinase U-type, mitochondrial	Svensson *et al*., 2011; Kazak *et al*., 2015
CKMT1B	Creatine kinase U-type, mitochondrial	
COBL	Protein cordon-bleu	Svensson *et al*., 2011
HMGCS2	Hydroxymethylglutaryl-CoA synthase, mitochondrial	
TGM2	Protein-glutamine gamma-glutamyltransferase 2	
PRDM16	Histone-lysine N-methyltransferase PRDM16	Seale *et al*., 2007
DIO2	Type II iodothyronine deiodinase	Cannon and Nedergaard, 2004
ELOVL3	Elongation of very long chain fatty acids protein 3	Tvrdik *et al*., 1997
PPARGC1A	Peroxisome proliferator-activated receptor gamma coactivator 1-alpha	Bostrom *et al*., 2012
EBF2	Early B cell factor 2	Wang *et al*., 2014
PM20D1	Peptidase M20 domain containing 1	Long *et al*., 2016
CIDEA	Cell death activator CIDE-A	Barneda *et al*., 2013
FGF21	Fibroblast growth factor 21	Lee *et al*., 2014
TBX1	T-box transcription factor TBX1	Wu *et al*., 2012
TMEM26	Transmembrane protein 26	
GK	Glyserol kinase	Weir *et al*., 2018
CITED1	Cbp/p300-interacting transactivator 1	Sharp *et al*., 2012
HOXC8	Homeobox protein Hox-C8	
HOXC9	Homeobox protein Hox-C9	

4.2. Solute carrier (SLC) transporters

4.2.1. SLC transporters: classifications and functions

Solute carrier (SLC) transporters participate in various biological processes by transporting essential nutrients, both macro and micro nutrients, disposing the waste products, and shuttling the metabolites between organels [Zhang *et al*., 2019; Kenthirapalan *et al*., 2016]. SLC transporters serve as metabolic gates and enable the cells to uptake the available substrates to generate energy or to maintain homeostasis. Other physiological functions including tissue

development, oxidative stress, and neurological regulation also require the SLC transporters contribution. Cell membrane transporters majorly include ATP-binding cassettes (ABC) and SLC transporters [Zhang *et al*., 2019]. Human SLC transporter families consist of 400 genes and 52 subfamilies. A comprehensive similarity relationship of SLCs superfamily is described in **Figure 4**. SLCs play important role in transmembrane transport of various substrates such as inorganic ions, fatty acids, amino acids, and neurotransmitters. The SLCs are majorly classified into six groups (**Figure 4**).

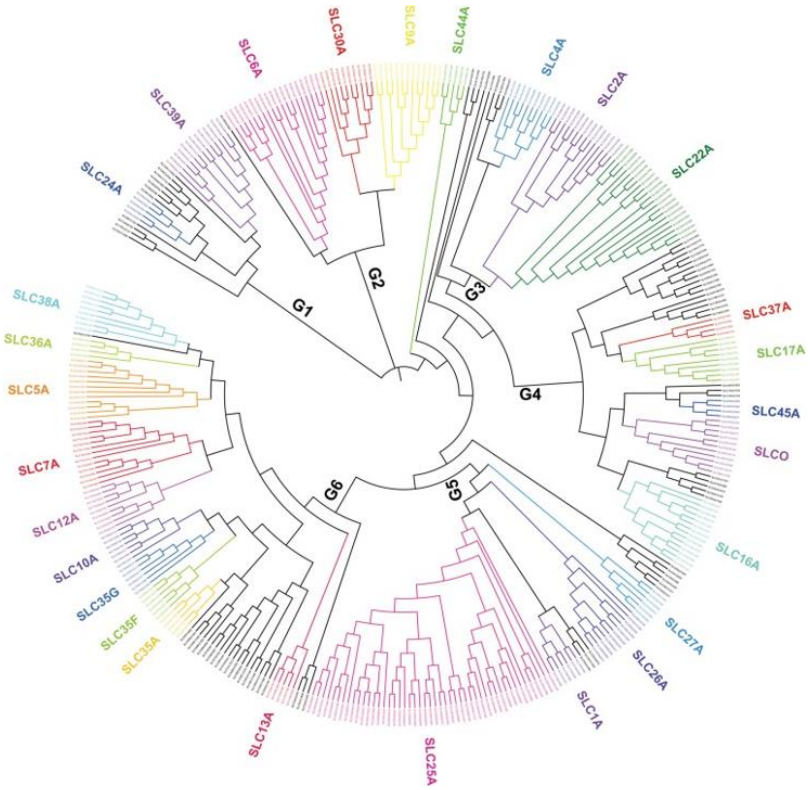

Figure 4. *The phylogenetic tree of SLC superfamily with six classifications [Zhang et al., 2019]*

There are 4 modes of transmembrane transport by SLCs: cotransporter/coupled transporter, exchanger, facilitated/passive transporter, and orphan transporter (**Figure 5**). Cotransporter is defined as the transport of one substrate via concentration gradient coupled with other molecules [Zhang *et al*., 2019]. Sodium/glucose symporter, which belongs to *SLC5A* family, was the first discovered cotransporter. It transports Na^+ and glucose in the same directions across the epithelial cell membrane providing glucose for glycolysis. Exchanger mode transports two substrates across the membrane in the opposite direction. Sodium/hydrogen exchanger 3, encoded by *SLC9A3,* facilitates the transport of Na^+ and H^+ in opposing directions to eliminate acids generated by active metabolism thus pH in the intestinal epithelial cells is maintained at

normal level [Zhang *et al*., 2019; Hediger *et al*., 2012]. The third mode of transmembrane transport is the facilitated transporter that mediate the substrate translocation without coupled molecules or by spontaneous passive transport. Thiamine transporter 2, encoded by *SLC19A3* and later will be described more detail, is one of the facilitating transporter. A major player in thermogenesis UCP1, also known as *SLC25A7*, transfers the H^+ across the inner mitochondrial membrane according to its electrochemical gradient. The orphan transporter group is comprised of transporters with unidentified substrates and function [Hediger *et al*., 2012].

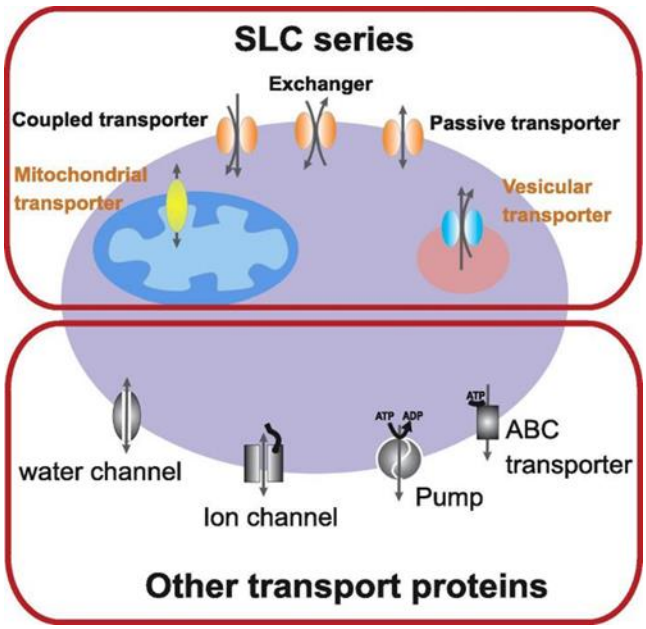

Figure 5. *SLC and non-SLC transporters expressed in plasma membrane [Hediger et al., 2012]*

Glucose transporters GLUT4, encoded by *SLC2A4*, are well-studied transporters expressed ubiquitously in adipose tissue, muscle, and cardiac tissues [Mueckler and Thorens, 2013]. GLUT4 has been identified as differentiated adipocyte marker and translocates glucose in an insulin-dependent manner. The deficiency or loss of function of GLUT4 causes glucose intolerance in mice while the overexpression of GLUT4 in adipose tissue improve the insulin resistance [Yang *et al*., 2005]. Fatty acids transporter-1 (FATP1), encoded by *SLC27A1*, has also been identified as one of adipocyte markers [Wade *et al*., 2021]. FATP1 translocation to the plasma membrane is triggered by insulin leading to the elevation of fatty acids uptake [Kim *et al*., 2004]. Deletion of FATP1 in mice resulted in the delayed fatty acid uptake from serum upon insulin injection. The expression of FATP1 in BAT is important to maintain core body temperature upon prolonged cold exposure [Wu *et al*., 2006]. Cold exposure triggers its

localization to the plasma membrane, therefore, the availability of fatty acids as main resource of metabolic fuel can be sustained.

4.2.2. Amino acid transporters

Amino acid transporters belong to *SLC7A* family, which is classified into subgroups: cationic amino acid transporters (CATs) and hetero(di)meric amino acid transporters (HATs) (**Figure 6a**) [Verrey *et al*., 2004]. CATs, encoded by *SLC7A1-4*, possess 14 putative transmembrane segments and are glycosylated (**Figure 6b**).

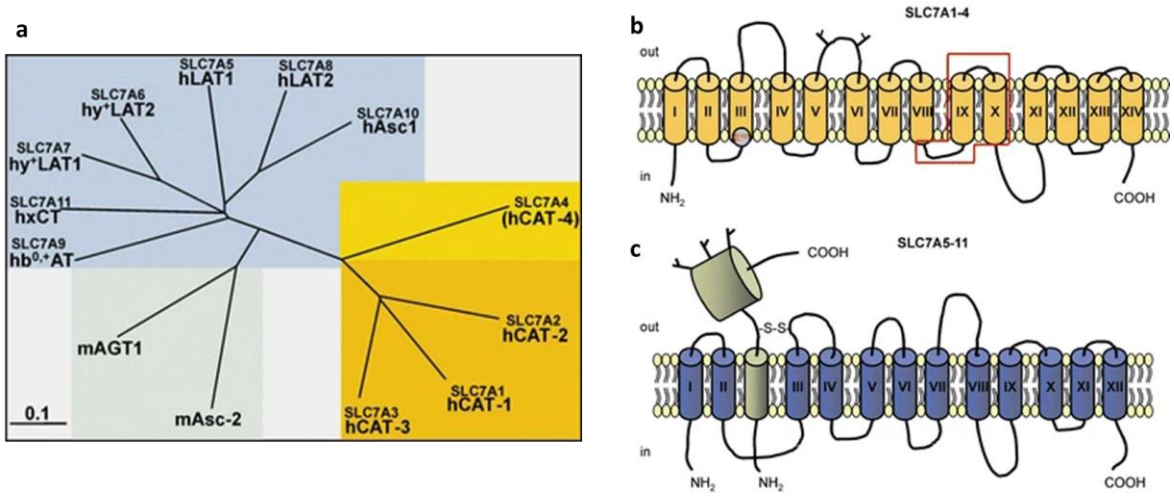

Figure 6. *Phylogenetic tree (a) and putative structure (b-c) of SLC7 amino acid transporters [Verrey et al., 2004]. The SLC7 family is composed of two subfamilies formed by the cationic amino acid transporters (CAT, SLC1–4) and the glycoprotein-associated amino acid transporters [gpaAT, light chains of heterodimeric amino acid transporters (HAT-lc), SLC5–11 and mouse neutral amino acid, ala, ser, cys-preferring transporter-2 (mAsc-2) and aspartate/glutamate transporter-1 (AGT1)].*

CAT1-3, encoded by *SLC7A1-3*, have been well-known as cationic amino acids transporters but the function of CAT4 (*SLC7A4*) remains unclear [Verrey *et al*., 2004]. CAT1 is ubiquitously expressed except in adult liver. CAT1 plays a major role in maintaining the substrate availability of NO-producing cells such as endothelial cells. Homozygous CAT1 KO mice die immediately after birth and exert a smaller body size as compared to WT-littermates due to severe anemia [Perkins *et al*., 1997]. CAT2a is expressed in liver, skeletal muscle, and pancreas, while CAT2b expression in inducible in several cell types. Abundant expression of CAT2b is observed only after cytokine or LPS treatment in most cell types along with the inducible isoform of NO-synthase. Homozygous KO of CAT2 in mice did not exert any abnormal phenotypes indicating the role of CAT2 is dispensable. However, the NO generation is diminished in peritoneal macrophages of CAT2 KO mice underlining the crucial role of CAT2b for substrates

sustainability. CAT3 is mainly expressed in mesoderm and central neurons in adult mice and rats [Hosokawa *et al*., 1999; Ito and Groudine, 1997]. CAT3 is abundantly expressed in human thymus. Unlike CAT1 and CAT2, CAT3 expression did not correlate with NO production [Verrey *et al*., 2004]. CAT4 is expressed in brain, testis, and placenta [Sperandeo *et al*., 1998] and its substrates and functions are unknown.

HATs are also identified as glycoprotein-associated amino acids transporters encoded by *SLC7A5-SLC7A11*. Model of HAT is constructed by a light chain (*SLC7A5-11*) with 12 putative transmembrane helices associated with heavy chain 4F2hc (*CD98, SLC3A2*) or rBAT (*SLC3A1*) through a conserved disulfide bridge (**Figure 6c**). L-type amino acid transporter-1 (LAT1) is encoded by *SLC7A5* gene and mediates the transport of neutral amino acids when expressed with 4F2hc. LAT1 also contributes in the uptake of branched-chain and aromatic amino acids. LAT1-4F2hc function is strongly trans-stimulated by intracellular amino acids and the stoichiometry of this exchange is 1:1 [Meier *et al*., 2002]. LAT2 (encoded by *SLC7A8*) also play role in transporting neutral L-amino acids in a sodium-independent mechanism. In addition, it also transports triiodothyronine (T3) and thyroxine (T4). LAT2 is a high affinity transporter for alanine, serine, threonine, cysteine, phenylalanine, tyrosine, arginine, and tryptophan. Similar to LAT1, LAT2 facilitates the transport of neutral amino acids when associated with 4F2hc.

4.2.3. Alanine-serine-cysteine transporter-1 (ASC-1)

Human ASC-1 is the light subunit encoded by *SLC7A10* and belongs to the LAT subfamily and is bridged through Cys154 to 4F2hc heavy subunit (**Figure 7a**) [Yan *et al*., 2019]. ASC-1 is a sodium-independent transporter that has high affinity for the small neutral D- and L-amino acids, preferentially by exchanger mechanism. It has a main role in modulating the glutamatergic transmission through mobilization of D-serine at the glutamatergic synapse [Brown *et al*., 2013]. ASC-1 has multiple substrates such as L-alanine, L-cysteine, glycine, and both isoform of serine. ASC-1 is abundantly expressed in brain and is being investigated as a therapeutic target for schizophrenia [Rosenberg *et al*., 2013]. Inhibition of ASC-1 may elevate the level of extracellular glycine and D-serine in critical brain regions. A small molecule BMS-466442 has been characterized as a selective inhibitor of ASC-1 with IC_{50} 36.8±11.68 nM and 19.7±6.7 nM for human ASC-1 expressing cells and primary cultures (**Figure 7b**) [Brown *et al*, 2013].

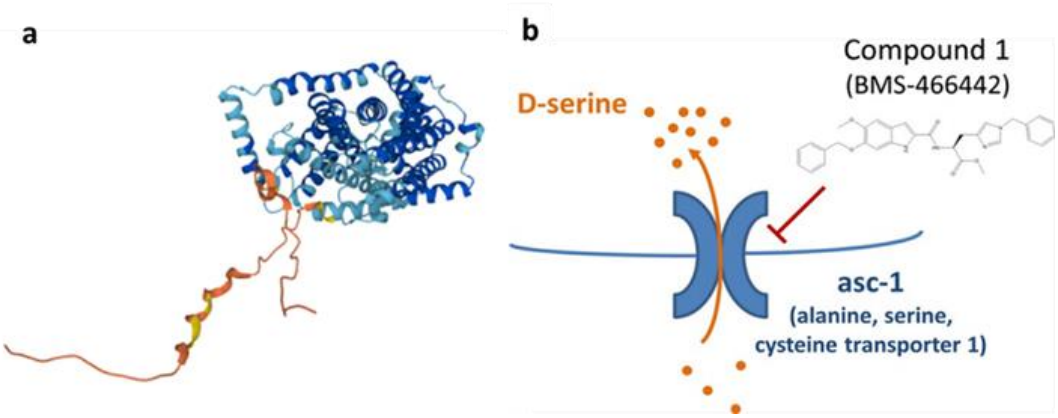

Figure 7. *3D structure of ASC-1 (a) and selective inhibition by BMS-466442 (b).*

The role of ASC-1 in synaptic system has been elucidated, however, its role in metabolic regulation has not been explored. ASC-1 was identified as surface marker of mice white adipocytes [Ussar *et al*., 2014]. The protein expression of ASC-1 is higher in cell membrane of SC WAT as compared to BAT [Ussar *et al*., 2014]. A later study reported that a subpopulation of preadipocytes expressing ASC-1 exerted lower capacity to differentiate to beige adipocytes as compared to ASC-1 negative cells [Suwandhi *et al*., 2021]. Other study reported that ASC-1 expression is negatively correlated with waist-to-hip ration and its impairment by BMS-466442 decreased the OCR of human primary adipocytes [Jersin *et al*., 2021]. The inhibition of ASC-1 in adipocytes also reduced serine uptake and total glutathione levels. As the consequences, ROS production was promoted leading to oxidative stress and cellular damage [Jersin *et al*., 2021].

4.2.4. Thiamine metabolism

Thiamine, which belongs to vitamin B family, was first discovered in 1912. The recommended daily intake of thiamine for adults is 1-1.4 mg/day. Thiamine can be synthesized by bacteria, fungi, and plants, but not by mammals thus thiamine is an essential vitamin for humans. Thiamine can be obtained from the intestinal microflora and dietary sources in the form of free thiamine. In several countries, thiamine deficiency becomes a serious problem due to inadequate intake or consumption of antithiamine factors. Thiamine fortification program has been performed to overcome thiamine deficiency, especially in infants. Food sources of thiamine are meat and meat products, cereals and grains, vegetables, dairy products, and fruits. Thiamine half-life in humans is 9 to 18 days. Under normal physiological and nutritional conditions, the liver of adult humans can reserve thiamine for 3 weeks in average and the reserved thiamine can

be rapidly diminished in disease or surgery [Manzanares *et al*., 2011; Maguire *et al*., 2018]. Thiamine deficiency can cause a number of severe disease, such as *Beriberi* and Wernicke's encephalopathy. Several studies also report that thiamine deficiency is correlated with type 1 and type 2 diabetes (Jermendy, 2006; Saito *et al*., 1987]. A significant thiamine deficiency was found in patients prior to bariatric surgery and this condition was observed based on measurement of serum thiamine concentration [Peterson *et al*., 2016]. In diabetic animal models, thiamine treatment reduced fasting glucose and HbA1c levels [Thornalley *et al*., 2010]. Gonzalez-Ortiz *et al*. (2011) reported that short term treatment of thiamine with dose 150 mg/day could significantly improve the level of fasting glucose in individuals with type 2 diabetes.

There are two ways to evaluate the thiamine status, which are considered as gold standards: by assessing the level of TPP-saturation of a thiamine-dependent enzyme (erythrocyte transketolase (ETK) assay) and by measuring erythrocyte TPP concentration [Whitfield *et al*., 2018; Maguire *et al*., 2018]. The ETK assay provides an informative result as it displays actual functionality of thiamine [Whitfield *et al*., 2018]. Erythrocyte TPP measurement from whole blood is recognized as a reliable measure of thiamine status, which some regard as equivalent or superior to ETK assay. Erythrocyte TPP measurement may have an advantage over ETK assay for detecting tissue thiamine accumulation, but the functionality status cannot be observed [Maguire *et al*., 2018]. The results of ETK assay may depend on the storage and processing conditions of blood samples [Puxty *et al.*, 1985]. Direct measurement of whole blood TPP mass is more reliable regarding the context of hemoglobin mass, which is expressed in nanogram of TPP per gram of hemoglobin units (ng/g Hb), and it will be correct for unavoidable pipetting related volume sampling error [Talwar *et al*., 2000]. **Table 2** describe the advantages and disadvantages of thiamine biomarkers evaluation [Whitfield *et al*., 2018].

Table 2. *Thiamine biomarkers used to measure recent intake and thiamine status*

BIOMARKERS	SPECIMEN	ADVANTAGES	DISADVANTAGES
Direct measurement			
Thiamine	Plasma	Indicates recent intake	Not an indicator of thiamine status
TMP	Plasma	Indicates recent intake	Not an indicator of thiamine status
TPP	Whole blood; erythrocyte	Biologically active vitamin and indicator of thiamine status	Unstable if specimen is not properly handled
Indirect/functional measurement			
ETK assay	Washed erythrocyte	Functional assay of biological activity	Assay is not readily available

Thiamine is present in humans in various forms such as free-thiamine, thiamine monophosphate (TMP), TPP, and thiamine triphosphate (TTP) [Losa *et al*., 2005]. The distribution of thiamine derivatives in human whole blood and plasma is described in **Table 3**. Functional activity of the tissues determine the form of presence thiamine. The largest amount of thiamine exist as TPP, counting for 80% of total body thiamine. TPP is essential as it participates in various biological processes in the cytosol, mitochondria, and peroxisome. In the cytosol, TPP plays role in the pentose phosphate pathway, involved as a cofactor of transketolase enzyme. Transketolase is an important linker of pentose phosphate pathway to glycolysis, feeding excess sugar phosphate into the main carbohydrate metabolic pathways. The pentose pathway plays main role in producing the reducing equivalents, NADPH, that are important for ribose-5-phosphate generation for high-energy ribonucleotide synthesis. The status of low thiamine level can be reflected by abnormal expression and activity of transketolase enzyme [Ortigoza-Escobar *et al*., 2016].

Table 3. *Distribution of thiamine derivatives in human whole blood and plasma with the percent of total thiamine derivatives in each specimen type (n.d: not detectable) [Withfield et al., 2018].*

Specimen	Thiamine (nmol/L)	TMP (nmol/L)	TDP (nmol/L)	TTP (nmol/L)
Whole blood	4 ± 3 (2.4%)	10 ± 4 (6.1%)	138 ± 33 (83.6%)	13 ± 4 (7.9%)
Plasma	11 ± 3 (68.7%)	5 ± 2 (31.3%)	n.d	n.d

In the mitochondria, TPP is an important cofactor for several complexes including pyruvate dehydrogenase complex (catalyzing the conversion of pyruvate into acetyl-CoA), oxoglutarate dehydrogenase complex (catalyzing the carboxylation of α-glutarate in tricarboxylic acid (TCA) cycle), and BCKDH complex (catalyzing the decarboxylation of branched short-chain α-ketoacids) [Ortigoza-Escobar *et al*., 2017; Tittman, 2009]. TPP is the coenzyme for E1 component of BCKDH complex, leading to its activation. In contrast, BCKDH kinase (BDK) phosphorylates E1 of BCKDH leading to its inactivation. It has been reported that BDK is also sensitive to the inhibition by TPP [Harper *et al*., 1984]. The TPP-binding site of the E1 component is associated with the active site of the BCKDH, which is also the phosphorylation region of BDK. Noguchi *et al*. (2018) reported that TPP inhibited BDK in BCKDH-BDK complex and the mechanism of inhibition was significantly increased by the presence of free Ca^{2+} in a physiological range concentration. Their finding explains the mechanism of the elevation of branched-chain amino acid (BCAA) oxidation during skeletal muscle exercise by the increase of mitochondrial free Ca^{2+} level. Yoneshiro *et al*. (2019) reported that human brown

adipose tissue regulates the circulating BCAA levels upon cold exposure through mitochondrial BCAA transporter encoded by SLC25A44 gene. The clearance of circulating BCAA by BAT resulted in the elevation of BCAA oxidation by BCKDH and controlled the energy homeostasis. The presence of thiamine during BCAA clearance by BAT is essential to maintain the activity of BCKDH. The role of TPP as cofactor in several mitochondrial enzymes is displayed in **Figure 8** [Whitfield *et al*., 2018].

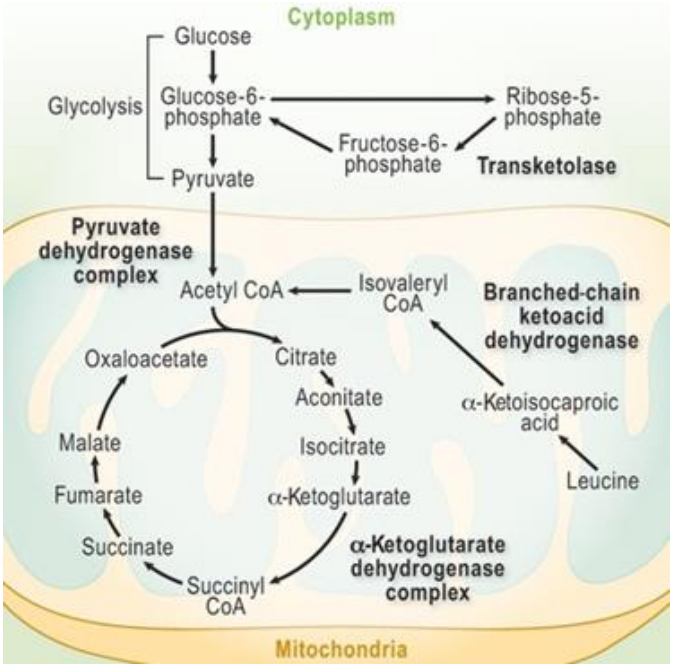

Figure 8. *TPP is required as cofactor of several mitochondrial enzymes, shown in bold text.*

As mentioned above, TPP is an important cofactor of pyruvate dehydrogenase (PDH), which catalyzes the conversion of pyruvate to Acetyl-CoA. Thiamine deficiency compromises the PDH activity resulting in the accumulation of pyruvate in the cytosol that triggers the upregulation of lactate dehydrogenase (LDH) activity [Ciszak *et al*., 2003]. The elevation of LDH activity results in the accumulation of lactate in the cytosol. It has been known that lactate concentrations are chronically increased in obese patient with diabetes [Chen *et al*., 1993; Lovejoy *et al*., 1990]. The elevation of lactate concentration due to irresponsiveness of PDH in adipocytes precedes the onset of insulin resistance in obese patients [Wu *et al*., 2016]. These findings suggested that the declined activity of PDH due to thiamine deficiency may mediate metabolic syndrome or insulin resistance in obese individuals.

In the peroxisome, TPP plays role as a cofactor of 2-hydroxyacyl-CoA lyase (HACL1), which is important in fatty acids degradation. HACL1, along with 2-hydroxyphytanolyl-CoA lyase (2-HPCL), were first discovered when studying α-oxidation of phytanic acid. HACL1 is involved in two pathways, including the degradation of 3-methyl-branched fatty acids (e.g.phytanic acid) and the shortening of 2-hydroxy long-chain fatty acids. HACL1 plays a significant role in catalyzing the cleavage step that involves the splitting of carbon-carbon bond between the first and second carbon atom in a 2-hydroxyacyl-CoA intermediate, resulting in the production of aldehyde and formyl-CoA. Formyl-CoA is then quickly converted into formate and subsequently to CO_2. Hitherto, there is no report regarding the deficiency of HACL1 in humans, but its activity is significantly affected by thiamine deficiency [Casteels *et al*., 2017].

4.2.5. Thiamine transporters (ThTrs)

Free thiamine uptake is performed by thiamine transporter 1 (ThTr1) and 2 (ThTr2), which belong to *SLC19* family alongside with folate transporter (encoded by *SLC19A1*). Both thiamine transporters are located in cell membrane with 12 transmembrane domains. The expression of both transporters are enriched in small and large intestines. In human, ThTr1 is expressed in the apical and basolateral membrane domains of polarized enterocytes and ThTr2 is expressed in the apical brush-border membrane domain (Said *et al*., 2004]. Human ThTr2 seems to play more significant role in thiamine uptake in intestine because the deficiency of ThTr1 does not affect the plasma thiamine levels. Both thiamine transporters mediate the uptake of thiamine, which exists as cation at physiological pH, across the cell membrane using differences in pH as a driving force [Ganapathy *et al*., 2004]. Thiamine influx into cells via ThTrs is enhanced by an outwardly directed H^+ gradient ($pH_{out}>pH_{in}$), suggesting thiamine/H^+ antiport as the transport mechanism (**Figure 9**).

ThTr1 is encoded by *SLC19A2* gene and possess a high affinity to thiamine. *SLC19A2* gene has 6 exons and 5 introns with 22.5 kb length. ThTr1 shares 40% homology with folate transporter, which is encoded by *SLC19A1* gene. Human ThTr1 consist of 497 amino acids containing 12 transmembrane alpha helixes with NH_2 and COO^- terminus regions facing to cytosol and two N-glycosylation sites in putative extracellular domains [Ganapathy *et al*., 2004]. Autosomal recessive thiamine-responsive megaloblastic anemia (TRMA) occurs when *SLC19A2* gene is disrupted by mutations. Among 136 TRMA patients, 58 different mutations have been

reported and 48.3% of them affected exon 2 [Marcé-Grau, 2019]. Several studies have been reported to discover the function of ThTr1. The fibroblast of TRMA patients carrying homozygous mutations c.1074G>A and c885delT had lower thiamine uptake activity as compared to control cells [Fleming *et al*., 1999; Scharfe *et al*., 2000]. It was also reported that the administration of high dose thiamine improve the activity of mitochondrial complex 1 in a TRMA patient. Several studies have also reported that mutation in *SLC19A2* gene resulted in various disease, mainly megaloblastic anemia, in Tunisian, Indian, and Chinese population [Gritli *et al*., 2001; Manimaran *et al*., 2016; Xian *et al*., 2018].

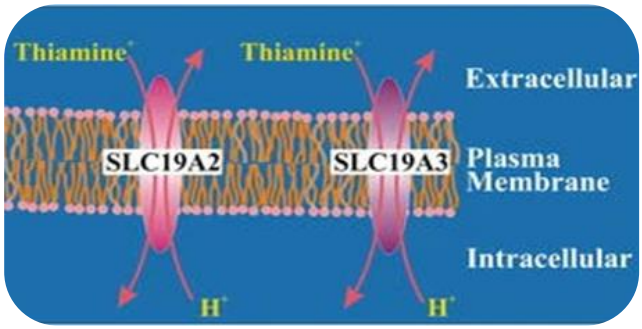

Figure 9. *Proposed thiamine transport into the cells by ThTr1 and ThTr2 [Ganapathy et al., 2004]*

ThTr2 is encoded by *SLC19A3* and mediates thiamine uptake by facilitated transport mechanism. Human *SLC19A3* encodes a 496 amino acid residue protein with predicted molecular weight 56 kDa. The protein is constructed by 12 transmembrane alpha helixes flanked by cytoplasmic N- and C-terminal regiosn [Marce-Grau *et al*., 2019]. ThTr2 shares sequence similarity with FLT and ThTr1 [Eudy *et al*., 2000]. It is ubiquitously expressed in human tissues, however, a recent study reported that ThTr2 is highly expressed in human adipose visceral and subcutaneous abdominal tissue [Melé *et al*., 2015; Pereira *et al*., 2021]. The inhibition of ThTr2 significantly affected the thiamine absorption in intestine and renal reabsorption leading to thiamine deficiency. Loss-of-function mutation affecting this gene interrupt thiamine transporter function resulting in biotin responsive basal ganglia disease that is also known as thiamine metabolism dysfunction syndrome 2 (THMD2) [Ozand *et al*., 1998]. A more recent study reported the involvement of ThTr2 in high glucose-induced damage in retinal pericytes [Beltramo *et al*., 2020].

Disturbance on the thiamine transporters activity can attenuate the metabolic processes, mainly in those pathways that require thiamine or its derivative. Several thiamine transporter

inhibitors have been studied mostly in CACO2 cell line, which is a cell model for intestine cells [Zhang *et al*., 2014; Giacomini *et al*., 2017]. Fedratinib that contain 2,4-diaminopyrimidine in the structure can interact with thiamine transporters, and it is more potent in inhibiting ThTr2 [Zhang *et al*., 2014; Giacomini *et al*., 2017]. The IC_{50} value of potent thiamine inhibitors is described in **Table 4**.

Table 4. *IC_{50} of potent thiamine inhibitors on thiamine uptake [Giacomini et al., 2017]*

Compound	IC_{50} Value for Thiamine uptake (μM)	
	ThTr2	ThTr1
Fedratinib	1.36 ± 0.59	7.10 ± 1.26
Amprolium	0.620 ± 0.270	2.60 ± 0.93
Oxythiamine	66.4 ± 10.4	67.3 ± 7.50

5. Aims of the study

5.1. To find differentially expressed genes (DEGs) in human subcutaneous neck (SC) and deep neck (DN) derived white and brown adipocytes.

- Characterizing the molecular identity of human brown adipocytes derived from deep neck region.
- Predicting the brown adipocyte content and browning probability of human neck derived adipocytes by using available web tools.

5.2. To reveal the importance of alanine-serine-cysteine transporter-1 (ASC-1) and thiamine transporters (ThTrs) on thermogenesis of human neck-derived adipocytes.

- Studying the effect of potent inhibitors of ASC-1 and ThTrs on heat generation of human neck-derived adipocytes by monitoring oxygen consumption and quantification of thermogenesis by determining uncoupling activity of UCP1.
- Elucidating the important role of ASC-1 in mediating the uptake of amino acids in deep neck adipocytes by measuring amino acids concentration in the conditioned culture fluid during adrenergic stimulation in the presence of ASC-1 selective inhibitor
- Investigating the consequence of the restricted uptake of amino acids or thiamine on the expression of thermogenic genes and mitochondrial complex subunits.
- Evaluating the thiamine direct stimulation on mitochondrial thiamine pyrophosphate-dependent pyruvate dehydrogenase (PDH) activity in cell membrane-permeabilized adipocytes by measuring mitochondrial and proton leak respiration driven by PDH substrate.
- Analyzing the effect of ThTrs potent inhibitors on the expression of thermogenic genes in human neck tissue biopsies.

6. Materials and methods

6.1. Ethics statement

Tissue collection was approved by the Medical Research Council of Hungary (20571-2/2017/EKU) followed by the EU Member States' Directive 2004/23/EC on presumed consent practice for tissue collection. All experiments were carried out in accordance with the guidelines of the Helsinki Declaration. Written informed consent was obtained from all participants before the surgical procedure.

6.2. Materials

Table 5. *Compounds used in cell culture and differentiation*

COMPOUNDS	COMPANY
Apo-Transferin Human	Sigma-Aldrich #T2252
Biotin	Sigma-Aldrich #B4639
Collagenase from Clostridium histolyticum	Sigma-Aldrich #C1639
Dexamthasone	Sigma-Aldrich #D1756
Dibutyryl-cAMP	Sigma-Aldrich #D0627
DMSO	Sigma-Aldrich #D2650
DMEM nutrient mixture F-12	Sigma-Aldrich #D8437
Thiamine-free DMEM F-12 medium	Gibco cat#ME2107367
Fetal bovine serum	Gibco #10270
Hydrocortisone	Sigma-Aldrich #H0888
3-Isobutyl-1-methylxantin (IBMX)	Sigma-Aldrich #15879
Insulin solution human	Sigma-Aldrich #19278
Pantothenic acid	Sigma-Aldrich #P5155
Penicilin-Streptomycin	Sigma-Aldrich #P43333
Rosiglitazone	Cayman Chemicals #71740

Table 6. *SLC inhibitors and chemical compounds used in OCR measurement*

COMPOUNDS	COMPANY
Thiamine	Sigma-Aldrich #731188
Thiamine pyrophosphate (TPP)	Sigma-Aldrich #PHR1369
BMS-466442	Aobious, Inc, #AOB6567
Fedratinib	Selleck Chemicals LLC #S2736
Amprolium	Sigma-Aldrich #137-88-2
Devimistat	MedChem Express #HY-15453
Oxythiamine	Sigma-Aldrich #614-05-1
Oligomycine	Sigma-Aldrich #495455
Antimycin A	Sigma-Aldrich #A8674
3-Guaidinopropionic acid	Sigma-Aldrich #G6878
Seahorse XF Medium	Agilent #103575-100
Cell membrane permeabilizer	Agilent cat#102504-100

Table 7*. Compounds of mitochondrial assay solution*

COMPOUNDS	COMPANY
Mannitol	Sigma-Aldrich #M4125
Sucrose	Sigma-Aldrich #S0389
KH_2PO_4	Sigma-Aldrich #P5655
$MgCl_2$	Sigma-Aldrich #M8266
HEPES	Sigma-Aldrich #H3375
EGTA	Sigma-Aldrich #E3889
BSA	Sigma-Aldrich #A7070
ADP	Sigma-Aldrich #01905
Pyruvate	Sigma-Aldrich #P76209
Malate	Sigma-Aldrich #M7397

Table 8. *Gene primers and probes*

GENES	ASSAY ID
SLC19A3	Hs00228858_m1
SLC19A2	Hs00949693_m1
SLC25A19	Hs01001439_m1
UCP1	Hs00222453_m1
PPARGC1A	Hs01016719_m1
PRDM16	Hs00537016_m1
CITED1	Hs00918445_g1
TBX1	Hs00271949_m1
DIO2	Hs00255341_m1
SLC7A10	Hs00219813_m1
CKMT2	Hs00176502_m1
PM20D1	Hs00399438_m1
CKMT1A/B	Hs00179727_m1
ELOVL3	Hs00537016_m1
GAPDH	Hs99999905_m1

Table 9. *Antibodies used in immunoblotting*

ANTIBODY	COMPANY	CAT. NUMBER	DILUTION
UCP1	R&D Systems, Minneapolis, MN, USA	MAB6158	1:750
SLC19A3	Novus Biologicals, Centennial, CO, USA	NBP1-69703	1:500
SLC19A2	Abcam, Cambridge, MA, USA	Ab229680	1:500
SLC25A19	Novus Biologicals, Centennial, CO, USA	NBP1-80528	1:500
PDHA1	Invitrogen, USA	459400	1:1000
PGC1α	Novus Biologicals, Centennial, CO, USA	NBP1-04676	1:1000
ASC-1	Abnova, Neihu Disctrict, Taipei City, Taiwan	H00056301-B01P	1:500
CKMT2	Novus Biologicals, Centennial CO, USA	NBP2-13841	1:2000
HRP-conjugated goat **anti-rabbit** IgG	Advansta, San Jose, CA, USA	R-05072-500	1:5000
HRP-conjugated goat **anti-mouse** IgG	Advansta, San Jose, CA, USA	R-05071-500	1:5000

6.3. Isolation of SC and DN derived human adipose stromal cells (hASCs)

During thyroid surgeries, a pair of DN and SC adipose tissue samples was obtained to rule out inter-individual variations. The samples were given by Dr. Ferenc Gyory and surgeries were performed in Department of Surgery, Faculty of Medicine, University of Debrecen. The age of the donors range from 45-73 years old. Patients with known diabetes, malignant tumor or with abnormal thyroid hormone levels at the time of surgery were excluded. Adipose tissue specimens were dissected from blood vessels and connective tissues and minced into small pieces. The minced tissues were digested in 120 U/mL collagenase-containing PBS for 1 hour in 37 ^{o}C water bath. The tube was gently mixed every 15 minutes. The completely disaggregated tissue was filtered to remove the tissue debris. The cell suspension was centrifuged for 10 minutes at 200 g and the pellet of stromal vascular fraction (SVF) was re-suspended in DMEM-F12 medium containing 10% FBS, 100 U/mL penicillin-streptomycin, 33 µM biotin and 17µM pantothenic acid. SVF were seeded into 6-well plates at a density of 15000 cells/cm^2 and cultured in serum-containing medium at 37 $^{\circ}$C in 5% CO_2 for 24 hours to attach. Floating cells were removed with PBS and the attached hASCs were cultured until they reached confluency. Cells were mycoplasma-free as it was proved by PCR analysis.

6.4. Adipocyte differentiation: white and brown adipocytes

hASCs were seeded in 6-well plates and differentiated into adipocytes (ADIP) under regular adipogenic medium and brown adipocytes (B-ADIP) under long-term rosiglitazone treatment. ADIP differentiation was induced for three days using DMEM-F12 medium supplemented with 33 µM biotin, 17 µM pantothenic acid, 10 µg/mL human Apo-transferrin, 20 nM human insulin, 100 nM hydrocortisone, 200 pM T3, 2 µM rosiglitazone, 25 nM dexamethasone, and 500 µM IBMX [Toth *et al*., 2020]. B-ADIP differentiation was induced for three days using DMEM-F12 medium supplemented with 33 µM biotin, 17 µM pantothenic acid, 10 µg/mL apo-transferrin, 0.85 µM human insulin, 200 pM T3, 1 µM dexamethasone, and 500 µM IBMX. After three days, dexamethasone and IBMX were omitted from both differentiation medium. From day 4-14, hydrocortisone was constantly present in the ADIP differentiation cocktail [Kristof *et al*., 2015]. Rosiglitazone and higher concentration of insulin were presence in the B-ADIP differentiation cocktail since day 4-14 of differentiation [Elabd *et al*., 2009; Toth *et al*., 2020; Arianti *et al*., 2021].

6.5. Cell culture and pharmacological inhibitor of SLC target treatment

SC and DN preadipocytes were seeded on 6-well plates and differentiated into ADIP and B-ADIPs. After 14 days of differentiation, ADIPs and B-ADIPs were treated with single bolus of dibutyryl-cAMP 500 µM for 10 hours. BMS-466442 100 nM was administered to selectively inhibit ASC-1. Fedratinib 1µM or amprolium 300 µM was administered to inhibit ThTr activity. Oxythiamine 300 µM or devimistat 75 µM was administered to inhibit the activity of TPP-requiring enzymes. In thiamine concentration dependence thermogenic experiments, we used custom-made thiamine free culture fluid treating adipocytes with the gradually increasing concentration of thiamine 40 nM, 200 nM, 1 µM, 5 µM, or 25 µM in the presence or absence of cAMP stimulation for 10 hours.

6.6. Total RNA isolation and RT-qPCR

Total RNA was isolated from differentiated adipocytes using triazole reagent. Total RNA concentration was measured by nanodrop spectrophotometer after DNase treatment. TaqMan reverse transcription reagent was applied to generate cDNA by following manufacturer's instruction. A LightCycler 480 (Roche Diagnostics) was utilized to determine the normalized expression of gene of interest. Validated TaqMan qPCR assay designed and supplied by Applied

Biosystems were used according to manufacturer's instruction. Human GAPDH was used as endogenous control. The list of gene primers and probes used in this study is summarized in **Table 8**. All samples were analyzed in triplicate. Gene expression values were calculated by the comparative Ct method. ΔCt represents the threshold cycle (Ct) of the target minus that of GAPDH.

6.7. Western Blot

Differentiated ADIPs and B-ADIPS were washed with cold PBS and collected in SDS buffer. The samples were boiled in 100^{o}C for 10 minutes and loaded onto SDS polyacrylamide gel. Proteins were transferred onto PVDF Immobilon-P Transfer Membrane followed by blocking in Tris-buffered saline containing 0.05% Tween-20 TBS (TTBS) and skimmed milk for 1 hour. Membranes were probed by primary antibodies (**Table 9**) overnight at 4^{o}C. Next, membranes were washed with TTBS 3x15 minutes and followed by incubation with horseradish-peroxidase-conjugated species-corresponding secondary antibodies for 1 h at room temperature. Immunoblots were developed with Immobilon western chemiluminescent substrate. Blot images were taken using a ProteinSimple AlphaImager® HP instrument. Densitometry analysis of immunoblots was performed by using Image J software.

6.8. Oxygen consumption measurement by Seahorse

OCR and ECAR were measured using an XF96 oxymeter (Seahorse Biosciences, North Billerica, MA, USA). Small chamber was created between cells and sensors (**Figure 10)** allowing us to detect a very rapid changes of oxygen concentration as the cells respire to produce ATP through oxidative phosphorylation. XF Seahorse analyzer provides a kinetic measurement of respiration by measuring the concentration of oxygen consumed by cells from the medium (oxygen consumption rate). XF seahorse analyzer also detect the lactic acid production through glycolysis by measuring protons released by cells that acidify the medium (extracellular acidification rate). After recording the baseline OCR, 500 µM dibutyryl-cAMP, 100 nM BMS-466442, 1 µM fedratinib, 300 µM amprolium, 75 µM devimistat, 300 µM oxythiamine or combination of cAMP and SLC inhibitor were injected to the cells. Then, stimulated OCR was recorded every 30 minutes. The adipocytes were treated with the creatine analogue 2 mM β-guanidinopropionic acid (β-GPA) which interferes with creatine-driven substrate cycle [Kazak *et al*., 2015]. Proton leak respiration was determined after injecting ATP synthase blocker

(oligomycin) at 2 µM concentration. The respiration remaining after oligomycin injection is linked to the proton leak rate across the inner mitochondrial membrane [Ruas *et al.*, 2016]. Cells received a single bolus of Antimycin A at 10 µM concentration for baseline correction (measuring non-mitochondrial respiration). The OCR was normalized to protein content.

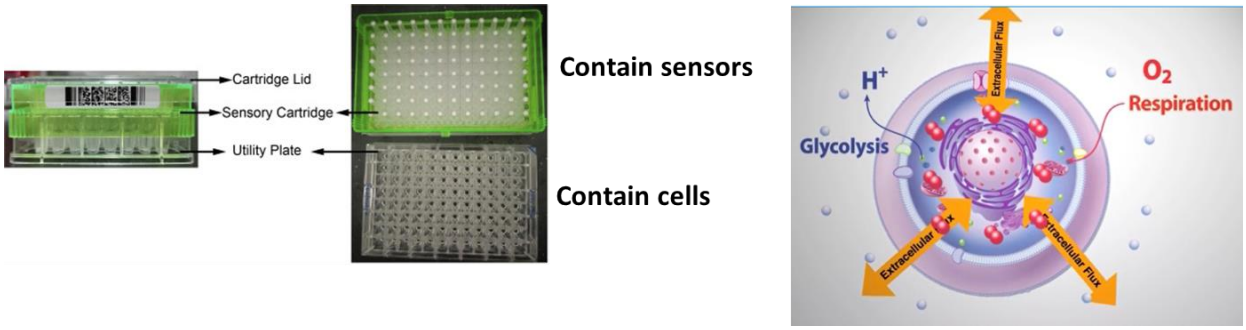

Figure 10. *Seahorse cartridge that contain sensors for oxygen and pH change in the medium and plate that contain cells (left panel). Seahorse analyzer can measure the level of oxygen consumed from the medium and proton released by the cells (right panel).*

For thiamine concentration dependence experiment, we incubated the adipocytes in thiamine free culture fluid 1h before the extracellular flux assay. After recording the baseline OCR, 500 µM dibutyryl-cAMP and gradually increasing concentrations of thiamine were injected. Then, stimulated OCR was recorded every 30 minutes in both types of experimental settings. Proton leak respiration was monitored after injecting oligomycin at 2 µM concentration. Cells received a single bolus of Antimycin A at 10 µM concentration for baseline correction (measuring non-mitochondrial respiration). The OCR was normalized to protein content.

6.9. Amino acid consumption measurement

Frozen cell culture supernatants were filtered using 3 kDa filters (Pall Corporation, Port Washington, NY, USA), then 10 µl of filtrate was derivatized with AccQ·Tag Ultra Derivatization Kit (Waters, Milford, MA, USA). Chromatographic separation was carried out on H-class UPLC (Waters) using AccQTag Ultra Column (2.1 X 100mm), AccQTag Eluent A and B and gradient provided in the AccQ-Tag Ultra Chemistry Kit (Waters). Detection of amino acid derivatives was performed at 260 nm in the PDA detector of the UPLC. Concentration of the amino acids was calculated with the Empower software (Waters) using a 7-point calibration curve.

Flux of amino acids into or from adipocytes was calculated by comparing concentration differences measured at starting and end point of 10 hours dibutyryl-cAMP treatment with or without the presence of ASC-1 inhibitor. The number of cells in wells was calculated using KOVA glasstic slide 10 with grids (Kova International Inc, Garden grove, California, USA, cat#K304680) as described in the manufacturer's manual.

6.10. Oxygen consumption measurement in cell membrane-permeabilized adipocyte

To study the direct effect of TPP on PDH activity, a Seahorse-based assay was optimized for adipocytes [Mikulas *et al*., 2020]. To SC and DN derived adipocytes a mitochondrial assay solution containing 600 mM mannitol, 210 mM sucrose, 30 mM KH_2PO_4, 1.5 mM $MgCl_2$, 6mM HEPES, 3 mM EGTA, 0.6% BSA, 4 mM ADP, and 10 mM pyruvate + 5 mM malate, pH 7.4, was added before the measurement. Membrane permeabilizer (Agilent cat#102504-100, Santa Clara, CA, USA) at 1 nM concentration and 300 µM TPP were administered to the adipocytes after recording the basal OCR for 10 minutes. Then, OCR of permabilized adipocytes was recorded every 5 minutes. Proton leak respiration was determined after injecting oligomycin at 2 µM concentration. Permeabilized cells received a single bolus of Antimycin A at 10 µM concentration for baseline correction (measuring non-mitochondrial respiration).

6.11. RNA-Sequencing analysis

Total RNA sample quality was checked on Agilent BioAnalyzer using Eukaryotic Total RNA Nano Kit according to the Manufacturer's protocol. Samples with RNA integrity number (RIN) value > 7 were accepted for the library preparation process. Libraries were prepared from total RNA using NEBNext® Ultra™ II RNA Library Prep for Illumina (New England BioLabs, Ipswich, MA, USA) according to the manufacturer's protocol. Briefly, poly-A RNAs were captured by oligo-dT conjugated magnetic beads then the mRNAs were eluted and fragmented at 940 °C. First-strand cDNA was generated by random priming reverse transcription and after second strand synthesis step, double-stranded cDNA was generated. After repairing ends, A-tailing and adapter ligation steps, adapter-ligated fragments were amplified in enrichment PCR and finally sequencing libraries were generated. Sequencing runs were executed on Illumina NextSeq500 instrument using single-end 75 cycles sequencing. After sequencing, the reads were aligned to the GRCh38 reference genome (with EnsEMBL 95 annotation) using STAR aligner (version 2.7.0a). FeatureCounts was used to quantify our reads to genes. Significantly

differentially expressed genes (DEGs) were defined based on adjusted p values < 0.05 and $\log^2$ fold change threshold > 0.85. Heatmap was generating by using GraphPad 8.0 and interactome map was constructed by using Gephi 9.0 based on interaction from STRING (https://string-db.org/).

6.12. Statistical analysis

The results are expressed as mean±SD. Normality of the data was tested by Kolmogorov-Smirnov test. The comparison between two treatments (comparing control versus treated group) was performed by paired t-test or unpaired t-test. The data were visualized and analyzed by using GraphPad Prism 8.0 (GraphPad Software, San Diego, CA, USA).

7. Results

7.1. Global transcriptome analysis in human SC and DN adipocytes

7.1.1. Molecular signature of human brown/beige adipocytes derived from deep neck tissue

Differentiated hASCs derived from SC and DN fat tissues (both ADIP and B-ADIP) and undifferentiated progenitors were cultivated and global transcriptomic analysis was performed to elucidate their molecular signature. We found 1049 genes which were differentially expressed in SC and DN adipocytes [Toth *et al*., 2020]. After 14 days differentiation, adipocytes markers such as GLUT-4 (encoded by *SLC2A4*), *PLIN1*, *ADIPOQ*, and *LEP* were induced and expressed at similar level in both ADIP and B-ADIP irrespective to anatomical origin (**Figure 11a**). Next, we investigated the expression pattern of classical brown and beige adipocytes. The expression of *ZIC1* was not induced by differentiation in either SC or DN derived adipocytes (**Figure 11b**). Other classical brown adipocyte markers such as *LHX8* and *EPSTI1* was expressed higher in DN derived ADIP and B-ADIP and their expression was already high in DN progenitors as compared to SC derived ones (**Figure 11b**). A selective marker for brown/beige preadipocyte *EBF2* [Wang *et al*., 2014], which regulate the brown/beige adipocyte identity, was expressed higher in DN as compared to SC preadipocytes and DN derived adipocytes, both ADIP and B-ADIP, maintained high expression of *EBF2* after differentiation (**Figure 11b**). DN derived adipocytes also expressed higher level of beige adipocyte marker *TBX1* as compared to SC ones (**Figure 11b**). The expression of UCP1 was induced after differentiation and DN derived adipocytes showed higher *UCP1* expression as compared to SC adipocytes irrespective to differentiation protocol (**Figure 11b**). DN derived adipocytes also expressed higher level of genes involved in UCP1-independent thermogenesis such as CKMT1a/b and PM20D1 (**Figure 11b**) [Kazak *et al*., 2015; Long *et al*., 2016]. In addition to higher expression of brown/beige adipocyte marker, DN derived adipocytes also possessed higher brown adipocyte content (BATLAS, [Perdikari *et al*., 2018]) and browning degree score (ProFAT, [Cheng *et al*., 2018]) as compared to SC derived ones (**Figure 11c-d**). DN B-ADIP showed the highest BATLAS and ProFAT scores (**Figure 11c-d**). Our data indicated that adipocytes derived from different anatomical origins possessed distinct molecular signature and DN derived adipocytes possessed classical brown and beige adipocyte identity. DN derived ADIP and B-ADIP had higher thermogenic capacity as compared to SC ones marked by higher expression level of thermogenic markers and both BATLAS and ProFAT scores.

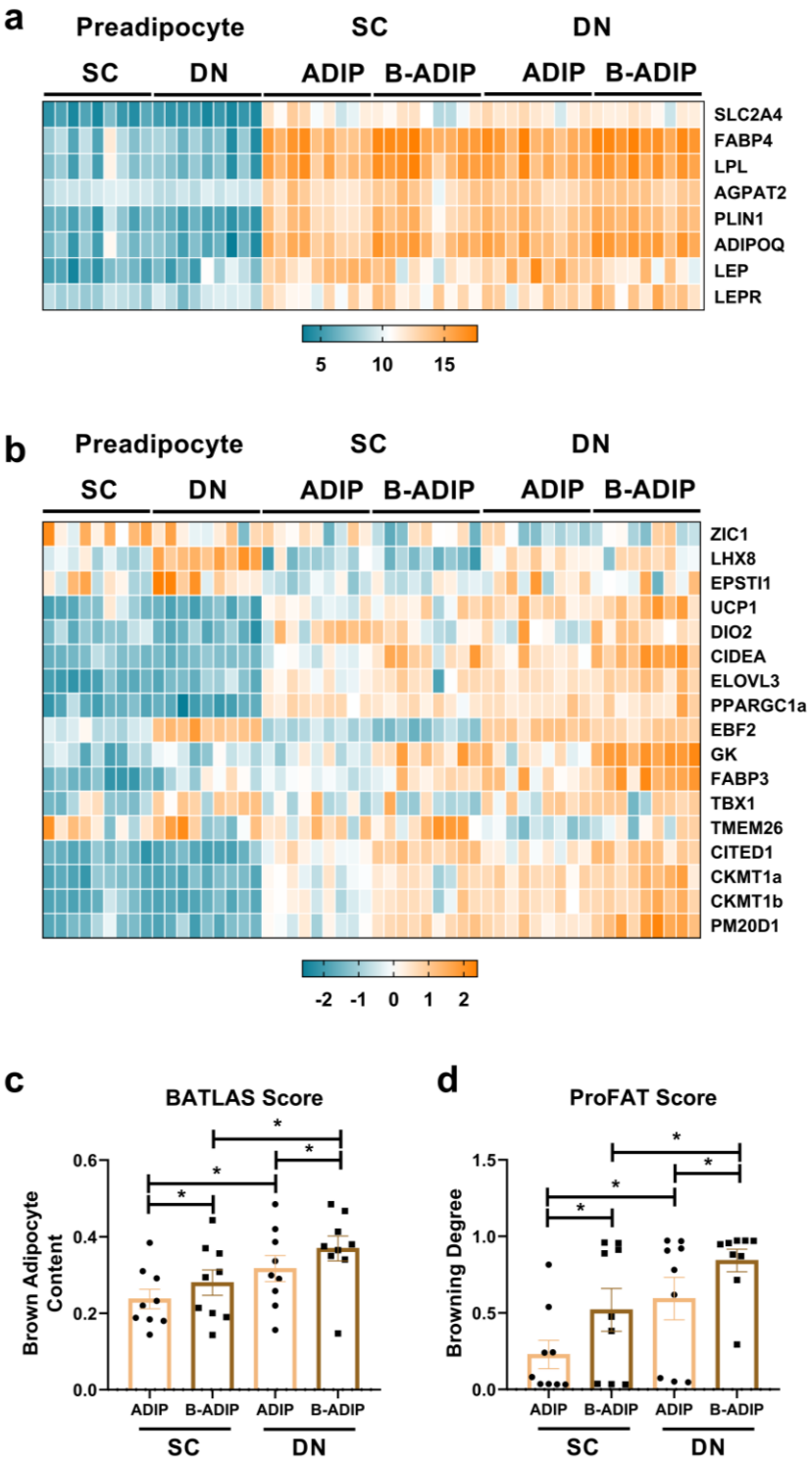

Figure 11. The molecular signature and browning capacity of human brown/beige adipocytes. *(a) Heatmap displaying the expression profiles of general adipocyte marker genes. (b) Heatmap displaying the expression profiles of brown/beige adipocytes. (c) Brown adipocyte content measures by BATLAS, n=9. (d) Browning degree measured by ProFAT, n=9. Statistical analysis by paired t-test. *p<0.05.*

7.1.2. Differential expression of SLC transporters

Active brown/beige adipocytes consume high amounts of cellular substrates including macro and micronutrients to provide sufficient fuel for heat generation. SLC transporters play a key role in mediating the uptake of substrates into active brown/beige adipocytes. Among the DEGs, we found 21 SLC transporters (**Figure 12a**) regulated by either the anatomical location (15 upregulated, 3 downregulated in DN versus SC ADIPs) or the applied differentiation protocol (3 upregulated in both SC and DN B-ADIPs).

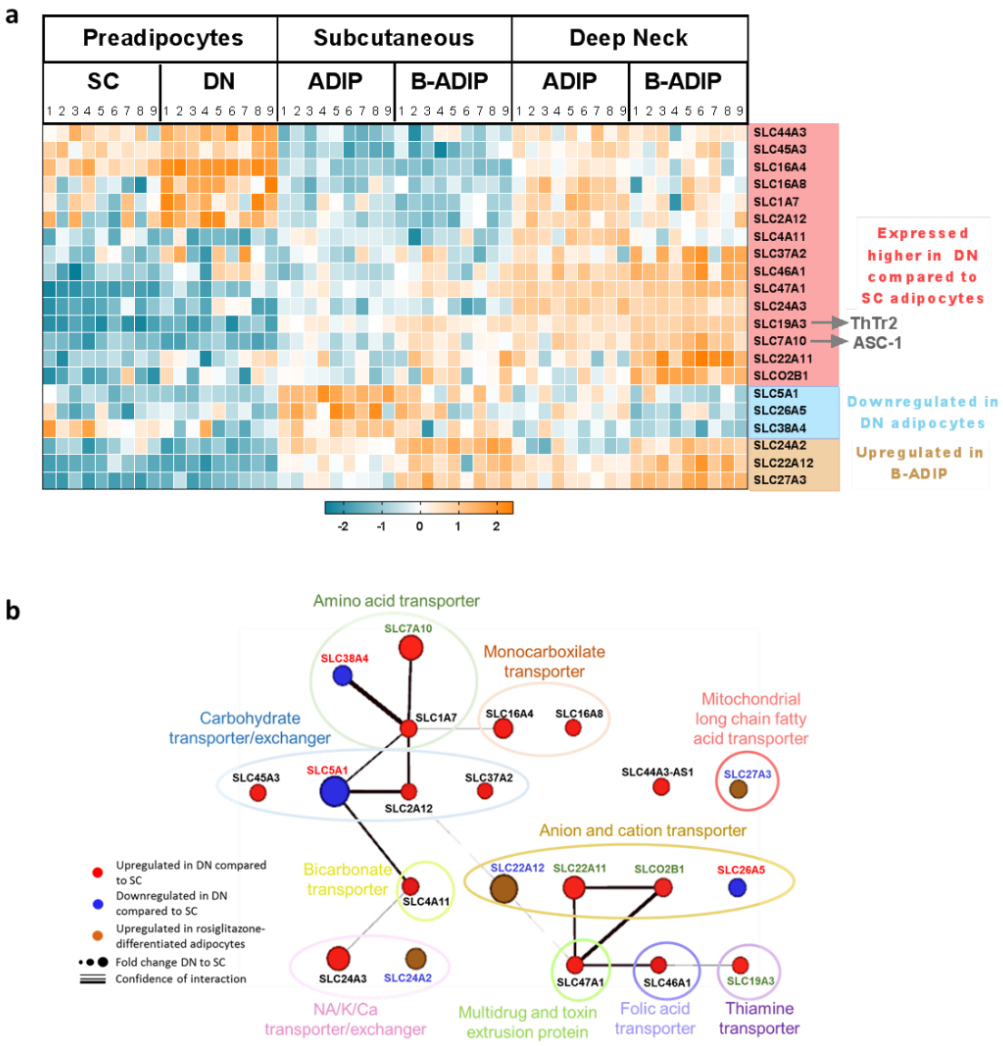

Figure 12. Heatmap displaying the expression profile (a) and interactome map of differentially expressed SLC transporter genes in human neck adipocytes. *Interactome map was generated by using Gephi 9.0.*

Among 21 SLC transporters, long chain fatty acid transporter encoded by *SLC27A3* is the only transporter localized in mitochondrial membrane, whereas other 20 SLC transporters are cell membrane transporters. SLC transporters are involved in various biological processes mediating the uptake of carbohydrate (*SLC45A3, SLC2A12, and SLC37A2*), amino acid (*SLC7A10* and *SLC1A7*), fatty acid (*SLC27A3*), cations/anions (*SLC22A11, SLC22A12,* and *SLCO2B1*), vitamins (*SLC19A3* and *SLC4A1*), monocarboxylate (*SLC16A4* and *SLC16A8*), bicarbonate (*SLC4A11*) and $Na^+/K^+/Ca^{2+}$ (*SLC24A2* and *SLC24A3*) (**Figure 12b**). The role of these transporters in nutrient uptake in human adipocytes derived from neck tissues have not been explored so far. In the following chapters, the potential role of neutral amino acids transporter (*SLC7A10*) and thiamine transporter (*SLC19A3*) in human primary adipocytes during thermogenic activation by cAMP is investigated in more details.

7.2. The importance of ASC-1 in efficient thermogenesis of human neck-derived adipocytes

7.2.1. ASC-1 expression pattern

In an attempt to explore potential thermogenic regulators, we found that major player of thermogenesis, *UCP1*, and other brown/beige marker genes were clustered with *SLC7A10* that encodes ASC-1. Our RNA-Seq data showed that DN derived adipocytes expressed higher level of *SLC7A10* as compared to SC derived adipocytes irrespective to differentiation protocols (**Figure 13a**). The expression pattern of *SLC7A10* was similar like *UCP1* expression pattern and we could validate our RNA-Seq data by RT-qPCR using independent donors (**Figure 13b**). We observed that the expression of *ASC-1* was low in both SC and DN progenitors and was induced during differentiation in parallel with *UCP1* expression levels (**Figure 13b-c**). We did not notice any different level of ASC-1 expression between two anatomical origins at protein level, but the expression of UCP1 was higher in DN as compared to SC adipocytes irrespective to differentiation protocols (**Figure 13c**).

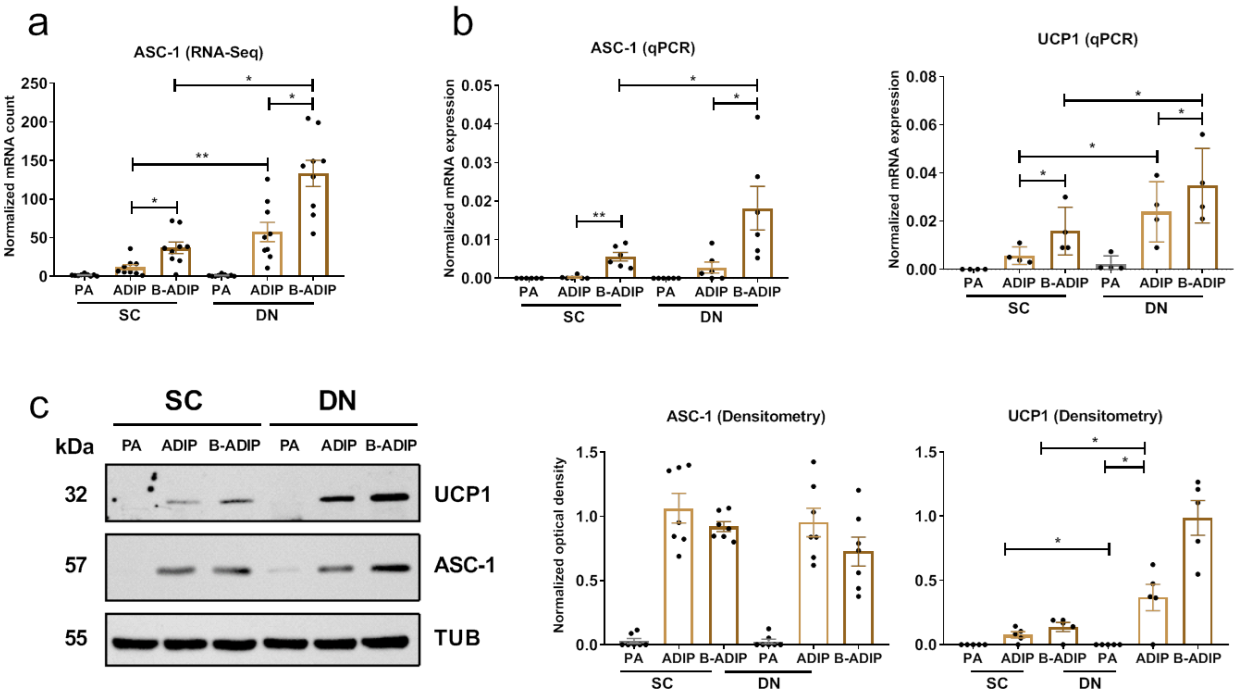

Figure 13. mRNA and protein expression of ASC-1 in human neck derived adipocytes. *(a) ASC-1 mRNA expression determined by RNA-seq, n=9 for all groups. Statistical analysis was performed by one-way ANOVA. (b) mRNA expression of ASC-1 and UCP1 detected by RT-qPCR, n=6 for all groups. (c) Detection and quantification of ASC-1 and UCP1 by immunoblotting and densitometry, n=7 for all groups. PA: preadipocytes, ADIP: adipocytes, B-ADIP: brown adipocytes. Statistical analysis was performed by paired t-test, *p<0.05, **p<0.01.*

7.2.2. Facilitated serine, cysteine, and glycine uptake by DN adipocytes is hampered by ASC-1 inhibitor during thermogenic activation

To understand the functional importance of ASC-1 in human adipocytes, we measured the consumption of ASC-1 cargos including alanine, serine, cysteine, glycine, threonine, and glutamate by DN ADIPs and B-ADIPs upon thermogenic activation by cAMP for 10 h. We observed that serine, cysteine, glycine, and threonine were consumed at basal rate into unstimulated DN ADIPs and B-ADIPs (**Figure 14**). DN ADIPs consumed significantly higher amount of serine and cysteine as compared to B-ADIPs (**Figure 14**). Thermogenic activation by cAMP resulted in higher uptake of these amino acids in DN ADIPs and B-ADIPS and the uptake was hindered in the presence of specific noncompetitive ASC-1 inhibitor, BMS-466442 (**Figure 14**). Intriguingly, alanine consumption into DN ADIPs was low and B-ADIPs even released alanine both in unstimulated and cAMP-stimulated conditions (**Figure 14**). Alanine release may indicate that B-ADIPs catabolize amino acids to provide sufficient fuels for TCA cycle and to

convert nitrogen to pyruvate forming alanine as part of a possible glucose-alanine cycle *in vivo* [Felig, 1973]. ASC-1 preferentially facilitates the transport of neutral amino acids in an exchange mode, therefore, alanine release may allow the uptake of more cysteine, serine, and glycine. We also observed that DN ADIPs and B-ADIPs transported a significant amount of glutamate out and even higher amount of glutamate was released during thermogenic activation (**Figure 14**). These data suggested that active DN adipocytes consume higher amount of serine, cysteine, and glycine and ASC-1 mediates these amino acids uptake.

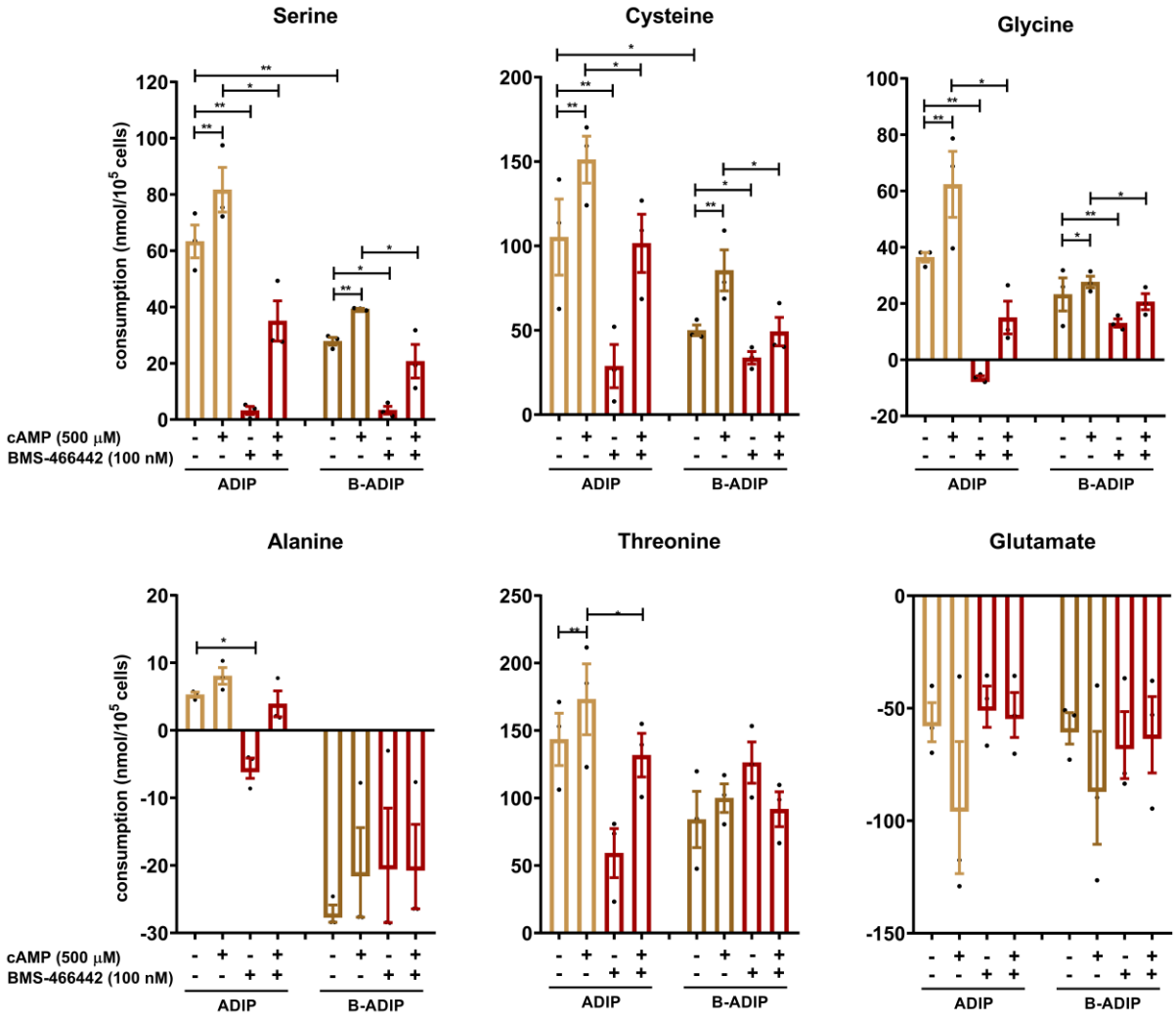

Figure 14. Effect of thermogenic induction and ASC-1 inhibitor (BMS-466442) treatment for 10 h on Serine, Cysteine, Glycine, Alanine, Threonine, and Glutamate consumption by human DN-derived adipocytes. *ADIP: adipocytes, B-ADIP: brown adipocytes. n=3 for al groups. Statistical analysis was performed by paired t-test, *p<0.05, **p<0.01.*

7.2.3. Inhibition of ASC-1 by its pharmacological inhibitor hampers UCP1-dependent and UCP1-independent oxygen consumption upon thermogenic activation

Next, we investigated the significance of ASC-1 in thermogenic activation of human adipocytes by measuring the OCR and observing the effect of ASC-1 inhibition by BMS-466442 during adrenergic stimulation. As expected, cAMP stimulation immediately elevated the OCR in ADIPs and B-ADIPS originated from both SC and DN (**Figure 15a-b**). The respiratory response of B-ADIPs was higher than ADIPs, both in SC and DN, and this observations was in line with higher expression of *UCP1* and other thermogenic markers [Toth *et al*., 2020]. In addition, DN derived adipocytes showed higher OCR as compared to SC ones (comparing **Figure 15a to Figure 15b**) supporting the previous data describing a higher thermogenic capacity of DN adipocytes (**Figure 11**). In unstimulated condition, the ASC-1 inhibitor significantly hampered cAMP-stimulated oxygen consumption of both SC and DN adipocytes (**Figure 15a-b**). ASC-1 blocking did not affect the oxygen consumption rate of resting SC and DN ADIPs and B-ADIPs (**Figure 15a-b**) despite the reduced uptake of ASC-1 cargos in unstimulated adipocytes (**Figure 14**) indicating that the ASC-1 contributes to cell respiration during thermogenic activation.

To investigate the effect of ASC-1 inhibition on UCP1-dependent portion of cellular respiration, oligomycin (ATP synthase blocker) was administered to the cells allowing us to estimate UCP1-dependent proton leak. We observed a decrease in UCP1-dependent proton leak of cAMP-stimulated SC and DN adipocytes (**Figure 15a-b**) indicating a significant influence of ASC-1 facilitated transport on mitochondrial proton gradient generation and its uncoupling. Contribution of a UCP1-independent respiration via creatine futile cycle to the cAMP-stimulated respiration was measured upon the injection of creatine analogue, β-GPA [Kazak *et al*., 2015]. B-GPA-inhibited portion of respiration was increased following cAMP stimulation and was abrogated by ASC-1 inhibitor in ADIPs and B-ADIPs irrespective to anatomical origins (**Figure 14a-b**). Non-mitochondrial respiration (**Figure 15a-b**), basal, and maximal ECAR (**Figure 16a-b**) were not affected by ASC-1 inhibitor. Our data pointed to the significance of ASC-1 in facilitating the uptake of amino acids needed for efficient thermogenic activation in human SC and DN derived adipocytes.

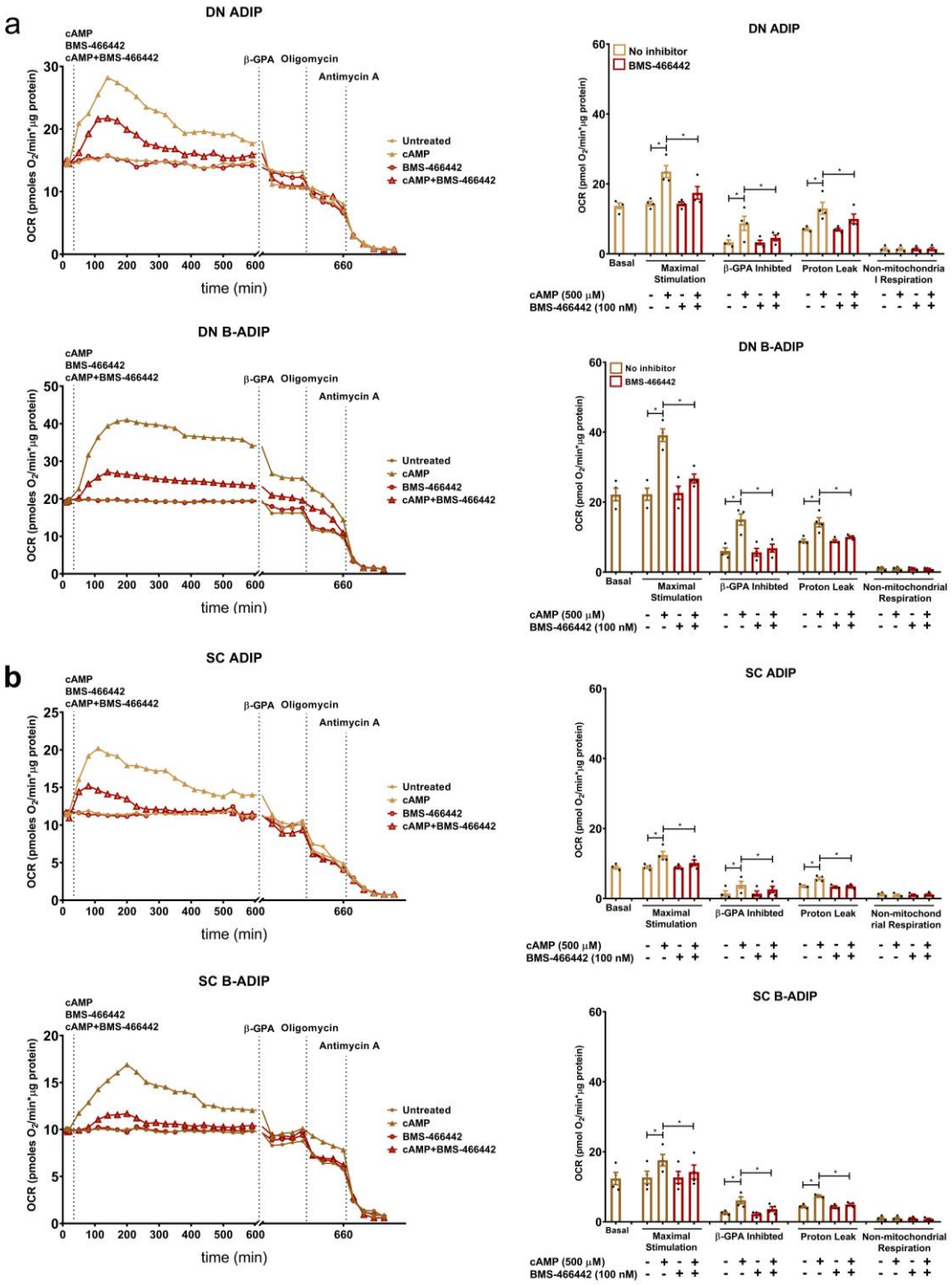

Figure 15. Effect of ASC-1 inhibitor on oxygen consumption rate of DN and SC derived adipocytes upon thermogenic activation. *(a-b) OCR of DN (a) and SC (b) adipocytes was detected for 10 h following cAMP stimulation without and with ASC-1 inhibition; representative curves of four measurements (left panels). OCR at basal, maximal stimulation, after b-GPA inhibition, oligomycin, and antimycin A addition (right panels) was quantified in adipocytes derived from four independent donors. n=4 for all groups. ADIP: adipocytes, B-ADIP: brown adipocytes. n=3 for all groups. Statistical analysis was performed by paired t-test, *p<0.05, **p<0.01.*

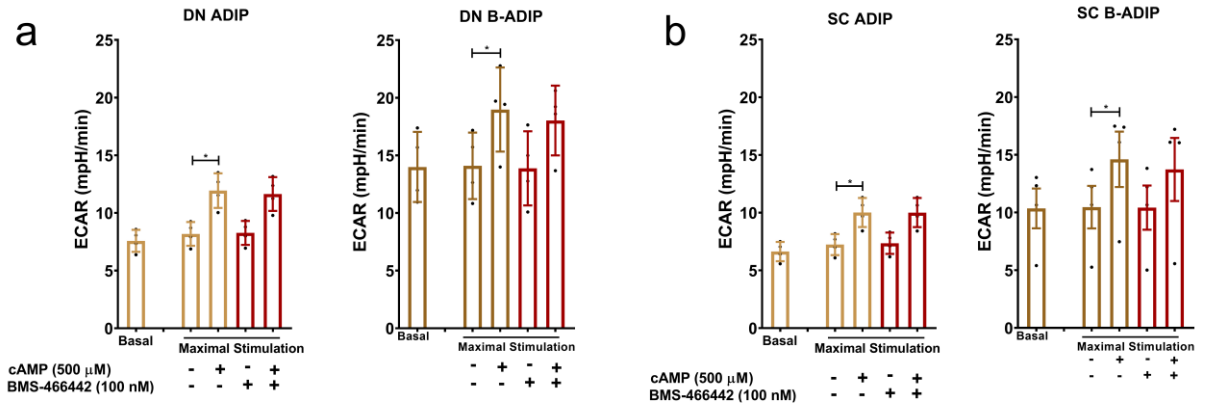

Figure 16. Effect of ASC-1 inhibitor on extracellular acidification rate of DN and SC derived adipocytes upon thermogenic activation. *ECARs of DN (a) and SC (b) adipocytes at basal and maximal stimulation; n=4 for all groups. ADIP: adipocytes, B-ADIP: brown adipocytes. n=3 for all groups. Statistical analysis was performed by paired t-test, *p<0.05, **p<0.01.*

7.2.4. cAMP-stimulated increase of browning markers and mitochondrial complex subunits expression are hindered by ASC-1 inhibitor

Observing the effect of ASC-1 inhibition on the respiration of stimulated adipocytes, we presumed that cAMP-induced expression of thermogenic genes was also influenced. DN derived adipocytes had the tendency to have a higher expression of PGC1a, CKMT2, and UCP1 as compared to SC ones (**Figure 17**). As expected, cAMP increased the expression of those genes in ADIPs and B-ADIPs irrespective to anatomical origins (**Figure 17**). Inhibition of ASC-1 led to decrease cAMP-dependent upregulation of PGC1a, CKMT2, and UCP1 at both mRNA and protein levels (**Figure 17**).

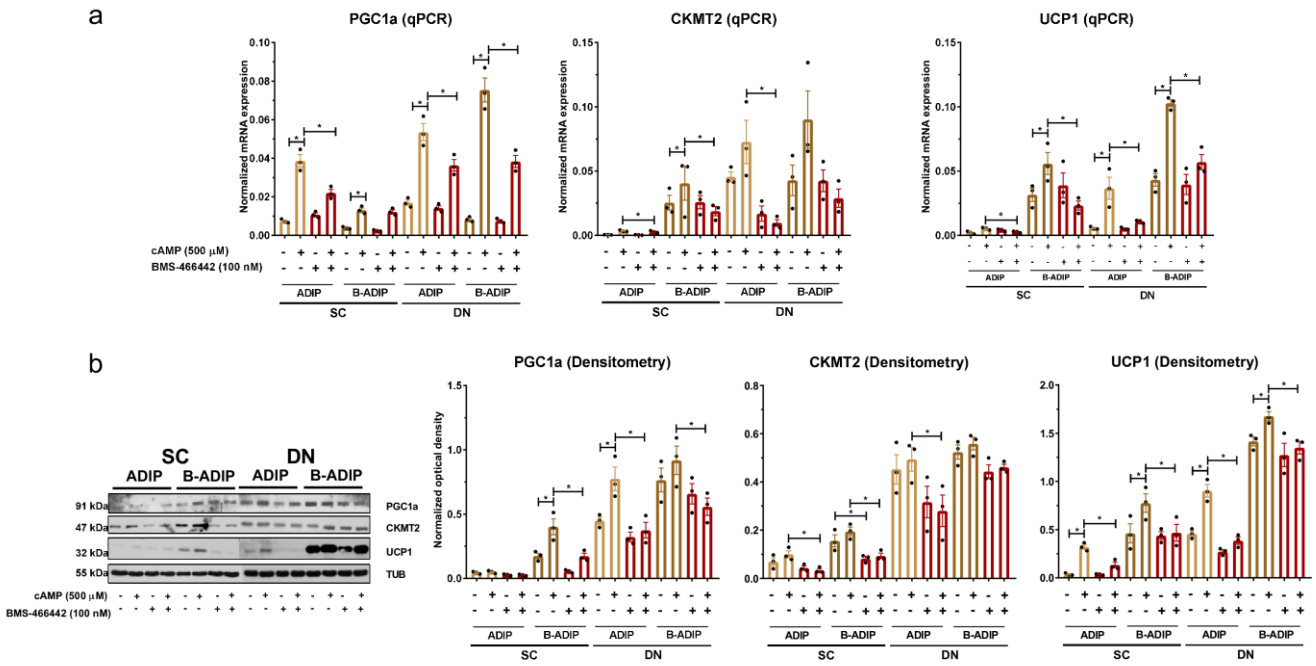

Figure 17. Effect of ASC-1 transporter inhibition on the expression of thermogenic markers in human neck-derived adipocytes. *mRNA (a) and protein (b) expression of PGC1a, CKMT2, and UCP1 detected by RT-qPCR and immunoblotting in human SC and DN adipocytes. n=3 for all groups. ADIP: adipocytes, B-ADIP: brown adipocytes. Statistical analysis was performed by paired t-test. *p<0.05, **p<0.01.*

We also investigated the effect of ASC-1 transporter inhibition on the mRNA expression of other brown/beige adipocyte markers as (**Table 1**) in SC and DN derived adipocytes. cAMP elevated the mRNA expression of *CKMT1a/b*, *PM20D1*, *ELOVL3*, *DIO2*, and *CITED1* which was hindered by ASC-1 inhibition (**Figure 18a-e**). The cAMP-induced elevation of *TBX1* expression, which was halted by ASC-1 inhibitor, was observed only in DN ADIPs (**Figure 18f**). Our data suggested that cAMP-induced upregulation of thermogenic genes in human neck derived adipocytes requires ASC-1 facilitated transport of serine, cysteine, and glycine.

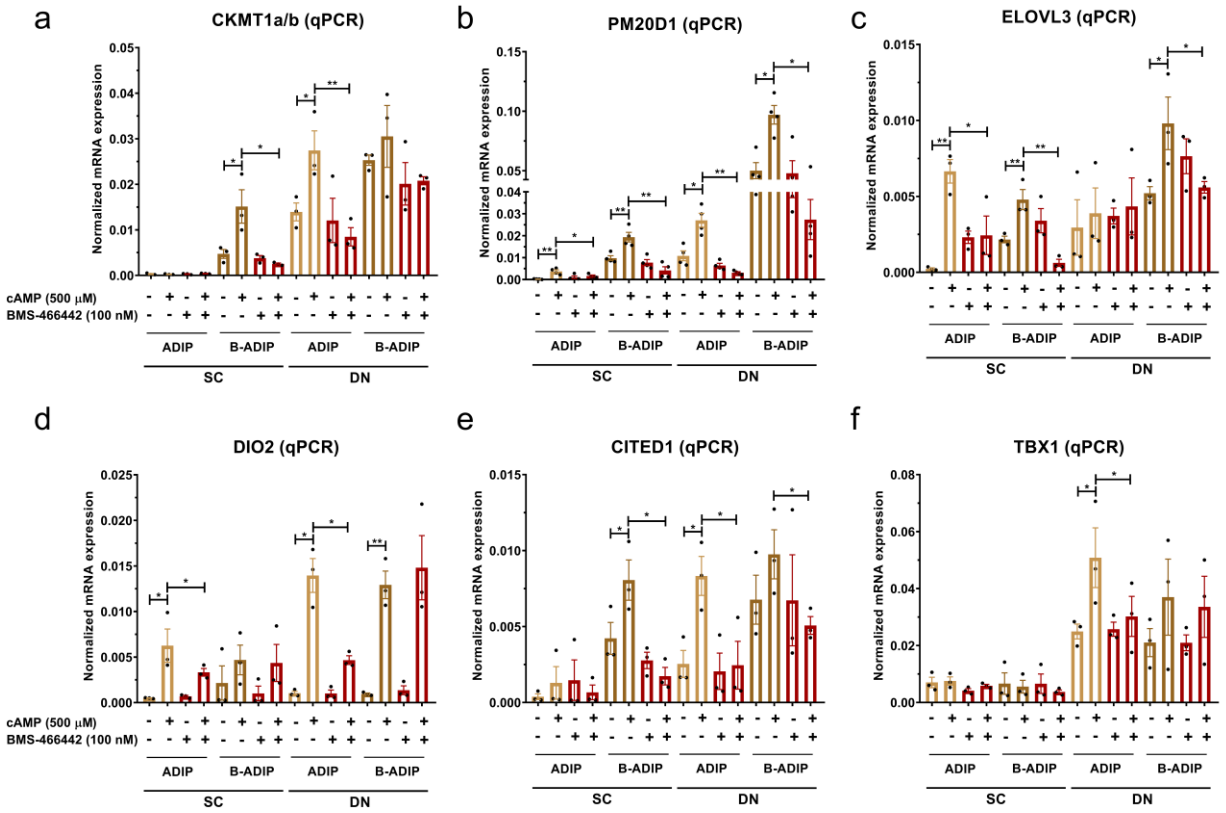

Figure 18. Effect of ASC-1 transporter inhibition on the mRNA expression of CKMT1a/b *(a), PM20D1 (b), ELOVL3 (c), DIO2 (d), CITED1 (e), and TBX1 (f) detected by RT-qPCR. n=3 for all groups. ADIP: adipocytes, B-ADIP: brown adipocytes. Statistical analysis was performed by paired t-test. *p<0.05, **p<0.01*

In addition to thermogenic markers, we also investigated the influence of ASC-1 inhibitor on the protein expression of mitochondrial complex subunits. Thermogenic activation by cAMP elevated the expression of complex I and II subunits in DN ADIPs (**Figure 19a-c**). We could not observe the cAMP-dependent upregulation in B-ADIPs since the basal expression of those complexes were already high. The cAMP-dependent upregulation of complex I, II, and IV was abrogated by ASC-1 inhibitor (**Figure 19a-c, e**). The expression of complex III and V was not influenced either by cAMP or ASC-1 inhibitor (**Figure 19d, f**). Although it was not significant, we observed that SC ADIPs had lower expression of complex V (**Figure 19f**).

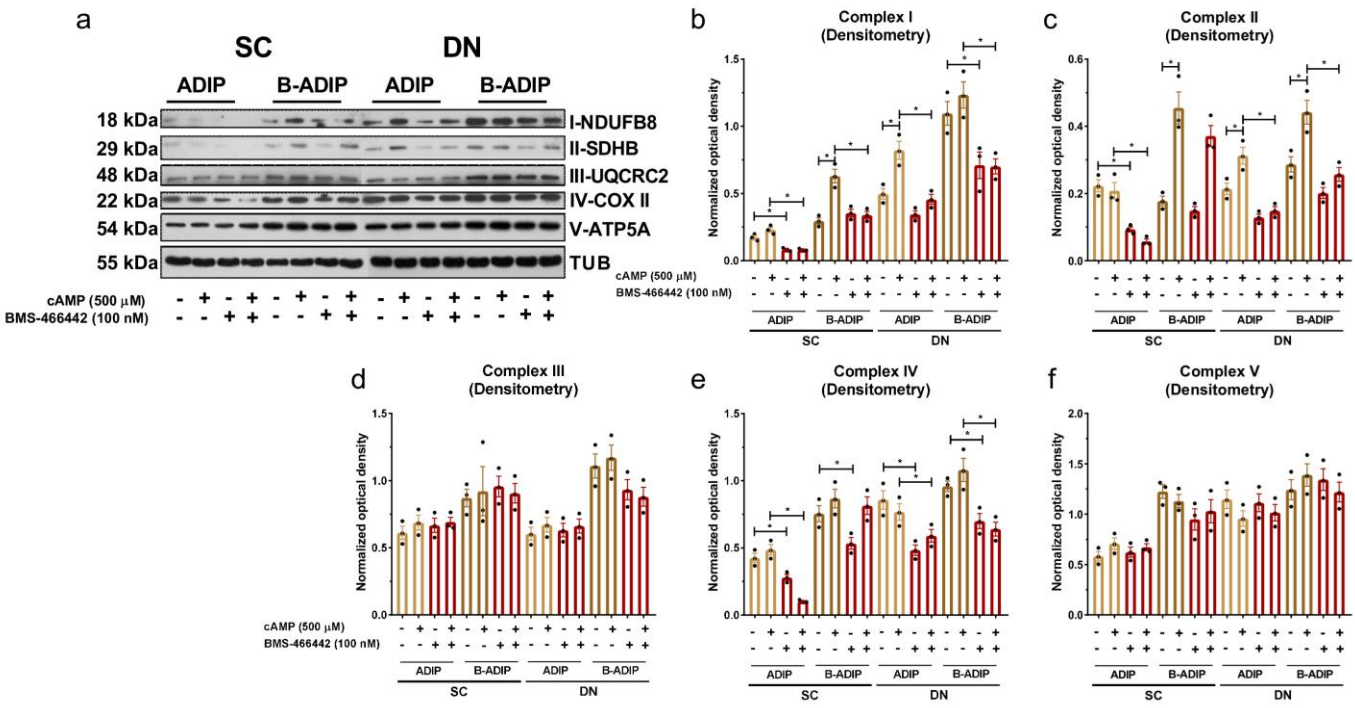

Figure 19. Effect of ASC-1 inhibitor on the expression of mitochondrial complex subunits in SC and DN derived adipocytes. *(a) Expression of mitochondrial complex subunits detected by immunoblotting. (b-f) Densitometry analysis of complex I-V immunoblotting. n=3 for all groups. ADIP: adipocytes, B-ADIP: brown adipocytes. Statistical analysis was performed by paired t-test. *p<0.05*

7.3. The significance of abundant thiamine and its transporters in efficient thermogenesis of human neck-derived adipocytes

7.3.1. UCP1 containing DN derived adipocytes expressed a high level of thiamine transporter 2

In a previous chapter, it has been shown that besides expressing higher brown/beige adipocytes markers, DN derived adipocytes also possessed higher brown adipocyte content and browning degree score quantified by BATLAS and ProFAT webtools [Perdikari *et al.*, 2020; Cheng *et al.*, 2018]. Among the 21 SLC transporters which were differentially expressed in SC and DN adipocytes, we found that the expression of ThTr2 (encoded by *SLC19A3*) was very low in preadipocytes and was robustly induced during differentiation (**Figure 20a**). ThTr2 expression was influenced by anatomical origins (higher in DN as compared to SC derived adipocytes) and differentiation protocols (higher in B-ADIPs as compared to ADIPs) and RT-qPCR analysis using independent donors could validate the RNA-Seq data (**Figure 20a**). Protein expression pattern of ThTr2 detected by immunoblotting were similar to the UCP1 indicating that ThTr2

was more expressed in high UCP1 containing DN derived adipocytes (**Figure 20b**). ThTr1, encoded by *SLC19A2*, possessed lower expression and was not differently expressed between SC and DN derived adipocytes (**Figure 20b-c**).

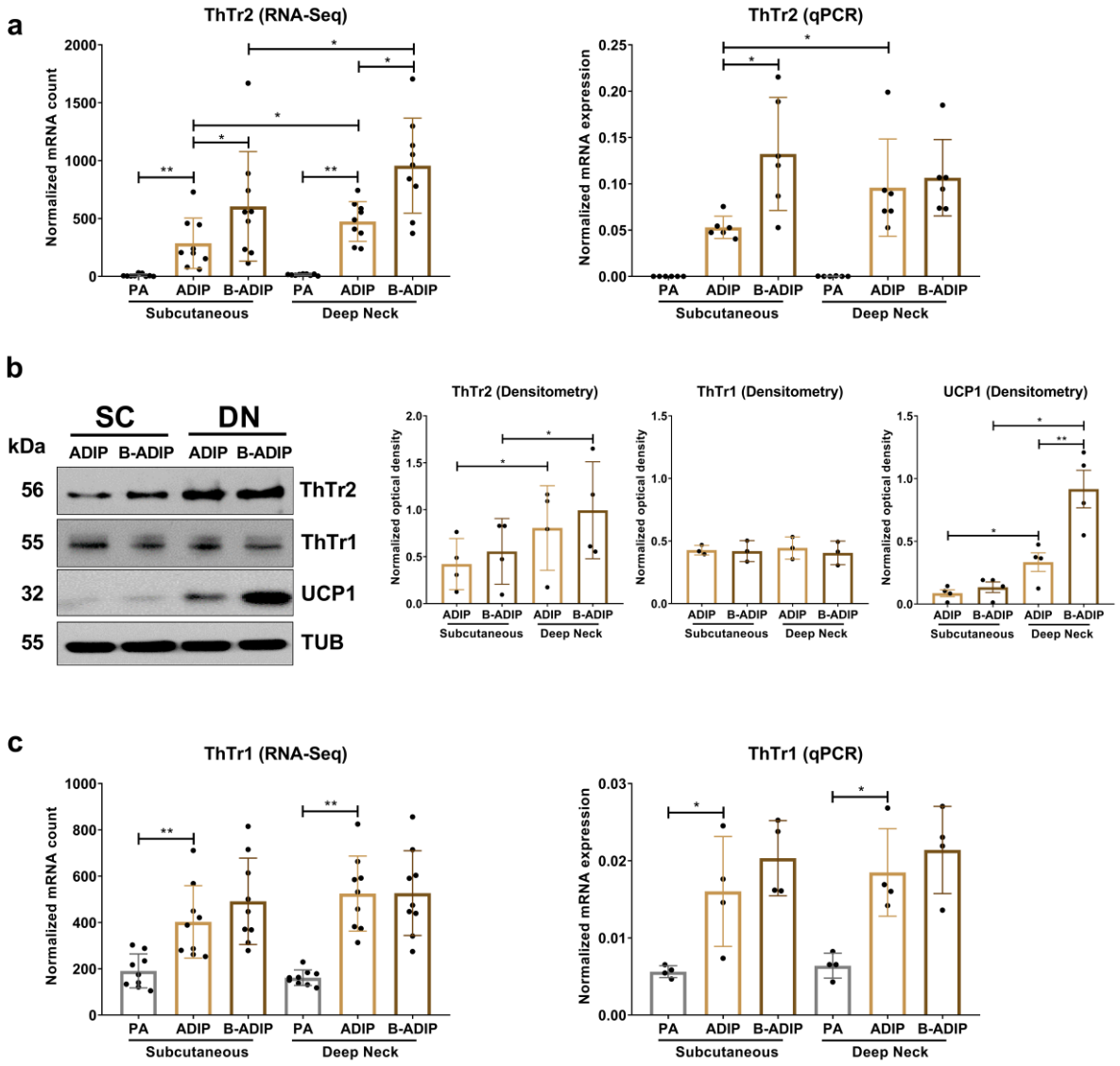

Figure 20. Expression pattern of thiamine transporters in SC and DN derived adipocytes. *(a) mRNA expression of ThTr2 based on RNA-Seq data (n=9) and detected by RT-qPCR (n=6). (b) Detection by immunoblotting and quantification of ThTr2, ThTr1, and UCP1 protein expression, n=4 or 3 (for ThTr1). (d) mRNA expression of ThTr2 based on RNA-Seq data (n=9) and detected by RT-qPCR (n=4). PA: preadipocytes, ADIP: adipocytes, B-ADIP: brown adipocytes. Statistical analysis was performed by unpaired t-test, *p<0.05, **p<0.01 or GLM (for RNA-Seq analysis).*

The expression of thiamine transporters was also checked in publicly accessible transcriptomic data set of adipocytes derived from human SC WAT (Min *et al*., 2019). ThTr2 expression was induced by differentiation and further elevated by adrenergic stimulation/forskolin (**Figure 21a**) while the expression of ThTr1 was not affected by either (**Figure 21b**). In a thermogenic adipocytes cluster [Min *et al*., 2019], adrenergic stimulation increased the mRNA expression of both ThTrs (**Figure 21c-d**). An RNA-Seq-based screening identified ThTr2 as adipose tissue-specific; its abundant expression in adipose tissue strongly correlated with the expression of mitochondrial genes suggesting a possible association between the expression of ThTr2 and brown/beige adipocytes (Pereira *et al*., 2021). Analysis of RNA-Seq data of Perdikari *et al*. (2018) reveals that ThTr2 expression is higher than ThTr1 expression (estimated by mRNA counts) in both human WAT and BAT obtained by needle biopsies from the neck area (**Figure 21e, f**). The TPP transporter that facilitates the transport to mitochondria (TPC), encoded by *SLC25A19*, is expressed higher in BAT as compared to WAT (**Figure 21g**). These data along with our observations (**Figure 1**) suggested that ThTr2 and thiamine might have a role in regulation of adipocyte thermogenesis.

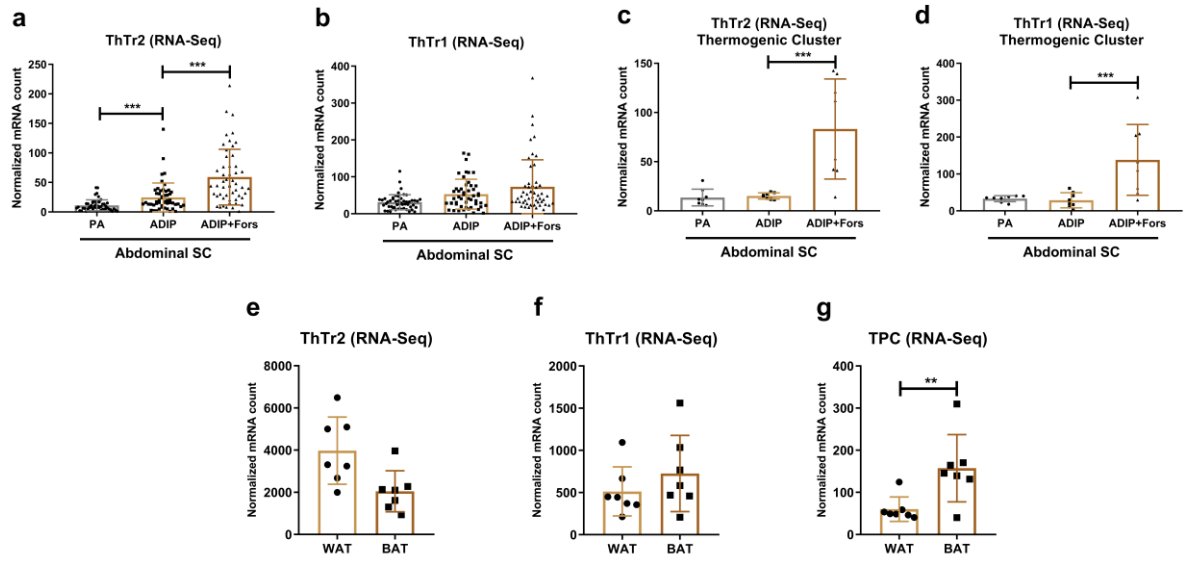

Figure 21. The expression of thiamine transporters in human abdominal subcutaneous adipocytes and neck tissue. *(a-d) Normalized mRNA counts of ThTr2 and ThTr1 of human abdominal SC derived adipocytes (n=52) and their thermogenic cluster (n=8). Based on available RNA-Seq data (www.ncbi.nlm.nih.gov/geo, accession number GSE134570) [Min et al., 2019]. (e-g) Normalized mRNA counts of ThTr2, ThTr1, and the mitochondrial TPP transporter (TPC) of human white and brown adipose tissue (WAT and BAT) obtained by needle biopsies. Based on available RNA-Seq data retrieved from the European Nucleotide Archive, accession number PRJEB20634 [Perdikari et al., 2018]. n=7. Statistical analysis of FASTQ files aligned to BAM were performed by DESeq2. **p<0.01, ***p<0.0001.*

7.3.2. Inhibition of ThTr2 hampered UCP1-dependent proton leak respiration

To investigate the importance of ThTr2 during thermogenic activation by cAMP in DN and SC derived adipocytes, we treated differentiated adipocytes with dibutyryl-cAMP (which mimics adrenergic stimulation *in vivo*) in the presence of a potent ThTr2 inhibitor, fedratinib [Zhang *et al*., 2014] and measured OCR in a regularly used culture medium which contains thiamine at 8.2 µM concentration. As anticipated, OCR was elevated immediately upon cAMP administration to DN derived ADIP while the response of SC derived ADIP was moderate (**Figure 22**). Fedratinib hindered the cAMP-stimulated elevation of OCR of ADIPs derived from both DN (**Figure 22a**, left and middle panels) and SC depots (**Figure 22b**, left and middle panels) during the 10 hours monitoring. Proton leak respiration that mainly correlates with UCP1-dependent heat generation was calculated upon the injection of oligomycin (ATP synthase blocker). We found that cAMP-stimulated proton leak respiration was reduced by fedratinib in both DN (**Figure 22a**, left and middle panels) and SC (**Figure 22b**, left and middle panels) ADIPs.

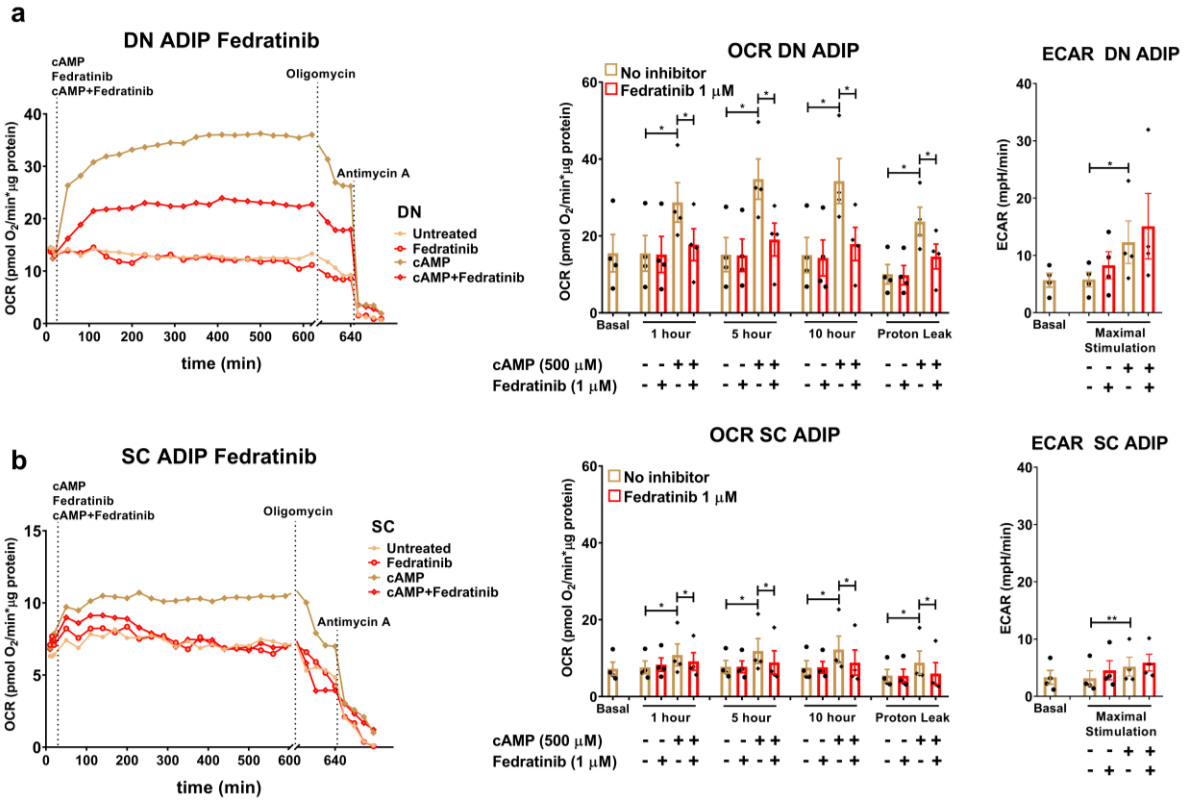

Figure 22. Effect of thiamine transporter 2 potent inhibitor (fedratinib) on the cAMP-induced oxygen consumption (OCR) and extracellular acidification (ECAR) rates in human deep neck (DN) and subcutaneous (SC) derived adipocytes. *SC and DN-derived preadipocytes were differentiated into ADIP, then OCRs were detected for 10 hours following the injection of dibutyryl-cAMP in the presence or*

*absence of fedratinib. Left panels show representative curves of 4 measurements. OCR at basal, 1, 5, and 10h post-injection, and after oligomycin addition (middle panels), and ECAR (right panels) were quantified in adipocytes derived from four independent donors. Statistical analysis was performed by unpaired t-test, *p<0.05, **p<0.01.*

Fedratinib can also inhibit tyrosine kinases including JAK2 [Zhang *et al*., 2014] and although tyrosine kinases are not known to be involved in adrenergic signaling of cultured adipocytes, we found it necessary to investigate the effect of other thiamine transporters inhibitor. We used thiamine analogue amprolium that inhibits the thiamine transport activity of both ThTr2 and ThTr1, with IC_{50} 0.620±0.27 and 2.60±0.93 µM, respectively (Giacomini *et al*, 2017). Amprolium was also effective in significantly decreasing cAMP-stimulated maximal and proton leak respiration in both DN (**Figure 23a**, left and middle panels) and SC (**Figure 23b**, left and middle panels) derived ADIPs. cAMP-stimulated ECAR was not affected by the inhibition of ThTr2 by fedratinib in the adipocytes (**Figure 22a-b**, right panels) whereas amprolium treatment resulted in its decrease (**Figure 23a-b**, right panels) in DN ADIP.

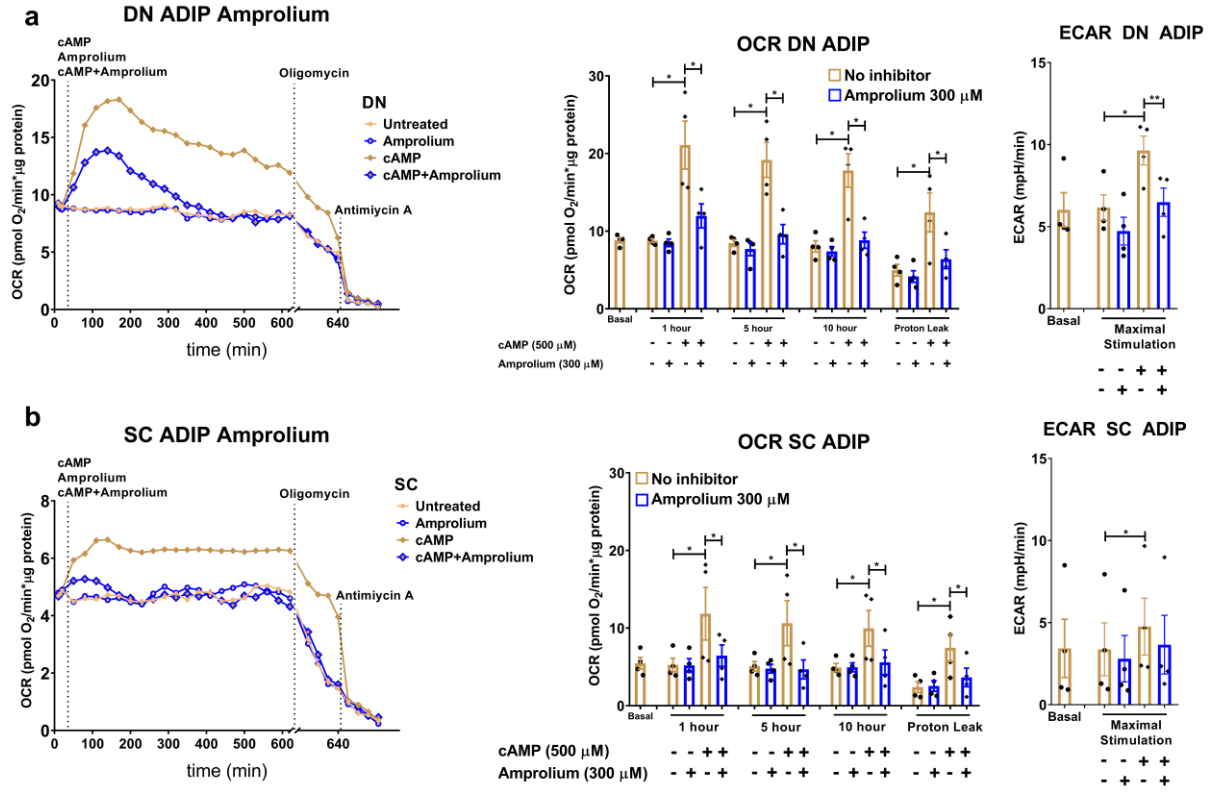

Figure 23. Effect of thiamine transporters potent inhibitor (amprolium) on the cAMP-induced oxygen consumption (OCR) and extracellular acidification (ECAR) rates in human deep neck (DN) and subcutaneous (SC) derived adipocytes*. SC and DN-derived preadipocytes were differentiated into ADIP,*

*then OCRs were detected for 10 hours following the injection of dibutyryl-cAMP in the presence or absence amprolium. Left panels show representative curves of 4 measurements. OCR at basal, 1, 5, and 10h post-injection, and after oligomycin addition (middle panels), and ECAR (right panels) were quantified in adipocytes derived from four independent donors. Statistical analysis was performed by unpaired t-test, *p<0.05, **p<0.01.*

We also investigated the effect of oxythiamine that competitively inhibit thiamine transport and thiamine pyrophosphokinase, restricting the level of TPP. Oxythiamine is pyrophosphorylated to oxythiamine-TPP which compete with the coenzyme function of TPP [Bunik *et al*., 2013]. Oxythiamine 300 µM decreased maximal respiration at 5 and 10 hours after its injection but did not affect proton leak respiration which was monitored upon oligomycin injection (data are not shown). It has been reported that oxythiamine does not inhibit ThTrs as efficiently as fedratinib or amprolium [Giacomini *et al*., 2017] suggesting that high thiamine uptake could still occur in the adipocytes upon oxythiamine treatment. This may explain why proton leak respiration was not influenced by oxthiamine at the applied concentration.

This inhibitory effect of fedratinib was also observed in DN and SC adipocytes with more pronounced browning (B-ADIPs) resulted from their differentiation with constant PPARγ stimulation by rosiglitazone (**Figure 24a-b**, left and middle panels). cAMP elevated the OCR in both DN and SC B-ADIPs which was abrogated by fedratinib (**Figure 24a-b**, left and middle panels). Fedratinib did not influence the ECAR of either DN or SC B-ADIPs (**Figure 24a-b**, right panel). The inhibitory effect of fedratinib and amprolium on OCR and proton leak respiration clearly show that continuous supply of thiamine through its transporters is needed for efficient thermogenic response of adipocytes.

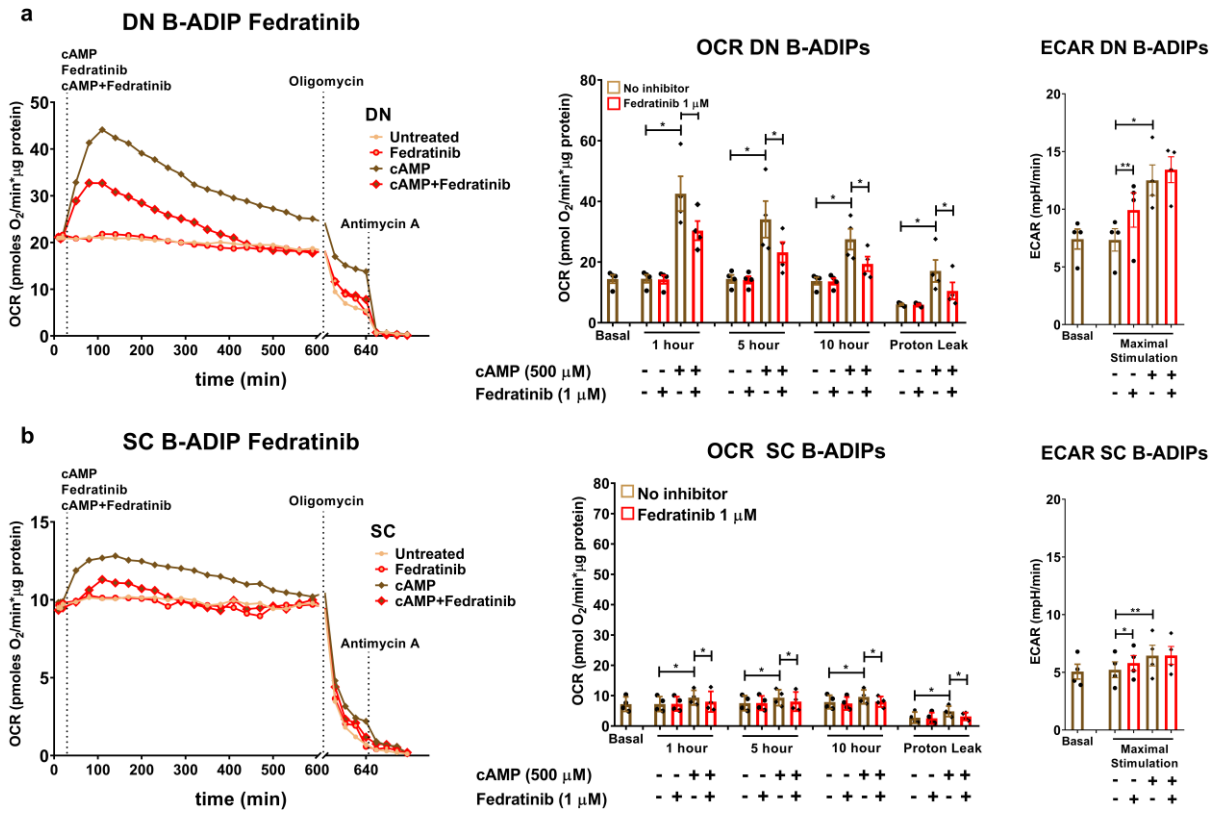

Figure 24. Effect of thiamine transporter 2-specific inhibitor (fedratinib) on oxygen consumption (OCR) and extracellular acidification (ECAR) rates in brown differentiated (B-ADIP) deep neck (DN) and subcutaneous (SC) derived adipocytes. *SC and DN progenitors were differentiated into brown adipocytes (B-ADIP) under long-term rosiglitazone treatment. After differentiation, adipocytes were treated with cAMP in the presence or absence of fedratinib. OCR in DN (a) and SC (b) B-ADIPs was detected for 10 hours; representative curves of four measurements (left panels). OCR at basal, maximal stimulation, and after oligomycin addition (middle panels) and ECAR (right panels) were quantified in adipocytes derived from four independent donors. Statistical analysis was performed by unpaired t-test, *p<0.05, **p<0.01.*

7.3.3. Thiamine enhances thermogenic activation in DN and SC-derived adipocytes in a concentration-dependent manner

We went further to investigate the significance of thiamine availability during thermogenic activation of adipocytes using a thiamine free culture medium and co-injection of cAMP with gradually increasing concentrations of thiamine (**Figure 25a**). In the absence of thiamine, as compared to 8.2 µM concentration present in regular culture medium, cAMP-stimulated OCR to maximal respiration rate was lower in both DN and SC ADIPs (comparing data on **Figure 25a** to **Figure 22 and 23**). cAMP-stimulated maximal respiration was increased already after addition of thiamine at 40 nM concentration (mild increase but significant) and elevated further at rising concentrations up to 25 µM (**Figure 25a**). To elucidate the effect of

increasing thiamine concentration on UCP1-dependent portion of cellular respiration, we calculated the OCR recorded following oligomycin administration and found that increasing thiamine concentration led to a higher proton leak respiration which could be observed already at the lowest used thiamine concentration, 40 nM (**Figure 25a**). These results demonstrates that abundant thiamine availability have a critical importance during thermogenic activation of human adipocytes.

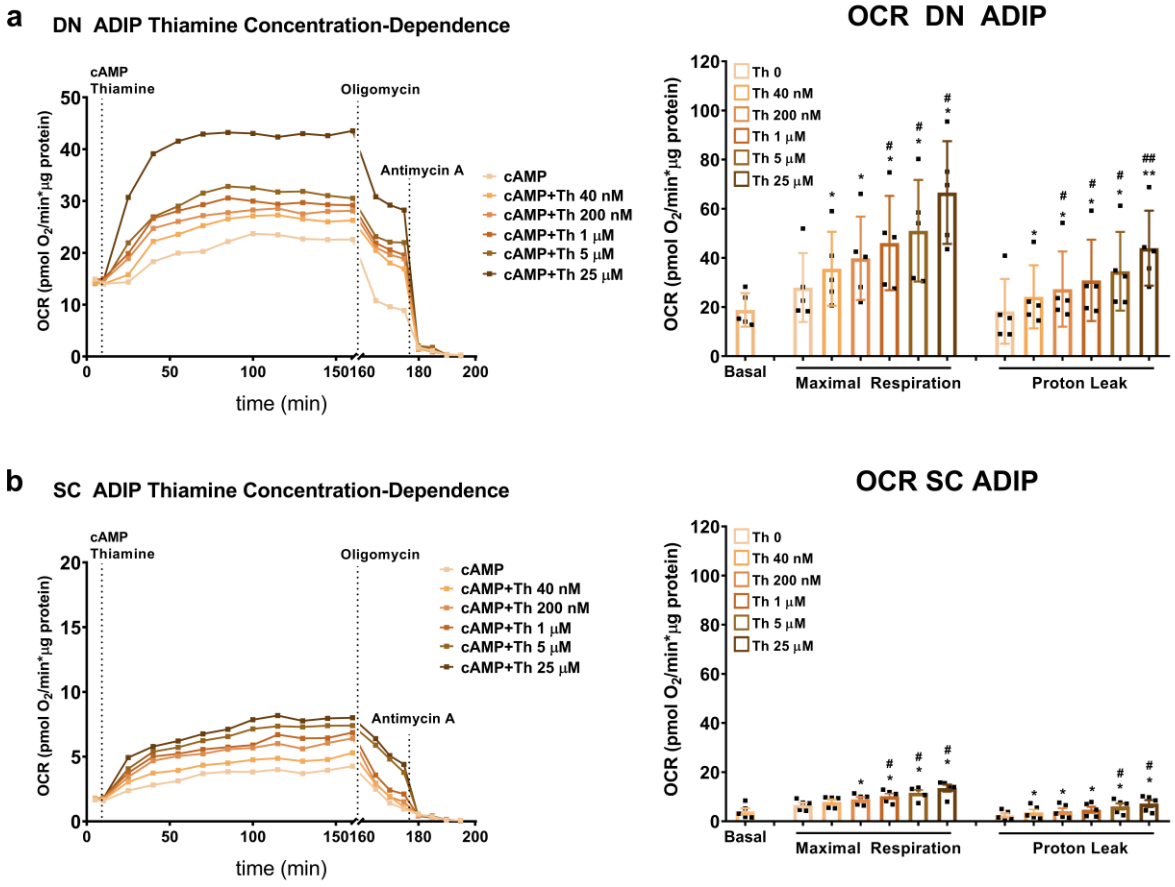

Figure 25. Effect of thiamine (Th) availability on the thermogenic activation of adipocytes. *After differentiation, ADIPs were incubated in thiamine free media for one hour, then treated with 500 μM dibutyryl-cAMP and gradually increasing concentrations of thiamine for 10 hours. (a-b) OCR of DN (a) and SC (b) ADIPs was monitored and representative curves of five measurements (left panels) are shown. OCR at basal and maximal stimulation, and after oligomycin addition (right panels) was quantified in adipocytes derived from five independent donors. Statistical analysis was performed by *comparing effect of each concentration of thiamine to the lack of thiamine and #higher than 40 nM concentrations to the effect of 40nM concentration. Statistical analysis was performed by unpaired t-test, */#p<0.05, **/##p<0.01.*

7.3.4. TPP enhances the activity of TPP-dependent PDH in permeabilized adipocytes

To further elucidate the mechanism of thermogenic action of thiamine, which is converted to the biochemically active compound TPP in cells, Seahorse-based respiration assay was optimized to monitor the activity of one of the TPP-dependent enzyme complexes, PDH, in cell membrane-permeabilized adipocytes which enabled us to study mitochondrial function without isolating mitochondria (**Figure 26a**). Pyruvate and malate, which are substrates for PDH and intermediates in TCA cycle, were added to drive NADH generation. Upon the injection of membrane permeabilizing agent, OCR dropped in both DN and SC derived ADIPs (**Figure 26b**). However, the difference in basal OCR between DN and SC ADIPs as well as responsiveness to oligomycin were maintained under the permeabilized conditions. TPP addition significantly increased both maximal mitochondrial and proton leak respiration in DN derived ADIPs while a less pronounced effect was observed in SC ADIPs (**Figure 26b**).

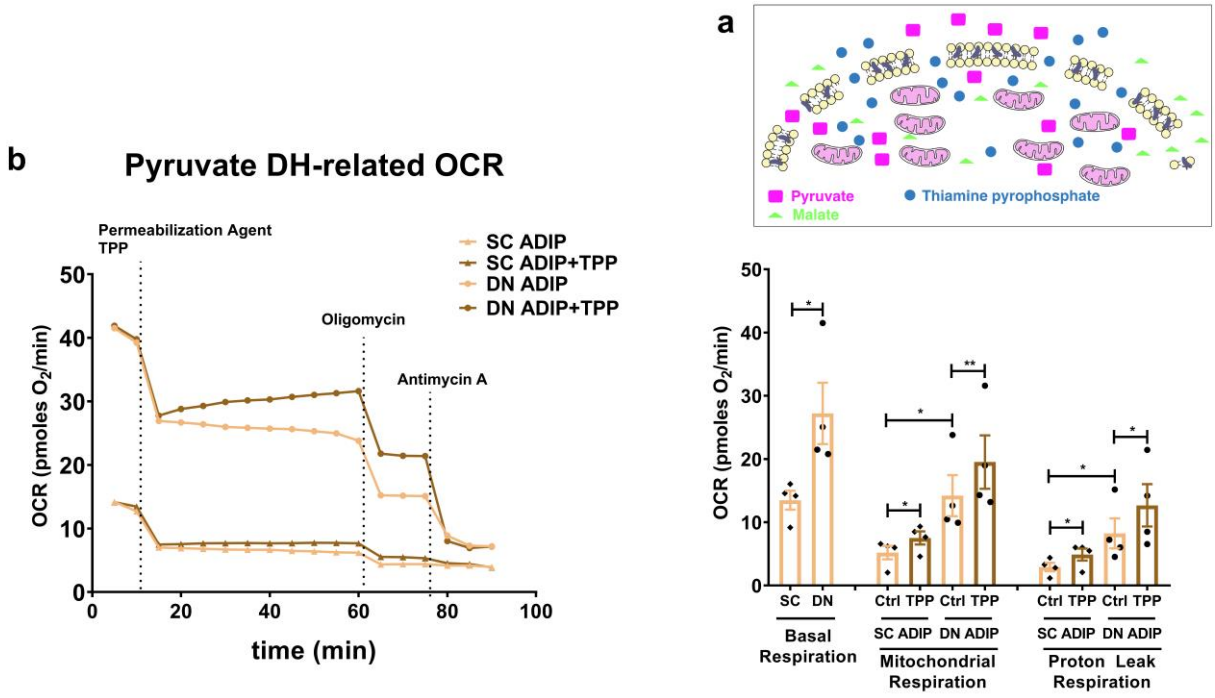

Figure 26. Effect of direct stimulation of pyruvate dehydrogenase (DH) by Th pyrophosphate (TPP) on the thermogenic activation of adipocytes. *After differentiation, ADIPs were incubated in thiamine free media for one hour, then treated with 500 µM dibutyryl-cAMP and gradually increasing concentrations of thiamine for 10 hours. (a) Scheme of cell membrane permeabilization experiment where ADIPs were incubated in mitochondrial assay solution. OCR was measured following injection of the cell permeabilizer and TPP. (b) Representative curves of four measurements (left panel). OCR at basal, mitochondrial respiration, and proton leak respiration were quantified from four independent donors (right panel). Statistical analysis was performed by unpaired t-test, *p<0.05, **p<0.01.*

TPC was expressed higher in DN as compared to SC derived adipocytes and its expression was increased by cAMP indicating the elevated demand of TPP in the mitochondria during thermogenic activation (**Figure 27a-b**). It is important to note that ThTr2 inhibition did not influence protein expression of TPC or PDHA1, and the latter was not affected by increasing thiamine availability either (**Figure 27c-d**). The results obtained with the permeabilized adipocytes suggest that TPP-dependent PDH entities, which generate metabolic fuel for thermogenesis, are not fully saturated with bound TPP in differentiated adipocytes. This implies that excess thiamine converted to TPP in stimulated adipocytes can increase respiration and thermogenesis through elevating the level of TPP bound enzymes and thereby NADH production.

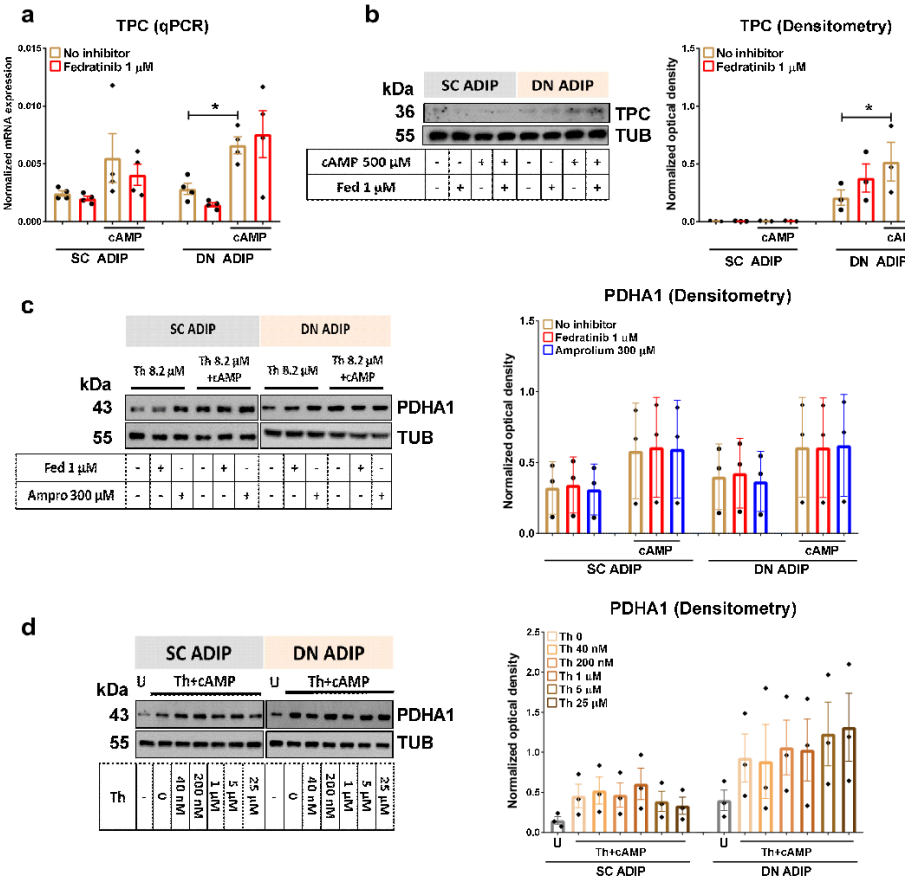

Figure 27. Expression of pyruvate dehydrogenase subunit alpha (PDHA1) and mitochondrial TPP transporter (TPC) in human deep neck (DN) and subcutaneous (SC) derived adipocytes. *(a, b) mRNA (n=4) and protein expression (n=3) of TPC in SC and DN derived adipocytes treated with 500 µM dibutyryl-cAMP in the presence of fedratinib for 10 hours. (c) Protein expression of PDHA1 in SC and DN derived ADIPs treated with 500 µM dibutyryl-cAMP in the presence of fedratinib or amprolium for 10 hours, n=3. (d) Protein expression of PDHA1 in SC and DN derived ADIPs treated with 500 µM dibutyryl-cAMP and gradually increasing concentrations of thiamine (Th) for 10 hours, n=3. U=untreated. Statistical analysis was performed by unpaired t-test. *p<0.05.*

We also investigated the effect of inhibiting another component of the PDH complex, the E2 subunit, in intact adipocytes. We treated the cells with cAMP analogue in the presence of lipoic acid antagonist, devimistat [Zachar *et al*., 2011]. Devimistat inhibited cAMP-stimulated elevation of OCR in both DN and SC ADIPs at 1, 5, and 10 hours after injection (data are not shown). It increased ECAR in SC but did not affect that in DN ADIP (data are not shown). Importantly, proton leak respiration was decreased upon addition of devimistat (data are not shown) indicating that continuous availability of co-factors for steady-state activity of TPP dependent enzymes is critical for maintaining effective thermogenic stimulation.

7.3.5. Inhibition of thiamine transport led to a lower expression of thermogenic genes in SC and DN derived adipocytes

The hampered thermogenesis observed in the presence of ThTr inhibitors raised the possibility that limited thiamine availability could influence thermogenic gene expression. As described in the previous chapter, DN ADIPs expressed higher level of UCP1 (**Figure 28a**) and PGC1a (**Figure 28b**) as compared to SC adipocytes. cAMP elevated mRNA and protein expression of these thermogenic marker genes in both SC and DN ADIPs at thiamine concentration present in the regular culture medium (**Figure 28a-c**). Inhibition of ThTrs by either fedratinib or amprolium resulted in attenuated cAMP-dependent upregulation of UCP1 and PGC1a (**Figure 28a-c**). Furthermore, the high expression of both UCP1 and PGC1a in DN ADIP was reduced as a result of inhibitor treatments even in unstimulated condition suggesting that continuous supply of thiamine is required to maintain a high basal expression of UCP1 and PGC1a. We also investigated the effect of fedratinib on other brown/beige markers (refer to **Table 1**). The cAMP-stimulated upregulation of thermogenic genes such as DIO2, CITED1, CIDEA, and TBX1 was abrogated in response to fedratinib during thermogenic activation in both SC and DN ADIPs (**Figure 28d-g**).

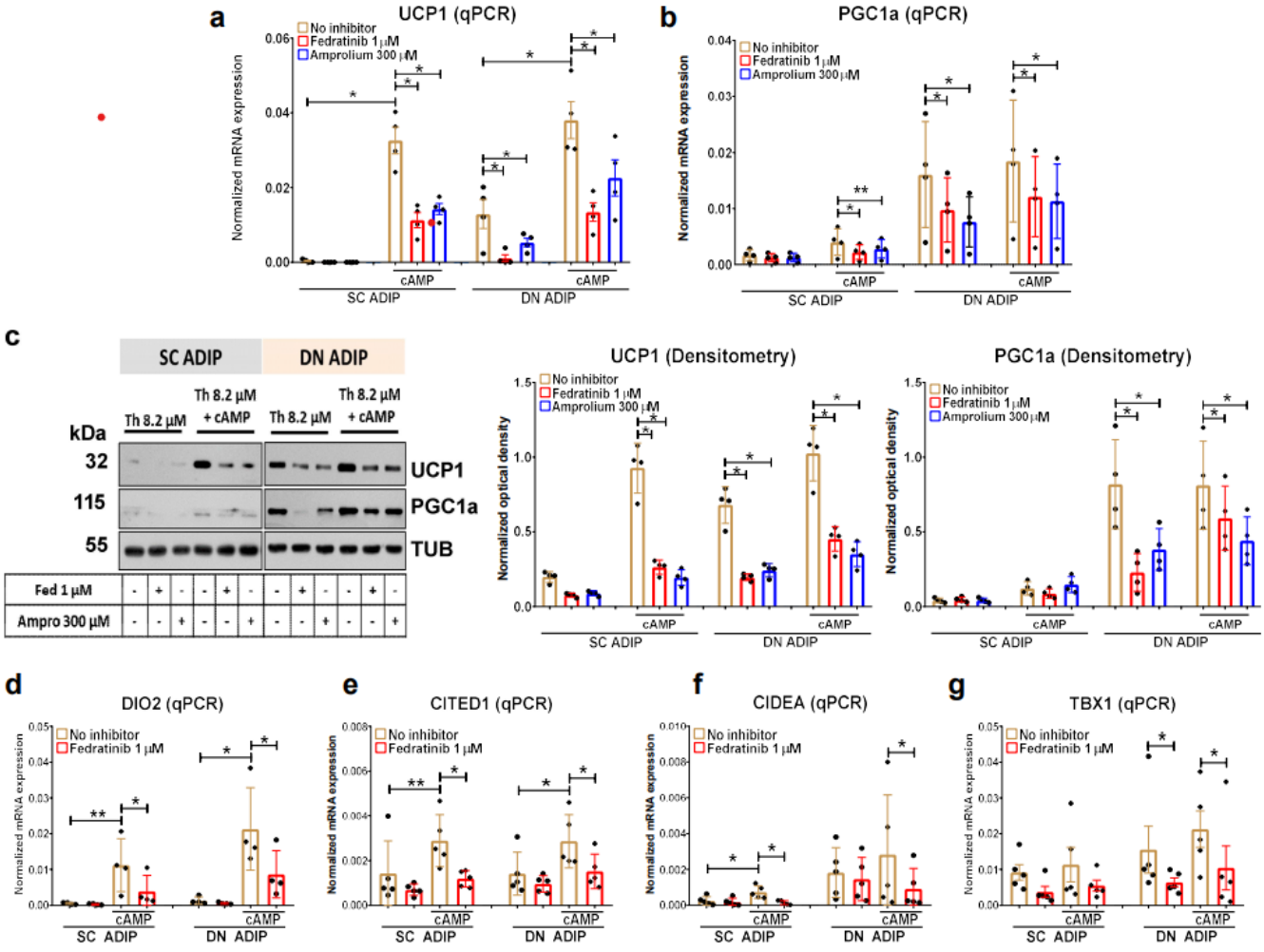

Figure 28. Effect of thiamine transporter inhibitors on the basal and cAMP induced expression of thermogenic marker genes in human deep neck (DN) and subcutaneous (SC) derived adipocytes. *After differentiation, ADIPs were treated with 500 µM dibutyryl-cAMP in the presence or absence of thiamine transporter inhibitors fedratinib (Fed) and amprolium (Ampro) for 10 hours. (a-b) mRNA expression of UCP1 and PGC1a detected by RT-qPCR, n=4. (c) Protein expression of UCP1 and PCG1a detected by immunoblotting, n=4. (d-g) mRNA expression of DIO2, CITED1, CIDEA, TBX1, and ThTr2 detected by RT-qPCR, n=5. Statistical analysis was performed by unpaired t-test, *p<0.05, **p<0.01.*

As fedratinib is a potent inhibitor of ThTr2, we also investigated whether fedratinib affected the expression of ThTr2 in SC and DN ADIPs. We did not observe any effect on the mRNA and protein expression of ThTr2 in SC and DN ADIPs, both in basal and stimulated condition (**Figure 29a-b**). These data suggested that fedratinib treatment reduced only ThTr2 activity but did not influence its expression. The mRNA and protein expression of ThTr1 was not affected either by fedratinib (**Figure 29c-d**).

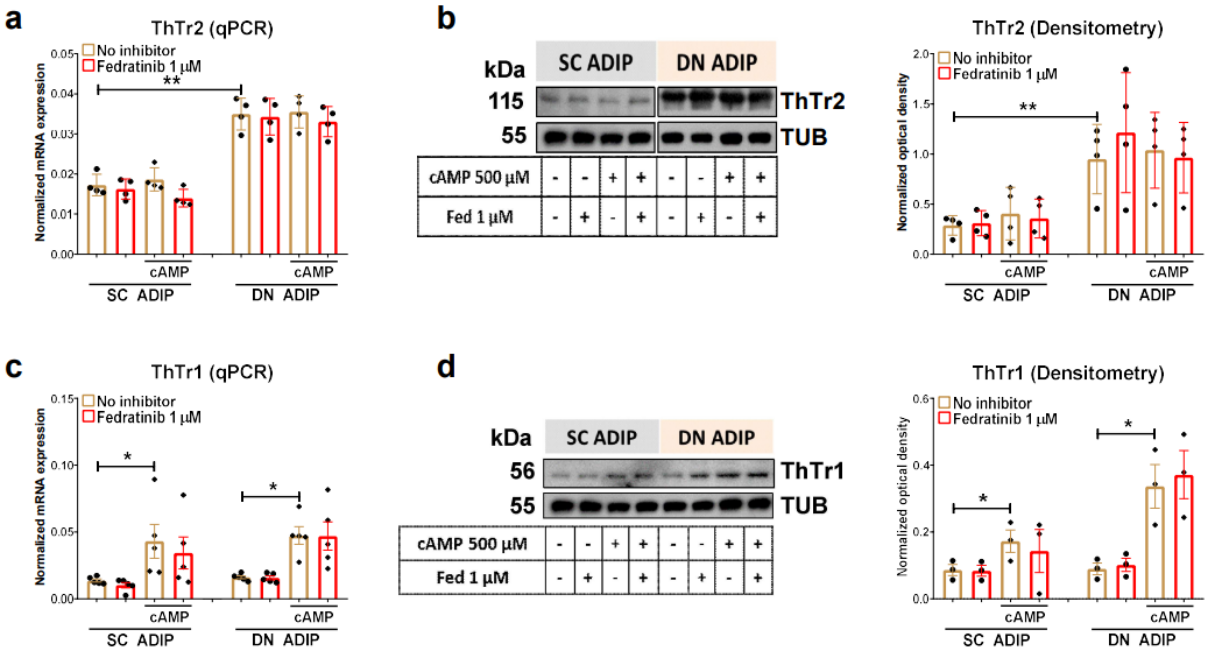

Figure 29. The expression of ThTr2 and ThTr1 was not affected by fedratinib in human deep neck (DN) and subcutaneous (SC) adipocytes. *ADIPs were differentiated and treated as in Figure 4. After differentiation, ADIPs were treated with 500 µM dibutyryl-cAMP in the presence or absence of fedratinib (Fed) for 10 hours. (a) mRNA expression of ThTr2 detected by RT-qPCR, n=4. (b) Protein expression of ThTr2 detected by immunoblotting, n=4. (c) mRNA expression of ThTr1 detected by RT-qPCR, n=4. (d) Protein expression of ThTr1 detected by immunoblotting, n=3. Statistical analysis was performed by unpaired t-test, *p<0.05.*

We also investigated the effect of fedratinib on thermogenic gene expression in SC and DN B-ADIPs. We found that cAMP could not induce further the upregulation of UCP1 and PGC1a as their basal expression in B-ADIP was already high (**Figure 30a-c**). However, we observed that ThTr2 inhibition resulted in the decreased expression of UCP1 and PGC1a (**Figure 30a-c**). In addition, we found that the expression of DIO2 and TBX1 was also hindered by fedratinib treatment (**Figure 30d, e**) demonstrating that thiamine transport is required for maintaining the high expression of thermogenic genes in thermogenically active B-ADIPs as well.

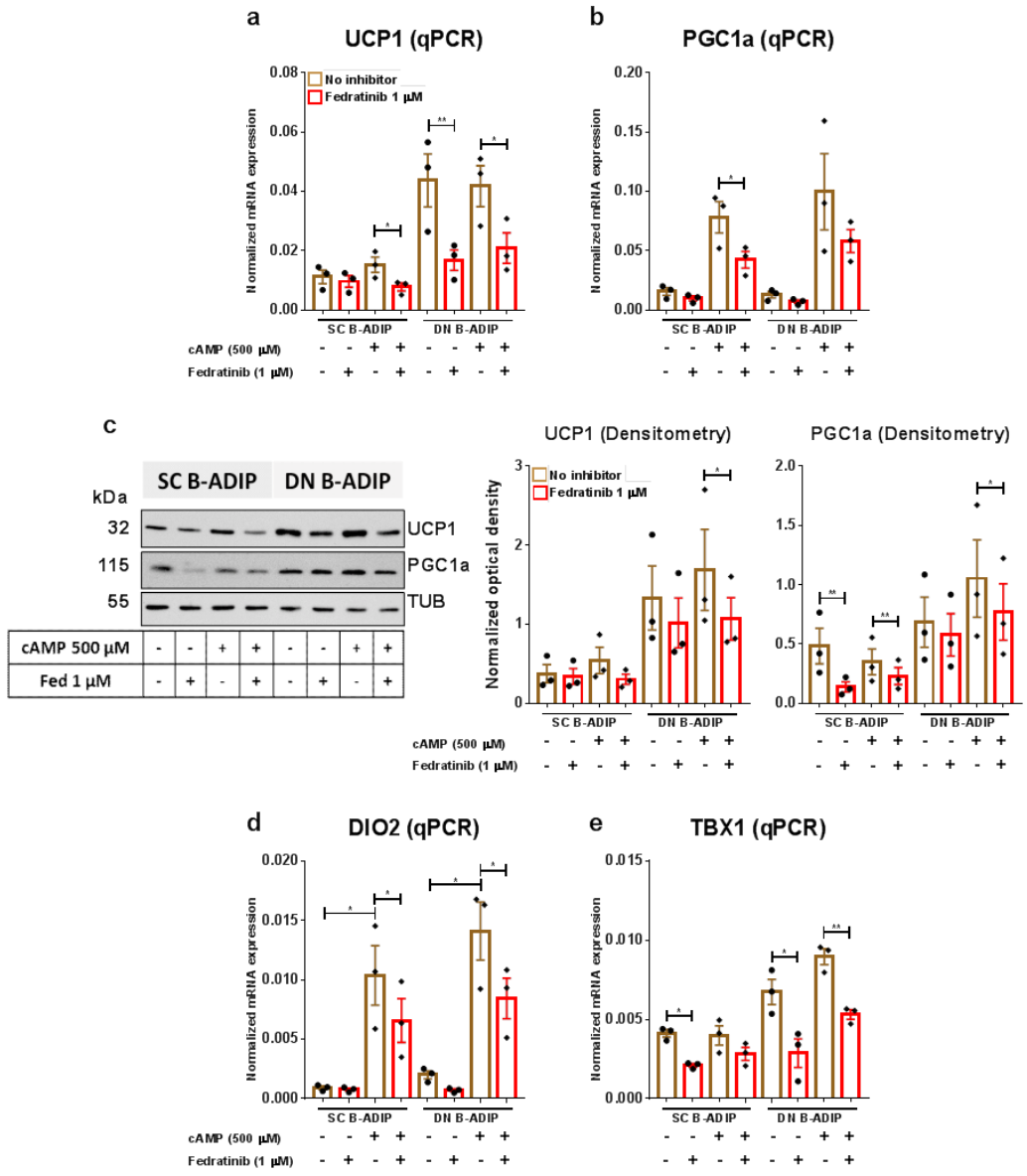

Figure 30. Effect of thiamine transporter 2 inhibitor fedratinib on the expression of thermogenic markers of subcutaneous (SC) and deep neck (DN) adipocytes differentiated with long term rosiglitazone treatment (B-ADIP). *After differentiation, B-ADIPs were treated with 500 µM dibutyryl-cAMP in the presence or absence of fedratinib (Fed) for 10 hours. (a-b) mRNA expression of UCP1 and PGC1a detected by qPCR. (c) Immunoblotting and densitometry of UCP1 and PGC1a protein expression in SC and DN B-ADIPs. (d, e) mRNA expression of DIO2 and TBX1 detected by qPCR. n=3 for all groups. Statistical analysis was performed by unpaired t-test, *p<0.05, **p<0.01.*

Next, we addressed the question whether inhibition of ThTr2 affects the protein expression of thermogenic markers and ThTrs *in situ*. Therefore, we dissected pairs of SC and DN biopsies into three pieces which were incubated in culture media with 8.2 µM thiamine. The first sample served as a control, the second was treated with cAMP analogue, and the third one

was co-treated with the cAMP analogue and fedratinib or amprolium. In accordance with the literature and our observations *ex vivo*, UCP1 and PGC1a was expressed at a higher level in DN compared to SC biopsies. UCP1 and PGC1a was remarkably upregulated in response to cAMP-dependent activation, which effect was significantly inhibited by fedratinib and amprolium in both SC and DN adipose tissues (**Figure 31a-b**). We also checked the expression of both thiamine transporters *in situ*. The expression of ThTrs was not affected by the cAMP analogue or its co-administration with the ThTrs potent inhibitors (**Figure 31c-d**).

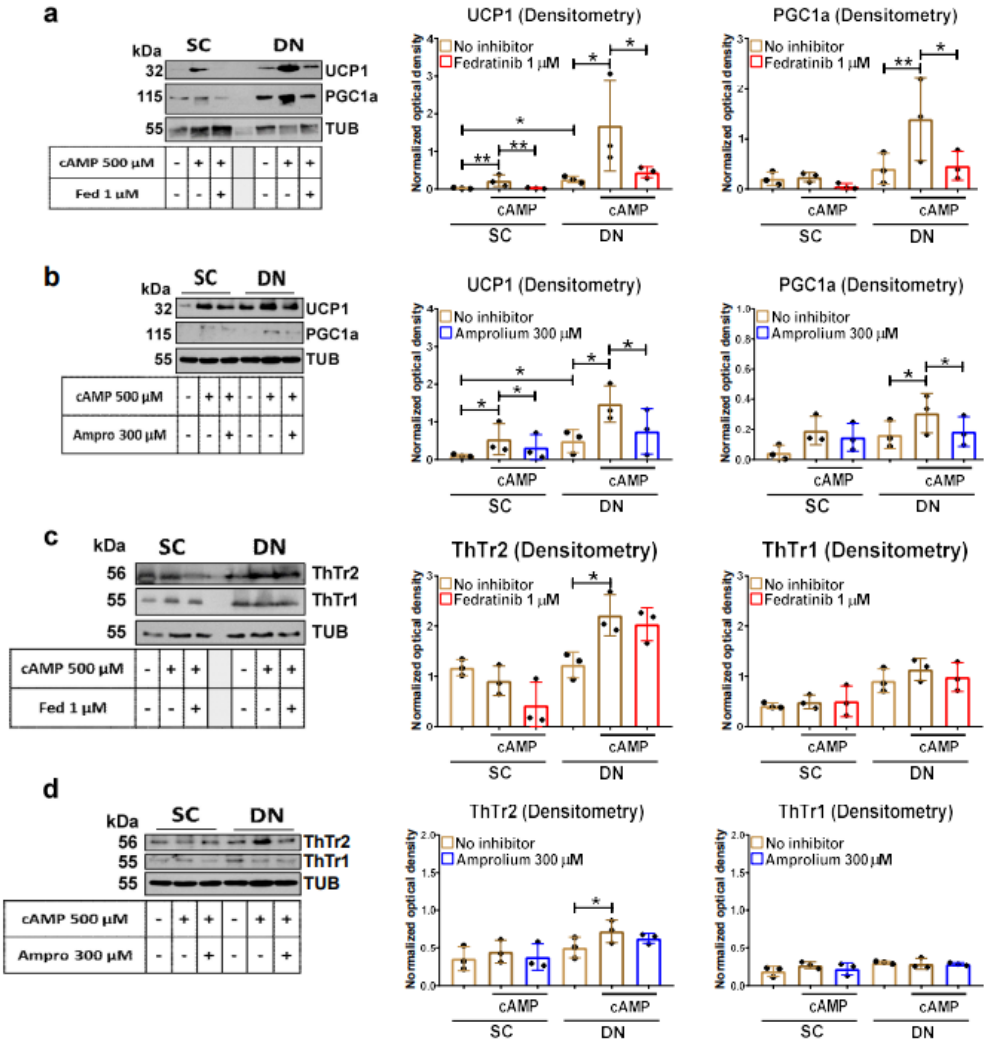

Figure 31. Effect of thiamine transporter inhibitors on the protein expression of thermogenic markers in huma neck biopsies during thermogenic activation. *(a, b) Protein expression of UCP1 and PGC1a in human SC and DN biopsies detected by immunoblotting in the presence of fedratinib (a) or amprolium (b). (c, d) Protein expression of ThTr2 and ThTr1 detected by immunoblotting in the presence of fedratinib (c) or amprolium (d). *p<0.05, **p<0.01, statistical analysis was performed by unpaired t-test.*

7.3.6. Induction of thermogenic gene expression by thiamine in a concentration-dependent manner

As we observed that there was an increase of proton leak respiration following a gradually increasing concentration of thiamine, we hypothesized that thiamine availability also regulated the expression of thermogenic markers. Using thiamine free culture fluid, we could observe that cAMP-stimulated upregulation of UCP1 and PGC1a were potentiated by applying increasing concentrations of thiamine (**Figure 32a-c**). Thiamine potentiated the expression of UCP1 at 40 nM and 1 µM in SC and DN ADIPs, respectively. The effect of thiamine on PGC1a expression was already observed at 40 nM in both SC and DN ADIPs. The influence of thiamine concentration on other thermogenic markers was also investigated. We found that thiamine potentiated cAMP-stimulated upregulation at its low concentration (**Figure 33a-d**). These results indicated that thiamine could potentiate the cAMP-stimulated expression of thermogenic genes.

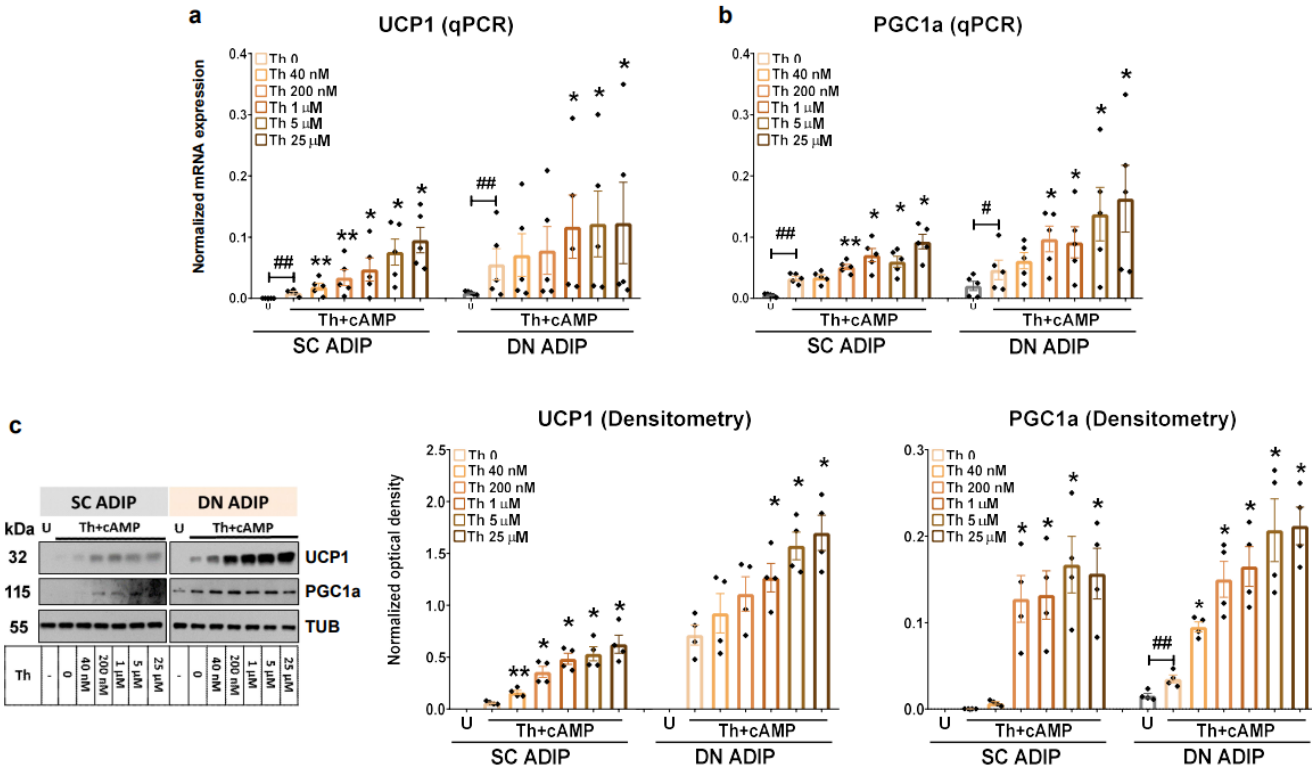

Figure 32. Effect of increasing concentration of thiamine (Th) on thermogenic gene induction in human deep neck (DN) and subcutaneous (SC) derived adipocytes. *After differentiation, ADIPs were incubated in thiamine free media for one hour, then treated with 500 µM dibutyryl-cAMP and gradually increasing concentrations of thiamine for 10 hours. (a-b) mRNA expression of UCP1 and PGC1a assessed by RT-qPCR, n=5. (c) UCP1 and PGC1a protein expression detected by immunoblotting, n=4. U: untreated. Statistical analysis was performed by unpaired t-test (*/#p<0.05, **/##p<0.01), *comparing data at each concentration of thiamine to the lack of thiamine or # comparing the indicated groups.*

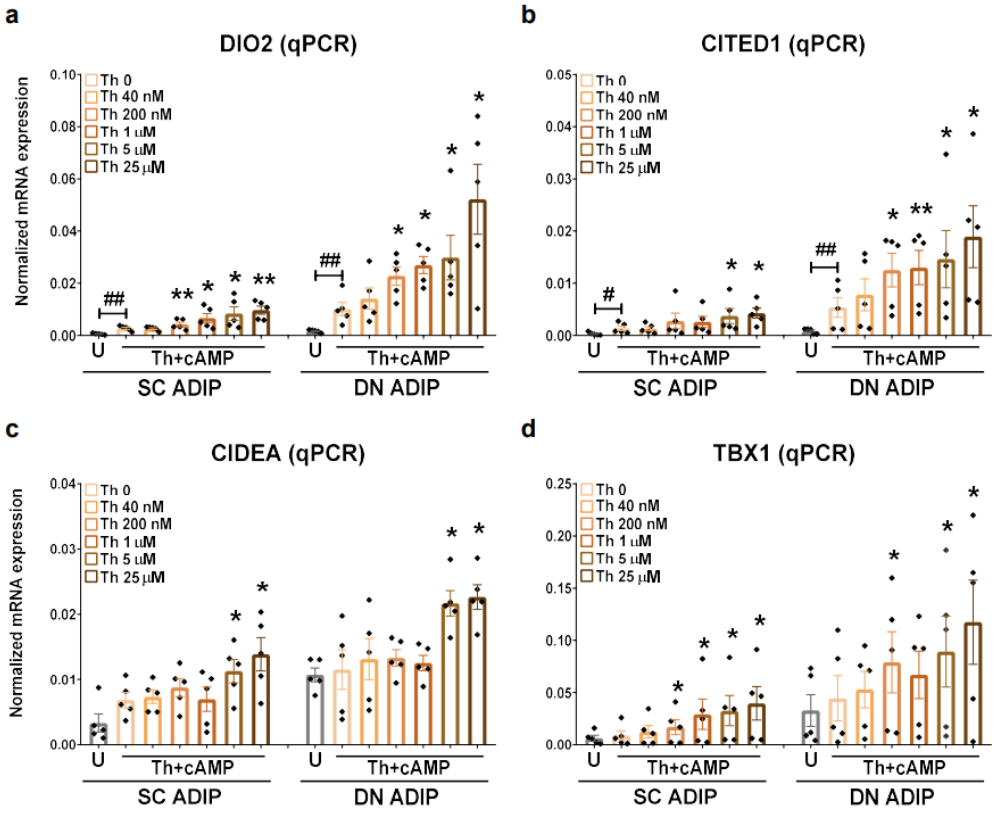

Figure 33. Effect of increasing concentration of thiamine (Th) on thermogenic gene induction in human deep neck (DN) and subcutaneous (SC) derived adipocytes. *After differentiation, ADIPs were incubated in thiamine free media for one hour, then treated with 500 µM dibutyryl-cAMP and gradually increasing concentrations of thiamine for 10 hours. (a-d) mRNA expression of DIO2, CITED1, CIDEA, and TBX1 assessed by RT-qPCR, n=5. U: untreated. Statistical analysis was performed by unpaired t-test (*/#p<0.05, **/##p<0.01), *comparing data at each concentration of thiamine to the lack of thiamine or # comparing the indicated groups.*

8. Discussion

8.1. Human DN derived adipocytes possess an overlap molecular signature of classical brown and beige adipocyte markers

Hitherto, there is discrepancy regarding the molecular identity of human BAT, particularly BAT which is located in supraclavicular and cervical region. We addressed a question whether human adipocytes derived from DN possess classical brown adipocyte identity or it is more resemble to beige adipocyte. We characterized human neck derived adipocytes by performing global transcriptomic analysis and analyzed the expression pattern of established markers for classical brown and beige adipocytes. The differentiated adipocytes derived from two anatomical origins, SC and DN depots, showed a similar expression pattern of general adipocytes such as *LEP, AIDPOQ, LEP, LEPR,* and *FABP4* indicating that the adipogenic program can be applied to hASCs derived from both anatomical origins and the differentiation rate of adipocytes originated from SC and DN are equal (**Figure 11a**).

When we investigated the expression pattern of classical brown and beige adipocyte markers, we found that those markers were differently expressed between SC and DN. Similar to other studies in human supraclavicular and deep neck, we found that the expression of UCP1 was higher in DN than SC adipocytes. The expression of *EBF2* which determine the brown adipocyte commitment was already high in DN preadipocyte and its high expression was maintained after differentiation. The expression of one of classical brown adipocyte marker, *LHX8*, and beige markers such as *CIDEA, CITED1, PM20D1 KCNK3,* and *TBX1* was significantly higher in DN adipocytes (**Figure 11b**). The expression of *CIDEA, CITED1,* and *PM20D1* was also upregulated by rosiglitazone irrespective to anatomical origins. Intriguingly, well-known thermogenic markers such as *PGC1a* and *ELOVL3* were not differently expressed between SC and derived adipocytes. Our results suggest that hASCs isolated from DN tissues consist of a mixture of progenitors which have potential to differentiate to classical brown or beige adipocytes. These findings are in accordance with Jespersen *et al*., (2013) reporting that there is an overlap molecular signature between classical brown and beige adipocyte in human BAT isolated from supraclavicular region.

In line with higher expression of thermogenic markers, DN derived adipocytes also possess higher brown adipocyte content and browning capacity score (**Figure 11c-d**) measured by BATLAS and ProFAT, respectively [Perdikari *et al*., 2018; Cheng *et al*., 2018]. Both web tools

were developed based on transcriptomic profiles of mice and human WAT and BAT. BATLAS can estimate the brown adipocyte content in a heterogeneous population of adipocytes, whereas ProFAT can predict the browning probability based on transcriptomic data [Perdikari *et al*., 2018; Cheng *et al*., 2018]. Regardless the anatomical origins, rosiglitazone increased the BATLAS and ProFAT score (**Figure 11c-d**). DN B-ADIPs had the highest BATLAS and ProFAT scores among all groups indicating that high thermogenic capacity in DN derived adipocytes can be induced further. The response of adipocytes derived from SC tissue, which is marked by higher expression of beige markers and score of BATLAS and ProFAT, indicate that masked beige adipocyte are present and can be induced by rosiglitazone or beta-adrenergic stimulation.

8.2. The expression of SLC transporters facilitating the uptake of cellular metabolic substrates is upregulated in thermogenic adipocytes

SLC transporters comprise a dynamic work for living cells by transporting essential nutrients including macronutrients, such as glucose, fatty acids, and amino acids, and micronutrients, such as vitamins and minerals [Zhang *et al*., 2019]. Active brown/beige adipocytes consume higher amounts of nutrients to provide sufficient fuel for heat generation and SLC transporters play a crucial role in mediating the transport of those molecules. It has been extensively studied in mice and human that active BAT utilize high amount of glucose [Cypess *et al*., 2009; Virtanen *et al*., 2009]. The uptake of glucose in adipocyte is primarily mediated by GLUT4 (encoded by *SLC2A4*) [El Bacha *et al*., 2010]. GLUT4 has been regarded as the predominant insulin-dependent glucose transporter for decades until a study reported that there was another insulin-sensitive glucose transporter GLUT12, which is encoded by SLC2A12. Like GLUT4, GLUT12 translocate to cell membrane upon insulin stimulation. Our RNA-Seq analysis showed that the expression of *GLUT12* was significantly higher in DN as compared to SC adipocytes (**Figure 12**). As we found that expression of *GLUT4* is similar between SC and DN adipocytes (**Figure 11**), the upregulation of *GLUT12* in DN adipocytes indicate that DN adipocytes require an additional facilitated-glucose transport to fulfill a higher energy demand. A transgenic mice overexpression *GLUT12* exerted an increased insulin sensitivity and insulin-dependent glucose clearance [Purcell *et al*., 2011]. Adipose levels of *GLUT12* was found low in obese humans and mice suggesting that GLUT12 may have a significant role in the development

of obesity-associated insulin resistance. In the future, a functional study is needed to uncover the importance of GLUT12 during thermogenic activation in human adipocytes.

Long chain fatty acid transporter-1 (FATP1), encoded by *SLC27A1*, was expressed on the plasma membrane of mice BAT and its expression was elevated upon cold exposure in parallel to elevated fatty acid uptake [Wu *et al*., 2006]. In adipocytes, the translocation of FATP1 to plasma membrane is induced by insulin [Anderson and Stahl, 2014]. FATP1 also plays a pivotal role in regulating available long chain fatty acids from exogenous sources such as tissues undergoing high levels of beta-oxidation or triglyceride synthesis. The deletion of FATP1 in mice led to the decreased of basal fatty acid uptake and halted the cold-induced fatty acid uptake. As the results, FATP1-null mice were unable to maintain body core temperature during cold exposure [Wu *et al*., 2006]. We did not observe any difference in the expression of *FATP1* in SC and DN derived adipocytes, however, we found that one of fatty acid transporter family, FATP3 (encoded by *SLC27A3*), was expressed higher in DN than SC adipocytes and long-term rosiglitazone treatment increased its expression (**Figure 12**). The studies reported the function and cellular location of FATP3 are still limited. FATP3 plays a critical role in mediating fatty acids uptake in endothelial cells [Kazantzis and Stahl, 2012], however its function in other tissues or its role in pathological condition remain unclear. The expression of *FATP3* was significantly reduced in human abdominal adipose tissue biopsies upon 5-week calorie restriction [Bouwman *et al*., 2014]. FATP3 can localize to mitochondria [Pei *et al*., 2004] and has acyl-CoA ligase activity for long-chain and very-long-chain fatty acids. The function of FATP3 in human adipocyte during thermogenic activation was still unknown. The upregulation of FATP3 in thermogenic adipocytes may be related to UCP1 activation by long-chain fatty acids [Fedorenko *et al*., 2012; Bertholet and Kirichok, 2017].

Branched-chain amino acids (BCAAs), which is another important substrate during thermogenic activation, can be oxidized in the mitochondria of brown adipose tissue, into which they are transported by SLC25A44 [Yoneshiro *et al*., 2019]. We found that neutral amino acids transporter ASC-1, which we studied in more detail, and excitatory amino acid transporter 5 (EAAT5, encoded by *SLC1A7*) were expressed higher in DN as compared to SC adipocytes (**Figure 12**). Our data showed that UCP1-enriched DN adipocytes expressed higher SLC

transporters that mediate the uptake of metabolic substrates including glucose, fatty acids, and amino acids to fuel heat generation.

In addition to macronutrients transporters, SLC transporters that mediate the uptake of thiamine (described more detail in later chapter) and folic acid (encoded by *SLC46A1*) were also expressed higher in DN than SC adipocytes. Folic acid, in its active form tetrahydrofolate (THF) plays role in transporting single-carbon group which will be transferred to other molecules as part of biosynthesis process of biological molecules. The expression of Na/K/Ca exchanger NCKX3, encoded *SLC24A3* respectively, were also higher in DN adipocytes as compared to SC adipocytes while NCKX2 encoded by *SLC24A2* was expressed higher in B-ADIPs (**Figure 12**). These ion exchangers transport 1 Ca^{2+} and 1 K^{+} in exchange for 4 Na^{+}. Calcium cycling that involves ryanodine receptor (RyR) and SERCA1 is one of the UCP1-independent thermogenesis mechanism [Ikeda *et al*., 2017]. Further investigation is needed to confirm the involvement of calcium transporter in UCP1-independent thermogenesis by calcium cycling.

8.3. ASC-1 transporter facilitates the uptake of serine, cysteine, and glycine during thermogenic activation in human neck derived adipocytes

ASC-1, which is localized in the plasma membrane, mediates the transport of small neutral amino acids, both D- and L- form, in a sodium-independent manner [Verrey *et al*, 2004]. ASC-1 shows a high level of structural similarity to sodium-independent large neutral amino acid transporters (LAT2, encoded by SLC7A8) thus both transporters have overlapping substrates [Verrey *et al*, 2004; Brown *et al*, 2014]. ASC-1 is the main regulator of extracellular D-serine in synaptic systems as the deletion of ASC-1 ablated D-serine uptake in synaptosomes by up to 70% [Rutter *et al*., 2007]. The expression and function of ASC-1 in neuronal systems is already well-established as ASC-1 is currently targeted to treat schizophrenia but studies in adipose tissue are still limited.

Our data showed that *ASC-1* was expressed higher in thermogenic adipocytes, similarly to *UCP1* (**Figure 13a-b**). At the protein level, ASC-1 expression was moderately higher in ADIPs as compared to B-ADIPs irrespective to anatomical origins (**Figure 13c**). Our finding was in line with other human study using tissue samples obtained by needle biopsies that found a slightly higher ASC-1 mRNA expressed in SC white tissue as compared to DN tissue [Perdikari *et al*., 2018]. Previous studies identified ASC-1 as cell surface markers of white adipocytes in human

and mice [Ussar *et al*, 2014; Garcia *et al*, 2016]. Interestingly, ASC-1 mRNA is expressed at the same level in white and brown adipocytes isolated from SC and DN after immortalization suggesting that a loss of repression of ASC-1 occur in immortalized adipocytes [Ussar *et al*., 2014]. In mice, ASC-1 mRNA expression is less in beige adipocytes (differentiation under rosiglitazone) as compared to white adipocytes. The presence of ASC-1 in mice subpopulation of SC preadipocytes of adolescent adipose tissue and in differentiating preadipocyte cell line resulted in the inhibition of beige differentiation program [Suwandhi *et al*., 2021].

We have investigated the role of ASC-1 in facilitating the uptake of serine, cysteine, and glycine in the metabolism and regulation of thermogenic adipocytes. Our metabolomics data showed that DN adipocytes consumed higher amount of serine, cysteine and glycine during thermogenic activation and ASC-1 played an important role in maintaining these amino acids influx (**Figure 14**). Inhibition of ASC-1 resulted in reduced uptake of these amino acids in basal and cAMP-stimulated condition in DN adipocytes (**Figure 14**). Serine is an important metabolic source to generate one-carbon unit in mammalian cells [de Koning *et al*., 2003]. One-carbon units are generated through break down of serine by both serine hydroxymethyltransferase (SHMT) enzymes, SHMT1 and SHMT2. One-carbon unit metabolism form a functional interaction with mitochondrial oxidative phosphorylation (OXPHOS) system that is crucial for ATP generation in mammalian cells. In our study, we have shown that mitochondrial OXPHOS system was affected by ASC-1 activity modulation as cAMP-induced elevation of mitochondrial complex I and II protein expression was alleviated by ASC-1 inhibitor. The disturbance of serine influx that leads to the reduction of one-carbon unit level may be one of major factor causing the decreasing of mitochondrial complex protein expression. One-carbon units are also required for shifting the methylation to trans-sulfuration pathway during glutathione (GSH) synthesis as a response to oxidative stress [McCarthy *et al*., 2014]. Serine treatment in mice diminishes oxidative stress by enhancing glutathione synthesis and lowering hepatic reactive oxygen species (ROS) production [Zhou *et al*., 2017].

Cysteine is a semi-essential amino acid that contains sulfur. Level of cysteine are lower in blood of diabetic individuals and animal models [Herrmann *et al*., 2005]. Achari *et al*. (2017) reported that L-cysteine supplementation enhances insulin sensitivity in high glucose treated 3T3-L1 adipocytes cell line through elevation of GSH level and adiponectin secretion. As the result, 3T3-L1 adipocytes express higher GLUT-4 and utilizes higher amount of glucose thus

improving energy metabolism. Cysteine, glycine, and glutamate are important for glutathione synthesis by activity of glutamylcysteine synthetase [Lu, 2009].

8.4. The importance of ASC-1 in UCP1-dependent and UCP1-independent thermogenesis of human neck derived adipocytes

We investigated the significance of ASC-1 transporter in cAMP-stimulated OCR of human neck derived adipocytes in the presence of a specific non-competitive ASC-1 inhibitor BMS-466442. In unstimulated condition, BMS-466442 did not affect the OCR of both SC and DN adipocytes (**Figure 15**). The hampering of ASC-1 activity led to the alleviation of cAMP-stimulated OCR in both SC and DN adipocytes (**Figure 15**). We observed that UCP1-dependent proton leak respiration, which was monitored upon oligomycin injection, was reduced during thermogenic activation in the presence of ASC-1 inhibitor (**Figure 15**). These data demonstrate the significance of ASC-1-mediated amino acid uptake in efficient thermogenic response of human neck adipocytes. mRNA expression of ASC-1 is higher in abdominal SC tissue from lean as compared to obese individuals [Ussar *et al*., 2014; Jersin *et al*., 2021]. Serine catabolism also plays a crucial role in sustaining mitochondrial respiration [Lucas *et al*., 2018]. We also observed that the interruption of serine influx ablated the cAMP-induced increasing of oxygen consumption at maximal respiration and UCP1-dependent respiration.

Higher expression of ASC-1 may give an advantageous effect for thermogenic activation of masked beige adipocytes residing in abdominal SC tissue of lean individuals. In line with OCR data, cAMP-stimulated mRNA and protein expression of thermogenic regulators such as UCP1 and PGC1a was also reduced by ASC-1 inhibitor in both human SC and DN adipocytes (**Figure 17**). Furthermore, we also found that the cAMP-stimulated mRNA expression of ELOVL3, CITED1 and DIO2 in human neck-derived adipocytes was reduced by the ASC-1 inhibitor (**Figure 18**). This data once again invigorates the significance of ASC-1 on thermogenic activation in human neck-derived adipocytes.

The inhibition of ASC-1 also hampered the activation of creatine futile cycle, which is of the mechanism in the UCP1-independent thermogenesis. We observed a decrease in β-GPA-inhibited OCR (**Figure 15**) and CKMT2 expression in both SC and DN adipocytes (**Figure 17**). In addition, cAMP-induced mRNA expression of CKMT1a/b was also reduced by the ASC-1 inhibitor (**Figure 18**). CKMT1a/b, the mitochondrial creatine kinase 1a/b, phosphorylates the creatine generating

the phosphocreatine. CKMT1a/b plays an important essential role in UCP1-independent thermogenesis through the creatine futile cycle [Kazak *et al*., 2015]. Three amino acids including methionine, glycine and arginine are required to synthesize creatine [Da Silva *et al*., 2009]. The interruption of glycine influx by ASC-1 inhibitor may reduce the creatine synthesis leading to the decreasing of creatine futile cycle rate and creatine kinase expression. In addition to the creatine futile cycle, ASC-1 inhibition also reduced cAMP-stimulated mRNA expression of PM20D1 in human SC and DN adipocytes (**Figure 18**). PM20D1 was enriched in classical BAT as compared to epididymal WAT and PM20D1 administration increased the energy expenditure [Long *et al*., 2016]. PM20D1 regulates the synthesis of N-lipidated/N-fatty-acyl amino acids which function as endogenous uncouplers of mitochondrial respiration in a UCP1-independent manner.

ASC-1 has been recently identified as a novel regulator of energy metabolism reporting that ASC-1 overexpression reduces ROS formation, lipid accumulation, and insulin resistance and enhances mitochondrial respiration in human abdominal subcutaneous adipocytes [Jersin *et al*., 2021]. The important role of ASC-1 in controlling obesity has been also highlighted by the observation in multiple cohorts that its expression in visceral adipose tissue is inversely correlated with insulin resistance and adiposity [Jersin *et al*., 2021]. The capacity to dissipate energy as heat is lower in obese individuals [Jung *et al*., 1979; Rosenbaum and Leibel, 2010]. Based on our presented data, it can be presumed that decreased expression of ASC-1 in hypertrophic WAT of obese individuals may partially contribute to attenuated thermogenic response. This also might partially explain the fact that obese individuals possess high amounts of brownable but thermogenically inactive fat [Leitner *et al*., 2017]. Our findings suggested that stimulation of ASC-1 expression in adipose tissue of obese patients may have a beneficial effect on energy homeostasis and may be a promising therapeutic target for obesity and associated metabolic disturbance.

8.5. Abundant thiamine availability and its uptake by ThTrs is important for the effective thermogenic activation in human neck derived adipocytes

High energy demand in active brown/beige adipocytes might require the upregulation of SLC transporters to maintain an adequate influx of nutrients required for energy production. ThTr2 (encoded by *SLC19A3*) is one of the SLC transporters that were upregulated in DN adipocytes (**Figure 12**). ThTr2 expression was induced during the differentiation and was higher in DN as compared to SC adipocytes (**Figure 20a-b**). Based on integrative analysis utilizing human

transcriptomic and GWAS database, ThTr2 was identified as a novel human adipose-specific gene [Ahn *et al*., 2019]. A recent report demonstrated that SC adipose tissue isolated from individuals with obesity expressed lower ThTr2 as compared to lean individuals and the expression of ThTr2 positively correlated with weight loss [Pereira *et al*., 2021] suggesting its possible role in augmentation of energy metabolism. An *in vivo* study showed that ThTr2-deficient mice had decreased uptake of thiamine in intestine. However, ThTr1-deficient mice did not show a reduced thiamine uptake suggesting that ThTr2 can compensate for the loss of ThTr1. In addition, ThTr2 expression was upregulated in the intestine of ThTr1-deficient mice underlying the importance of the presence of ThTr2 in normal uptake of thiamine in mice [Reidling *et al*., 2010]. In humans, ThTr2 is postulated to play a major role in intestinal absorption because deficiency of ThTr1 does not alter plasma thiamine levels [Marce-Grau *et al*., 2019]. We observed that ThTr1 expression was induced during differentiation, however, we did not detect any different expression level between SC and DN adipocytes (**Figure 20b, c**). The expression of both ThTrs was elevated by forskolin but this response can only be observed in thermogenic cluster adipocytes derived from abdominal SC (**Figure 21c, d**, [Min *et al*., 2019]). In human neck tissues obtained by needle biopsies, we observed that both ThTrs were expressed at the same level in WAT and BAT (**Figure 21e, f**, [Perdikari *et al*., 2018]).

Thiamine, or vitamin B1, is transported into cells by ThTr and subsequently converted to the active form, TPP, by TPK. Several enzymes such as TK, a subunit of PDH, α-KGDH, and BCKDH complexes require TPP as their cofactors. As it was enriched in UCP1-containing thermogenic adipocytes, we intended to reveal the importance of ThTr2 during thermogenic activation in human neck derived adipocytes. Blocking of ThTr2 activity by its potent inhibitor, fedratinib, dampened the maximal and proton leak respiration of adipocytes stimulated for heat production (**Figure 22**). We could not exclude the fact that fedratinib is also a potent inhibitor of JAK2 and has been widely used in cancer therapy. This brings up the possibility that the observed effects of fedratinib on thermogenic activation might be resulted from the inhibition of an activated tyrosine kinase, especially in view that JAK2 KO mice were unable to upregulate BAT UCP1 following a HFD or after cold exposure [Shi *et al*., 2016]. However, involvement of JAK2 in BAT regulation could be demonstrated only in the presence of non-adipocyte tissue cells (which is not the case in our ex vivo differentiated adipocytes) and it was dispensable for induc-

tion of UCP1 thermogenesis in white adipose tissue through beige adipocytes, which are presumed to be dominant among DN adipocytes. Nevertheless, we decided to perform all critical experiments using a competitive general thiamine transporter inhibitor, amprolium which also exerted comparable effect like fedratinib (**Figure 23**). To the best of our knowledge, we are the first group reporting the significance of ThTrs activity during thermogenic activation in human adipocytes. The available thiamine in the culture media also affected maximal and proton leak respiration of human neck derived adipocytes in a concentration-dependent manner. The lack of thiamine halted the cAMP-stimulated elevation of maximal and proton leak respiration of the adipocytes (**Figure 25**). Our data suggest that thermogenically active brown/beige adipocytes require high amounts of thiamine taken up from the extracellular space majorly via ThTr2.

8.6. TPP-dependent pyruvate dehydrogenase activity can be stimulated by TPP in cell-permeabilized adipocytes

Cells with a greater energetic demand, such as active brown/beige adipocytes might need extra amount of thiamine to boost the activity of TPP-requiring enzymes that are responsible for energy metabolism. We elucidated the effect of direct stimulation by TPP supplementation on PDH activity in cell membrane-permeabilized adipocytes. TPP treatment increased the mitochondrial and proton leak respiration in the mitochondria within a special buffer that contained pyruvate and malate as substrates for energy production (**Figure 26**). We speculated that PDH, which is a key enzyme complex in catabolism, is initially not fully saturated by TPP in adipocytes that have not been activated for thermogenesis. The expression of mitochondrial TPP transporter/TPC was higher in thermogenic adipocytes and was further elevated by cAMP (**Figure 27a-b**). Other study reported that high-dose thiamine therapy improved dyslipidemia in streptozotocin-induced diabetic rats by elevating the expression and saturation of TK [Babaei-Jadidi *et al*., 2004]. TPP treatment also elevated oxygen consumption rate and ATP turnover of mouse brain mitochondria upon cardiopulmonary resuscitation [Ikeda *et al*., 2016].

It has been extensively studied in mice and human that active BAT utilize high amount of glucose [Cypess *et al*., 2009; Virtanen *et al*., 2009]. A recent study reported that during cold exposure, mouse BAT consumed labeled glucose to form pyruvate through glycolysis, and mitochondrial pyruvate carrier-1 (MPC1, encoded by SLC54A1) mediates the transport of pyruvate from the cytosol to mitochondria [Panic *et al*., 2020]. In the mitochondria, pyruvate is

converted to acetyl-CoA catalyzed by PDH. Weir *et al*. (2018) reported that pyruvate dehydrogenase subunit A (PDHA) were higher expressed in BAT isolated from deep neck as compared to WAT isolated from subcutaneous area. We also observed an increase in PDHA1 protein expression in DN as compared to SC Ad and dibutyryl-cAMP induced the elevation of PDHA1 expression (**Figure 27c, d**) In addition, based on Metabolite Set Enrichment Analysis (MSEA) of mouse sera, thiamine metabolism pathway was enriched upon cold exposure [Panic *et al*., 2020]. We also observed the upregulation of mitochondrial TPP transporter (encoded by SLC25A19) in cAMP-treated DN adipocytes suggesting the extra need of TPP in the mitochondria during thermogenic activation, probably for a more effective decarboxylation of pyruvate by PDH and for a proper function of α-ketoglutarate dehydrogenase in TCA cycle.

8.7. The expression of thermogenic marker genes in active human adipocytes is regulated by thiamine availability

We were surprised when we found that thiamine availability could be connected to the regulation of thermogenic genes. Inhibition of thiamine transport into stimulated adipocytes led to decreased expression of UCP1 and other thermogenic regulators upon adrenergic stimulation (**Figure 28, 30-31**). Addition of thiamine in thiamine free culture condition to the stimulated adipocytes could increase the expression of these genes in a concentration dependent manner (**Figure 32-33**). We can only speculate about the mechanism of how thiamine may contribute to induction of thermogenic genes during adrenergic stimulation of adipocytes. The 5´ non-coding region of the UCP1 gene contains regulatory elements that confer tissue specificity, differentiation dependence, and neuro-hormonal regulation to UCP1 gene transcription through interactions with a large number of transcription regulators including cAMP-responsive transcription factors as well as the PGC-1a co-regulator [Villaroya *et al*., 2017]. Transcriptional regulation of the UCP1 gene by cAMP-mediated signaling is provided by protein kinase A mediated rapid phosphorylation of the CREB transcription factor at the proximal UCP1 promoter region and p38 MAP kinase-mediated phosphorylation of ATF2 at the upstream enhancer region constituting a fast mechanism of regulation [Robidoux et a., 2005]. Thiamine or TPP may directly affect this orchestrated transcriptional regulation of UCP1 and other thermogenic regulators at these complex regulatory sites. Previous study reported that thiamine inhibits p53 DNA binding in living cells [McLure *et al*., 2004]. Phosphorylation mediated or TPP dependent

metabolic changes occurring during thermogenesis may also generate so far not identified, indirect gene regulatory signals.

8.8. Clinical significance

Thiamine deficiency, which is mainly caused by inadequate nutrition intake and defects in thiamine transporters, is a major factor of several diseases such as beriberi or Wernicke's encephalopathy and Korsakoff psychosis referred to as Wernicke-Korsakoff syndrome (WKS) [Cook *et al*., 1998]. The main symptoms of WKS are memory impairment, ataxia, confabulation, and hypothermia which is frequently reported as secondary symptom. Under normal physiological and nutritional conditions, a healthy human adult has approximately a 3-weeks reserve of thiamine in the liver [Maguire *et al*., 2018]. These reserves are rapidly depleted in chronic alcohol consumption that leads to disturbance of thiamine absorption [Cook *et al*., 1998; Cruickshank *et al*., 1988; Donnino *et al*., 2010]. It has been reported that thiamine deficiency leads to the lesion of the hypothalamus, which is the main regulator of body temperature and appetite [Tanev *et al*., 2008]. Human case studies have reported that parenteral administration of thiamine improved the hypothermic condition after 2 days of treatment [Hansen *et al*., 1984]. Our presented data suggest that in addition to causing disturbance in hypothalamic thermoregulation, thiamine deficiency may also compromise peripheral thermogenesis in brown/beige adipocytes contributing to hypothermia in WKS patients.

Alcohol consumption positively correlates with visceral fat accumulation in healthy individuals [Kim *et al*., 2012; Dorn *et al*., 2003], which may be partially caused by the perturbance of thiamine absorption and metabolism. Thiamine deficiency has also been reported in type 1 and 2 diabetes patients [Thornalley *et al*., 2007]. Thiamine supplementation (100 mg, 3x100 mg daily which is about 100x higher than recommended daily allowance) for 6 weeks improves glucose tolerance in hyperglycemic individuals [Alaei *et al*., 2013]. It has also been reported that thiamine supplementation may provide beneficial effects in type 2 diabetes patients by improving lipid and creatinine profiles [Al-Attas *et al*., 2014]. Obese individuals exerted significant thiamine deficiency before undergoing bariatric surgery [Carrodeguas *et al*., 2005; Flanchbaum *et al*., 2006; Nath *et al*., 2017; Peterson *et al*., 2016; Aron-Wisnewsky *et al*., 2016]. A recent study reported that subcutaneous adipose tissue isolated from obese individuals expressed lower ThTr2 as compared to lean individuals. The expression of ThTr2 in subcutaneous adipose tissue was positively correlated with weight loss [Pereira *et al*., 2021]

suggesting its possible role in augmentation of energy metabolism. A recent report demonstrated that SC adipose tissue isolated from individuals with obesity expressed lower ThTr2 as compared to lean individuals and the expression of ThTr2 positively correlated with weight loss [Pereira *et al*., 2021] suggesting its possible role in augmentation of energy metabolism. Thiamine supplementation prevented obesity and obesity-associated metabolic disorders in OLETF rats [Tanaka *et al*., 2010]. We have presented a functional ex vivo study revealing the importance of ThTr2, also ThTr1, during thermogenic activation and proposed the impact of thiamine availability in the regulation of thermogenic gene transcription. Our results raise the possibility to target molecular elements of the regulation of thiamine metabolism to augment heat generation by thermogenic adipocytes in obese individuals.

9. Summary

9.1. Molecular signature of human deep neck derived adipocytes

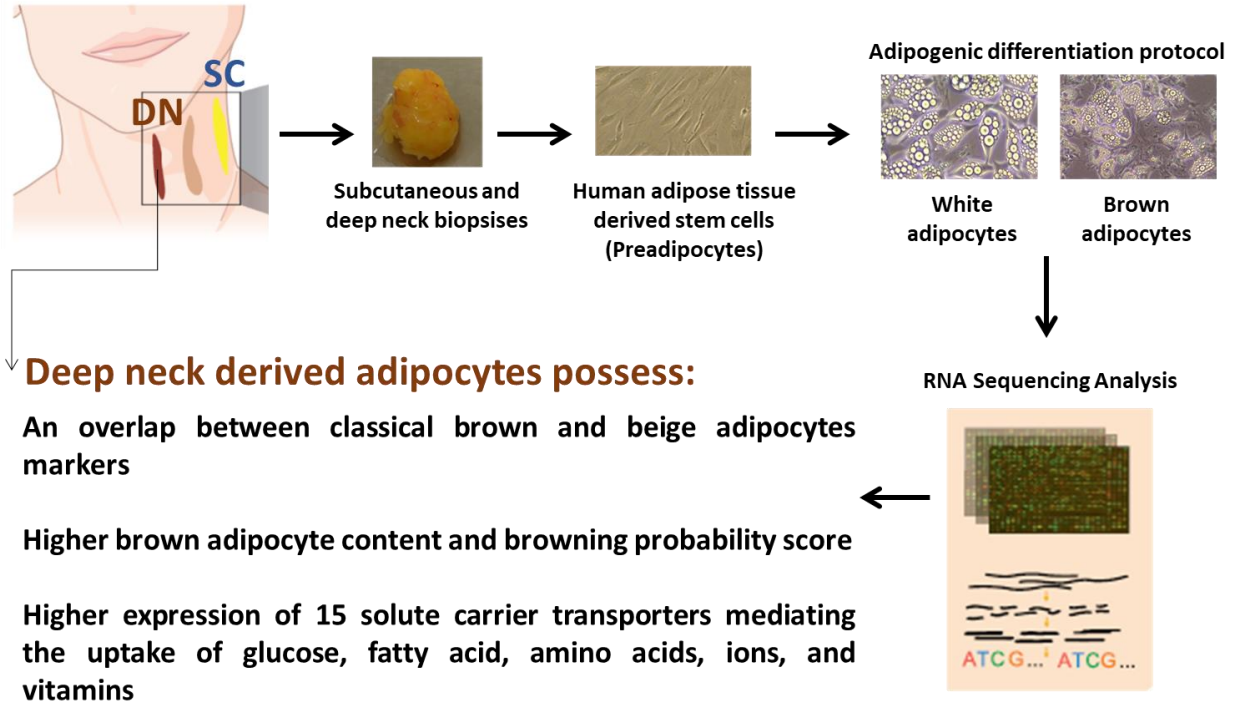

Figure 34. Molecular identity of human brown adipocytes originated from deep neck region *[Toth et al., 2020].*

- We isolated human adipose stem cells (hASCs) from human subcutaneous and deep neck tissues biopsies during thyroid surgery and differentiated the hASCs using adipogenic differentiation protocol. The differentiation rate was equal between subcutaneous and deep neck derived adipocytes, both white and brown adipocytes, indicated by similar expression pattern of general adipocyte markers such as *GLUT4*, *ADIPOQ*, *LEP*, and *LEPR*.
- By RNA-Sequencing analysis, we found that deep neck derived adipocytes expressed higher UCP1 as compared to subcutaneous irrespective to differentiation protocols. Deep neck derived adipocytes also had higher expression of classical brown (*LHX8*) and beige adipocyte markers (*TBX1*, *CITED1*, *PM20D1*, *KCNK3*, and *EBF2*) indicating that deep neck adipocytes possessed an overlapping molecular signature of classical brown and beige adipocytes.
- Brown adipocyte content and browning capacity was predicted by inputting the transcriptomic data to BATLAS and ProFAT web tools. Deep neck derived adipocytes

possessed higher BATLAS and ProFAT score as compared to subcutaneous ones irrespective to differentiation protocols. DN derived B-ADIPs showed the highest brown adipocyte content and browning capacity among all groups.

- 15 solute carrier transporters which are involved in the transport of glucose, fatty acids, amino acids, ions, and vitamins such as folic acid and thiamine were upregulated in DN as compared to SC adipocytes.

9.2. The importance of alanine-serine-cysteine transporter-1 in thermogenic activation of human neck adipocytes

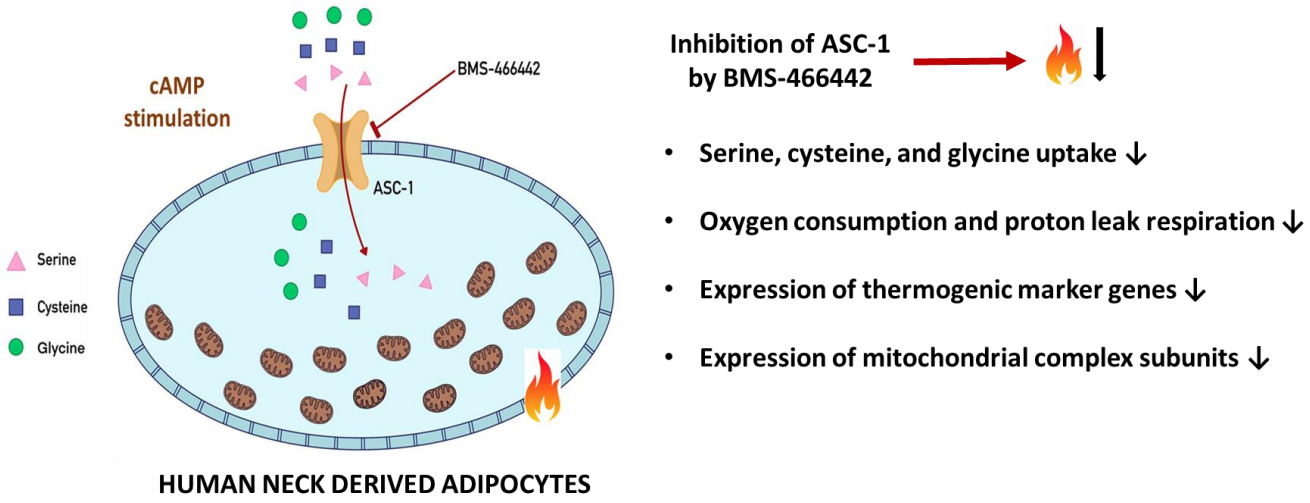

Figure 35. ASC-1 transporter play an important role in sustaining amino acids uptake during thermogenic activation of human neck derived adipocytes *[Arianti et al., 2021].*

- Human deep neck derived white and brown adipocytes consumed higher amount of serine, cysteine, and glycine during thermogenic activation by cAMP. In the presence of ASC-1 selective inhibitor, the uptake of those amino acids during thermogenic stimulation was dampened in both types of adipocytes.
- cAMP-stimulated oxygen consumption and proton leak respiration of subcutaneous and deep neck adipocytes was reduced by ASC-1 inhibitor. Creatine futile cycle that drives UCP1-independent heat generation was also reduced during thermogenic activation in the presence of ASC-1 inhibitor.
- In accordance with oxygen consumption data, the expression of thermogenic markers (*UCP1*, *CKMT1/2*, *PM20D1*, *ELOVL3*, *DIO2*, and *CITED1*), mitochondrial biogenesis regulator (*PGC1a*), and mitochondrial complex subunits was hampered by ASC-1 inhibitor during thermogenic stimulation.
- Our data suggested that ASC-1 mediated serine, cysteine, and glycine uptake is required for the efficient thermogenic response upon cAMP stimulation in human neck derived adipocytes. Stimulation of ASC-1 expression in adipose tissue of obese patients may have a beneficial effect on energy homeostasis and may be a promising therapeutic target for obesity and associated metabolic disturbance.

9.3. The significance of abundant thiamine and its transporters in efficient thermogenic response of human neck derived adipocytes

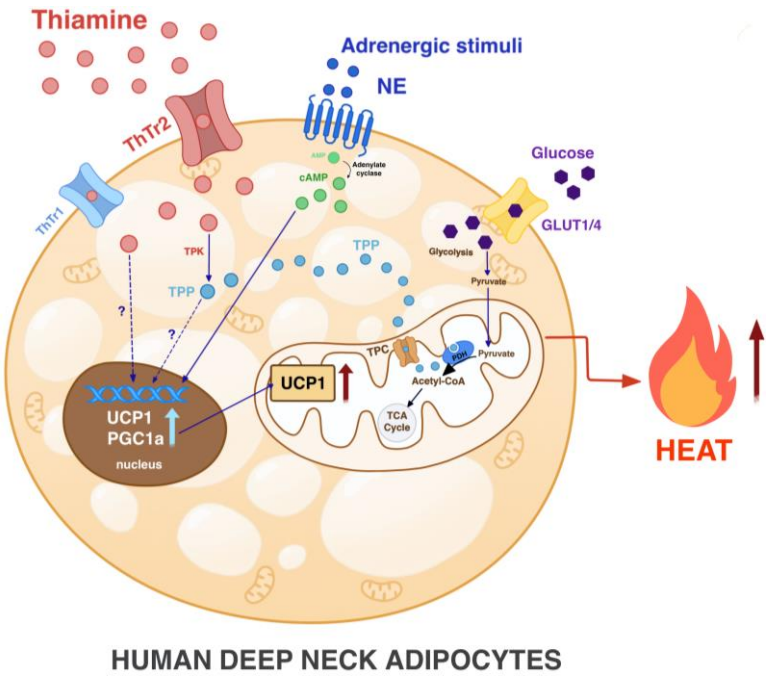

Figure 36. Abundant thiamine is required for efficient thermogenic activation in human neck derived adipocytes *[Arianti et al., 2022]*

- Abundance of thiamine is required for the efficient thermogenic response in human neck derived adipocytes during adrenergic stimulation. The inhibition of thiamine transport into the cells by applying potent inhibitors of the thiamine transporters led to the reduced oxygen consumption and proton leak respiration upon cAMP stimulation. The importance of thiamine availability during thermogenic activation was also proven when we applied thiamine free culture fluid and gradually increased the thiamine concentration. We found that thiamine enhanced the thermogenic activation of human neck adipocytes in a concentration-dependent manner.
- The activity of pyruvate dehydrogenase, which is thiamine pyrophosphate-dependent enzyme, can be enhanced by directly stimulating the cell membrane-permeabilized adipocytes with thiamine pyrophosphate and pyruvate dehydrogenase substrates. The UCP1-dependent proton leak respiration of permeabilized adipocytes was elevated by thiamine pyrophosphate. This indicates that excess thiamine converted to thiamine pyrophosphate during thermogenic activation can increase mitochondrial respiration and thermogenesis by

elevating the level of thiamine pyrophosphate bound enzymes and thereby NADH production.

- The expression of thermogenic markers during cAMP stimulation was also reduced when thiamine transport was inhibited by fedratinib and amprolium. In addition, we also found that thiamine potentiated the cAMP-stimulated thermogenic gene upregulation in a concentration-dependent manner.
- Thiamine deficiency, which is mainly caused by chronic alcohol consumption, leads to Wernicke-Korsakoff syndrome with hypothermia as a secondary symptom. Thiamine administration ameliorated the hypothermic condition suggesting the beneficial effect of thiamine in improving hypothalamic thermoregulation. Our presented data suggested that thiamine deficiency may also perturbs peripheral thermogenesis in thermogenic adipocytes contributing to hypothermia of Wernicke-Korsakoff syndrome patients.

10. References

Achari, A. E., & Jain, S. K. 2016. L-Cysteine supplementation increases adiponectin synthesis and secretion, and GLUT4 and glucose utilization by upregulating disulfide bond A-like protein expression mediated by MCP-1 inhibition in 3T3-L1 adipocytes exposed to high glucose. Molecular and Cellular Biochemistry 414: 105–113.

Ahn, J., Wu, H., & Lee, K. 2019. Integrative Analysis Revealing Human Adipose-Specific Genes and Consolidating Obesity Loci. Scientific Reports 9: 3087.

Alaei Shahmiri, F., Soares, M. J., Zhao, Y., & Sherriff, J. 2013. High-dose thiamine supplementation improves glucose tolerance in hyperglycemic individuals: a randomized, double-blind cross-over trial. European Journal of Nutrition 52: 1821–1824.

Al-Attas, O., Al-Daghri, N., Alokail, M., Abd-Alrahman, S., Vinodson, B., & Sabico, S. 2014. Metabolic benefits of six-month thiamine supplementation in patients with and without diabetes mellitus type 2. Clinical Medicine Insights Endocrinology and Diabetes 7: 1–6.

Anderson, C. M., & Stahl, A. 2013. SLC27 fatty acid transport proteins. Molecular Aspects of Medicine 34: 516–528.

Arianti, R., Vinnai, B. Á., Tóth, B. B., Shaw, A., Csősz, É., Vámos, A., Győry, F., Fischer-Posovszky, P., Wabitsch, M., Kristóf, E., & Fésüs, L. 2021. ASC-1 transporter-dependent amino acid uptake is required for the efficient thermogenic response of human adipocytes to adrenergic stimulation. FEBS Letters 595: 2085–2098.

Arianti, R., Vinnai, B. Á., Győry, F., M., Kristóf, E., & Fésüs, L. 2022. Availability of abundant thiamine determines efficiency of thermogenic activation in human neck area derived adipocytes. BioRxiv: https://doi.org/10.1101/2022.05.05.490662.

Aron-Wisnewsky, J., Verger, E. O., Bounaix, C., Dao, M. C., Oppert, J. M., Bouillot, J. L., Chevallier, J. M., & Clément, K. 2016. Nutritional and protein deficiencies in the short term following both gastric bypass and gastric banding. PloS One 11: e0149588.

Babaei-Jadidi, R., Karachalias, N., Kupich, C., Ahmed, N., & Thornalley, P. J. (2004). High-dose thiamine therapy counters dyslipidaemia in streptozotocin-induced diabetic rats. Diabetologia 47: 2235–2246.

Bal, N. C., Maurya, S. K., Sopariwala, D. H., Sahoo, S. K., Gupta, S. C., Shaikh, S. A., Pant, M., Rowland, L. A., Bombardier, E., Goonasekera, S. A., Tupling, A. R., Molkentin, J. D., & Periasamy, M. 2012. Sarcolipin is a newly identified regulator of muscle-based thermogenesis in mammals. Nature Medicine 18: 1575–1579.

Barneda, D., Frontini, A., Cinti, S., & Christian, M. 2013. Dynamic changes in lipid droplet-associated proteins in the "browning" of white adipose tissues. Biochimica et Biophysica Acta 1831: 924–933.

Beltramo, E., Mazzeo, A., Lopatina, T., Trento, M., & Porta, M. 2020. Thiamine transporter 2 is involved in high glucose-induced damage and altered thiamine availability in cell models of diabetic retinopathy. Diabetes & Vascular Disease Research 17: 1479164119878427.

Bertholet, A. M., & Kirichok, Y. 2017. UCP1: A transporter for H^+ and fatty acid anions. Biochimie 134: 28–34.

Boström, P., Wu, J., Jedrychowski, M. P., Korde, A., Ye, L., Lo, J. C., Rasbach, K. A., Boström, E. A., Choi, J. H., Long, J. Z., Kajimura, S., Zingaretti, M. C., Vind, B. F., Tu, H., Cinti, S., Højlund, K., Gygi, S. P., & Spiegelman, B. M. (2012). A PGC1-α-dependent myokine that drives brown-fat-like development of white fat and thermogenesis. Nature 481: 463–468.

Bouwman, F. G., Wang, P., van Baak, M., Saris, W. H., & Mariman, E. C. 2014. Increased β-oxidation with improved glucose uptake capacity in adipose tissue from obese after weight loss and maintenance. Obesity (Silver Spring, Md.) 22: 819–827.

Brown, J. M., Hunihan, L., Prack, M. M., Harden, D. G., Bronson, J., Dzierba, C. D., Gentles, R. G., Hendricson, A., Krause, R., Macor, J. E., & Westphal, R. S. 2014. In vitro Characterization of a small molecule inhibitor of the alanine serine cysteine transporter -1 (SLC7A10). Journal of Neurochemistry 129: 275–283.

Brychta, R. J., & Chen, K. Y. 2017. Cold-induced thermogenesis in humans. European Journal of Clinical Nutrition 7: 345–352.

Bunik, V. I., Tylicki, A., & Lukashev, N. V. 2013. Thiamin diphosphate-dependent enzymes: from enzymology to metabolic regulation, drug design and disease models. The FEBS journal 280: 6412–6442.

Cannon, B., & Nedergaard, J. 2004. Brown adipose tissue: function and physiological significance. Physiological Reviews 84: 277–359.

Carrodeguas, L., Kaidar-Person, O., Szomstein, S., Antozzi, P., & Rosenthal, R. 2005. Preoperative thiamine deficiency in obese population undergoing laparoscopic bariatric surgery. Surgery for Obesity and Related Diseases : Official Journal of the American Society for Bariatric Surgery 1: 517–522.

Casteels, M., Sniekers, M., Fraccascia, P., Mannaerts, G. P., & Van Veldhoven, P. P. 2007. The role of 2-hydroxyacyl-CoA lyase, a thiamin pyrophosphate-dependent enzyme, in the peroxisomal metabolism of 3-methyl-branched fatty acids and 2-hydroxy straight-chain fatty acids. Biochemical Society Transactions 35: 876–880.

Chang, S. H., Song, N. J., Choi, J. H., Yun, U. J., & Park, K. W. 2019. Mechanisms underlying UCP1 dependent and independent adipocyte thermogenesis. Obesity Reviews : An Official Journal of the International Association for the Study of Obesity 20: 241–251.

Chen, Y. D., Varasteh, B. B., & Reaven, G. M. 1993. Plasma lactate concentration in obesity and type 2 diabetes. Diabetes & Metabolism 19: 348–354.

Cheng, Y., Jiang, L., Keipert, S., Zhang, S., Hauser, A., Graf, E., Strom, T., Tschöp, M., Jastroch, M., & Perocchi, F. 2018. Prediction of adipose browning capacity by systematic integration of transcriptional profiles. Cell Reports 23: 3112–3125.

Chouchani, E. T., & Kajimura, S. 2019. Metabolic adaptation and maladaptation in adipose tissue. Nature Metabolism 1: 189–200.

Chouchani, E. T., Kazak, L., Jedrychowski, M. P., Lu, G. Z., Erickson, B. K., Szpyt, J., Pierce, K. A., Laznik-Bogoslavski, D., Vetrivelan, R., Clish, C. B., Robinson, A. J., Gygi, S. P., & Spiegelman, B. M. 2016. Mitochondrial ROS regulate thermogenic energy expenditure and sulfenylation of UCP1. Nature 532: 112–116.

Ciszak, E. M., Korotchkina, L. G., Dominiak, P. M., Sidhu, S., & Patel, M. S. 2003. Structural basis for flip-flop action of thiamin pyrophosphate-dependent enzymes revealed by human pyruvate dehydrogenase. The Journal of Biological Chemistry 278: 21240–21246.

Cohen, P., & Kajimura, S. 2021. The cellular and functional complexity of thermogenic fat. Nature Reviews. Molecular Cell Biology 22: 393–409.

Cook, C. C., Hallwood, P. M., & Thomson, A. D. 1998. B Vitamin deficiency and neuropsychiatric syndromes in alcohol misuse. Alcohol and Alcoholism 33: 317–336.

Cruickshank, A. M., Telfer, A. B., & Shenkin, A. 1988. Thiamine deficiency in the critically ill. Intensive Care Medicine 14: 384–387.

Cypess, A. M., Lehman, S., Williams, G., Tal, I., Rodman, D., Goldfine, A. B., Kuo, F. C., Palmer, E. L., Tseng, Y. H., Doria, A., Kolodny, G. M., & Kahn, C. R. 2009. Identification and importance of brown adipose tissue in adult humans. The New England Journal of Medicine 360: 1509–1517.

Cypess, A. M., White, A. P., Vernochet, C., Schulz, T. J., Xue, R., Sass, C. A., Huang, T. L., Roberts-Toler, C., Weiner, L. S., Sze, C., Chacko, A. T., Deschamps, L. N., Herder, L. M., Truchan, N., Glasgow, A. L., Holman, A. R., Gavrila, A., Hasselgren, P. O., Mori, M. A., Molla, M., … Tseng, Y. H. 2013. Anatomical localization, gene expression profiling and functional characterization of adult human neck brown fat. Nature Medicine 19: 635–639.

da Silva, R. P., Nissim, I., Brosnan, M. E., & Brosnan, J. T. 2009. Creatine synthesis: hepatic metabolism of guanidinoacetate and creatine in the rat in vitro and in vivo. American journal of physiology. Endocrinology and Metabolism 296: E256–E261.

de Koning, T. J., Snell, K., Duran, M., Berger, R., Poll-The, B. T., & Surtees, R. 2003. L-serine in disease and development. The Biochemical Journal 371: 653–661.

Donnino, M. W., Cocchi, M. N., Smithline, H., Carney, E., Chou, P. P., & Salciccioli, J. 2010. Coronary artery bypass graft surgery depletes plasma thiamine levels. Nutrition 26:133–136.

Dorn, J. M., Hovey, K., Muti, P., Freudenheim, J. L., Russell, M., Nochajski, T. H., & Trevisan, M. 2003. Alcohol drinking patterns differentially affect central adiposity as measured by abdominal height in women and men. The Journal of Nutrition 133: 2655–2662.

DosSantos, R. A., Alfadda, A., Eto, K., Kadowaki, T., & Silva, J. E. 2003. Evidence for a compensated thermogenic defect in transgenic mice lacking the mitochondrial glycerol-3-phosphate dehydrogenase gene. Endocrinology 144: 5469–5479.

El Bacha, T., Luz, M. & Da Poian, A. 2010. Dynamic adaptation of nutrient utilization in humans. Nature Education 3: 8.

Elabd, C., Chiellini, C., Carmona, M., Galitzky, J., Cochet, O., Petersen, R., Pénicaud, L., Kristiansen, K., Bouloumié, A., Casteilla, L., Dani, C., Ailhaud, G., & Amri, E. Z. 2009. Human

multipotent adipose-derived stem cells differentiate into functional brown adipocytes. Stem Cells 27:2753–2760.

Eudy, J. D., Spiegelstein, O., Barber, R. C., Wlodarczyk, B. J., Talbot, J., & Finnell, R. H. 2000. Identification and characterization of the human and mouse SLC19A3 gene: a novel member of the reduced folate family of micronutrient transporter genes. Molecular Genetics and Metabolism 71: 581–590.

Fedorenko, A., Lishko, P. V., & Kirichok, Y. 2012. Mechanism of fatty-acid-dependent UCP1 uncoupling in brown fat mitochondria. Cell 151: 400–413.

Felig P. 1973. The glucose-alanine cycle. Metabolism: Clinical and Experimental 22: 179–207.

Flancbaum, L., Belsley, S., Drake, V., Colarusso, T., & Tayler, E. 2006. Preoperative nutritional status of patients undergoing Roux-en-Y gastric bypass for morbid obesity. Journal of Gastrointestinal Surgery : Official Journal of the Society for Surgery of the Alimentary Tract 10:1033–1037.

Fleming, J. C., Tartaglini, E., Steinkamp, M. P., Schorderet, D. F., Cohen, N., & Neufeld, E. J. 1999. The gene mutated in thiamine-responsive anaemia with diabetes and deafness (TRMA) encodes a functional thiamine transporter. Nature Genetics 22: 305–308.

Ganapathy, V., Smith, S. B., & Prasad, P. D. 2004. SLC19: the folate/thiamine transporter family. Pflugers Archiv : European Journal of Physiology 447: 641–646.

Garcia, R. A., Roemmich, J. N., & Claycombe, K. J. 2016. Evaluation of markers of beige adipocytes in white adipose tissue of the mouse. Nutrition & Metabolism 13: 24.

Giacomini, M. M., Hao, J., Liang, X., Chandrasekhar, J., Twelves, J., Whitney, J. A., Lepist, E. I., & Ray, A. S. 2017. Interaction of 2,4-Diaminopyrimidine-Containing Drugs Including Fedratinib and Trimethoprim with Thiamine Transporters. Drug Metabolism and Disposition: the Biological Fate of Chemicals 45: 76–85.

Gonzalez-Hurtado, E., Lee, J., Choi, J., & Wolfgang, M. J. 2018. Fatty acid oxidation is required for active and quiescent brown adipose tissue maintenance and thermogenic programing. Molecular Metabolism 7: 45–56.

González-Ortiz, M., Martínez-Abundis, E., Robles-Cervantes, J. A., Ramírez-Ramírez, V., & Ramos-Zavala, M. G. 2011. Effect of thiamine administration on metabolic profile, cytokines and inflammatory markers in drug-naïve patients with type 2 diabetes. European Journal of Nutrition 50: 145–149.

Gritli, S., Omar, S., Tartaglini, E., Guannouni, S., Fleming, J. C., Steinkamp, M. P., Berul, C. I., Hafsia, R., Jilani, S. B., Belhani, A., Hamdi, M., & Neufeld, E. J. 2001. A novel mutation in the SLC19A2 gene in a Tunisian family with thiamine-responsive megaloblastic anaemia, diabetes and deafness syndrome. British Journal of Haematology 113: 508–513.

Haman, F., & Blondin, D. P. 2017. Shivering thermogenesis in humans: origin, contribution and metabolic requirement. Temperature 4: 217–226.

Hansen, B., Larsson, C., Wirén, J., & Hallgren, J. 1984. Hypothermia and infection in Wernicke's encephalopathy. Acta Medica Scandinavica 215: 185–187.

Harper, A. E., Miller, R. H., & Block, K. P. 1984. Branched-chain amino acid metabolism. Annual Review of Nutrition 4: 409–454.

Hediger, M. A., Clémençon, B., Burrier, R. E., & Bruford, E. A. 2013. The ABCs of membrane transporters in health and disease (SLC series): introduction. Molecular Aspects of Medicine 34: 95–107.

Herrmann, W., Schorr, H., Obeid, R., Makowski, J., Fowler, B., & Kuhlmann, M. K. 2005. Disturbed homocysteine and methionine cycle intermediates S-adenosylhomocysteine and S-adenosylmethionine are related to degree of renal insufficiency in type 2 diabetes. Clinical Chemistry 51: 891–897.

Hosokawa, H., Ninomiya, H., Sawamura, T., Sugimoto, Y., Ichikawa, A., Fujiwara, K., & Masaki, T. 1999. Neuron-specific expression of cationic amino acid transporter 3 in the adult rat brain. Brain Research 838: 158–165.

Ikeda, K., Kang, Q., Yoneshiro, T., Camporez, J. P., Maki, H., Homma, M., Shinoda, K., Chen, Y., Lu, X., Maretich, P., Tajima, K., Ajuwon, K. M., Soga, T., & Kajimura, S. 2017. UCP1-independent signaling involving SERCA2b-mediated calcium cycling regulates beige fat thermogenesis and systemic glucose homeostasis. Nature Medicine 23: 1454–1465.

Ikeda, K., Liu, X., Kida, K., Marutani, E., Hirai, S., Sakaguchi, M., Andersen, L. W., Bagchi, A., Cocchi, M. N., Berg, K. M., Ichinose, F., & Donnino, M. W. 2016. Thiamine as a neuroprotective agent after cardiac arrest. Resuscitation 105: 138–144.

Ito, K., & Groudine, M. 1997. A new member of the cationic amino acid transporter family is preferentially expressed in adult mouse brain. The Journal of Biological Chemistry 272: 26780–26786.

Jermendy G. 2006. Evaluating thiamine deficiency in patients with diabetes. Diabetes & Vascular Disease Research 3 120–121.

Jersin, R. Å., Tallapragada, D., Madsen, A., Skartveit, L., Fjære, E., McCann, A., Dyer, L., Willems, A., Bjune, J. I., Bjune, M. S., Våge, V., Nielsen, H. J., Thorsen, H. L., Nedrebø, B. G., Busch, C., Steen, V. M., Blüher, M., Jacobson, P., Svensson, P. A., Fernø, J., … Dankel, S. N. 2021. Role of the Neutral Amino Acid Transporter SLC7A10 in Adipocyte Lipid Storage, Obesity, and Insulin Resistance. Diabetes 70: 680–695.

Jespersen, N. Z., Larsen, T. J., Peijs, L., Daugaard, S., Homøe, P., Loft, A., de Jong, J., Mathur, N., Cannon, B., Nedergaard, J., Pedersen, B. K., Møller, K., & Scheele, C. 2013. A classical brown adipose tissue mRNA signature partly overlaps with brite in the supraclavicular region of adult humans. Cell Metabolism 17: 798–805.

Jung, R. T., Shetty, P. S., James, W. P., Barrand, M. A., & Callingham, B. A. 1979. Reduced thermogenesis in obesity. Nature 279: 322–323.

Kazak, L., Chouchani, E. T., Jedrychowski, M. P., Erickson, B. K., Shinoda, K., Cohen, P., Vetrivelan, R., Lu, G. Z., Laznik-Bogoslavski, D., Hasenfuss, S. C., Kajimura, S., Gygi, S. P., & Spiegelman, B. M. 2015. A creatine-driven substrate cycle enhances energy expenditure and thermogenesis in beige fat. Cell 163: 643–655.

Kazak, L., Chouchani, E. T., Lu, G. Z., Jedrychowski, M. P., Bare, C. J., Mina, A. I., Kumari, M., Zhang, S., Vuckovic, I., Laznik-Bogoslavski, D., Dzeja, P., Banks, A. S., Rosen, E. D., & Spiegelman, B. M. 2017. Genetic Depletion of Adipocyte Creatine Metabolism Inhibits Diet-Induced Thermogenesis and Drives Obesity. Cell Metabolism 26: 660–671.e3.

Kazantzis, M., & Stahl, A. 2012. Fatty acid transport proteins, implications in physiology and disease. Biochimica et Biophysica Acta 1821: 852–857.

Kenthirapalan, S., Waters, A. P., Matuschewski, K., & Kooij, T. W. 2016. Functional profiles of orphan membrane transporters in the life cycle of the malaria parasite. Nature Communications 7: 10519.

Kim, J. K., Gimeno, R. E., Higashimori, T., Kim, H. J., Choi, H., Punreddy, S., Mozell, R. L., Tan, G., Stricker-Krongrad, A., Hirsch, D. J., Fillmore, J. J., Liu, Z. X., Dong, J., Cline, G., Stahl, A., Lodish, H. F., & Shulman, G. I. 2004. Inactivation of fatty acid transport protein 1 prevents fat-induced insulin resistance in skeletal muscle. The Journal of Clinical Investigation 113: 756–763.

Kim, K. H., Oh, S. W., Kwon, H., Park, J. H., Choi, H., & Cho, B. 2012. Alcohol consumption and its relation to visceral and subcutaneous adipose tissues in healthy male Koreans. Annals of Nutrition & Metabolism 60: 52–61.

Kristóf, E., Doan-Xuan, Q. M., Bai, P., Bacso, Z., & Fésüs, L. 2015. Laser-scanning cytometry can quantify human adipocyte browning and proves effectiveness of irisin. Scientific Reports 5: 12540.

Lee, P., Linderman, J. D., Smith, S., Brychta, R. J., Wang, J., Idelson, C., Perron, R. M., Werner, C. D., Phan, G. Q., Kammula, U. S., Kebebew, E., Pacak, K., Chen, K. Y., & Celi, F. S. 2014. Irisin and FGF21 are cold-induced endocrine activators of brown fat function in humans. Cell Metabolism 19: 302–309.

Leitner, B. P., Huang, S., Brychta, R. J., Duckworth, C. J., Baskin, A. S., McGehee, S., Tal, I., Dieckmann, W., Gupta, G., Kolodny, G. M., Pacak, K., Herscovitch, P., Cypess, A. M., & Chen, K. Y. 2017. Mapping of human brown adipose tissue in lean and obese young men. Proceedings of the National Academy of Sciences of the U S A 114: 8649–8654.

Lidell, M. E., Betz, M. J., Dahlqvist Leinhard, O., Heglind, M., Elander, L., Slawik, M., Mussack, T., Nilsson, D., Romu, T., Nuutila, P., Virtanen, K. A., Beuschlein, F., Persson, A., Borga, M., & Enerbäck, S. 2013. Evidence for two types of brown adipose tissue in humans. Nature Medicine 19: 631–634.

Long, J. Z., Svensson, K. J., Bateman, L. A., Lin, H., Kamenecka, T., Lokurkar, I. A., Lou, J., Rao, R. R., Chang, M. R., Jedrychowski, M. P., Paulo, J. A., Gygi, S. P., Griffin, P. R., Nomura, D. K., & Spiegelman, B. M. 2016. The Secreted Enzyme PM20D1 Regulates Lipidated Amino Acid Uncouplers of Mitochondria. Cell 166: 424–435.

Losa, R., Sierra, M. I., Fernández, A., Blanco, D., & Buesa, J. M. 2005. Determination of thiamine and its phosphorylated forms in human plasma, erythrocytes and urine by HPLC and fluorescence detection: a preliminary study on cancer patients. Journal of Pharmaceutical and Biomedical Analysis 37: 1025–1029.

Lovejoy, J., Mellen, B., & Digirolamo, M. 1990. Lactate generation following glucose ingestion: relation to obesity, carbohydrate tolerance and insulin sensitivity. International Journal of Obesity 14: 843–855.

Lu S. C. 2009. Regulation of glutathione synthesis. Molecular Aspects of Medicine 30: 42–59.

Lucas, S., Chen, G., Aras, S., & Wang, J. 2018. Serine catabolism is essential to maintain mitochondrial respiration in mammalian cells. Life Science Alliance 1: e201800036.

Maguire, D., Talwar, D., Shiels, P. G., & McMillan, D. 2018. The role of thiamine dependent enzymes in obesity and obesity related chronic disease states: A systematic review. Clinical Nutrition ESPEN 25: 8–17.

Manimaran, P., Subramanian, V. S., Karthi, S., Gandhimathi, K., Varalakshmi, P., Ganesh, R., Rathinavel, A., Said, H. M., & Ashokkumar, B. 2016. Novel nonsense mutation (p.Ile411Metfs*12) in the SLC19A2 gene causing Thiamine Responsive Megaloblastic Anemia in an Indian patient. Clinica Chimica Acta; International Journal of Clinical Chemistry 452: 44–49.

Manzanares, W., & Hardy, G. 2011. Thiamine supplementation in the critically ill. Current Opinion in Clinical Nutrition and Metabolic Care 14: 610–617.

Marcé-Grau, A., Martí-Sánchez, L., Baide-Mairena, H., Ortigoza-Escobar, J. D., & Pérez-Dueñas, B. 2019. Genetic defects of thiamine transport and metabolism: A review of clinical phenotypes, genetics, and functional studies. Journal of Inherited Metabolic Disease 42: 581–597.

McCarthy M. J. 2014. Oxidative stress: a link between cardiovascular disease and psychiatric illness?. Acta Psychiatrica Scandinavica 130: 161–162.

McLure, K. G., Takagi, M., & Kastan, M. B. 2004. NAD+ modulates p53 DNA binding specificity and function. Molecular and Cellular Biology 24: 9958–9967.

Meier, C., Ristic, Z., Klauser, S., & Verrey, F. 2002. Activation of system L heterodimeric amino acid exchangers by intracellular substrates. The EMBO Journal 21: 580–589.

Melé, M., Ferreira, P. G., Reverter, F., DeLuca, D. S., Monlong, J., Sammeth, M., Young, T. R., Goldmann, J. M., Pervouchine, D. D., Sullivan, T. J., Johnson, R., Segrè, A. V., Djebali, S., Niarchou, A., GTEx Consortium, Wright, F. A., Lappalainen, T., Calvo, M., Getz, G., Dermitzakis, E. T., … Guigó, R. 2015. Human genomics. The human transcriptome across tissues and individuals. Science 348: 660–665.

Mikulás, K., Hermann, P., Gera, I., Komlódi, T., Horváth, G., Ambrus, A., & Tretter, L. 2018. Triethylene glycol dimethacrylate impairs bioenergetic functions and induces oxidative stress in mitochondria via inhibiting respiratory Complex I. Dental Materials : Official Publication of the Academy of Dental Materials 34: e166–e181.

Mills, E. L., Pierce, K. A., Jedrychowski, M. P., Garrity, R., Winther, S., Vidoni, S., Yoneshiro, T., Spinelli, J. B., Lu, G. Z., Kazak, L., Banks, A. S., Haigis, M. C., Kajimura, S., Murphy, M. P., Gygi, S. P., Clish, C. B., & Chouchani, E. T. 2018. Accumulation of succinate controls activation of adipose tissue thermogenesis. Nature 560: 102–106.

Min, S. Y., Desai, A., Yang, Z., Sharma, A., DeSouza, T., Genga, R., Kucukural, A., Lifshitz, L. M., Nielsen, S., Scheele, C., Maehr, R., Garber, M., & Corvera, S. 2019. Diverse repertoire of human adipocyte subtypes develops from transcriptionally distinct mesenchymal progenitor cells. Proceedings of the National Academy of Sciences of the U S A 116: 17970–17979.

Monemdjou, S., Kozak, L. P., & Harper, M. E. 1999. Mitochondrial proton leak in brown adipose tissue mitochondria of Ucp1-deficient mice is GDP insensitive. The American Journal of Physiology 276: E1073–E1082.

Mráček, T., Holzerová, E., Drahota, Z., Kovářová, N., Vrbacký, M., Ješina, P., & Houštěk, J. 2014. ROS generation and multiple forms of mammalian mitochondrial glycerol-3-phosphate dehydrogenase. Biochimica et Biophysica Acta 1837: 98–111.

Mueckler, M., & Thorens, B. 2013. The SLC2 (GLUT) family of membrane transporters. Molecular Aspects of Medicine 34: 121–138.

Nascimento, E., Sparks, L. M., Divoux, A., van Gisbergen, M. W., Broeders, E., Jörgensen, J. A., Schaart, G., Bouvy, N. D., van Marken Lichtenbelt, W. D., & Schrauwen, P. 2018. Genetic Markers of Brown Adipose Tissue Identity and In Vitro Brown Adipose Tissue Activity in Humans. Obesity 26: 135–140.

Nath, A., Tran, T., Shope, T. R., & Koch, T. R. 2017. Prevalence of clinical thiamine deficiency in individuals with medically complicated obesity. Nutrition Research 37: 29–36.

Noguchi, S., Kondo, Y., Ito, R., Katayama, T., Kazama, S., Kadota, Y., Kitaura, Y., Harris, R. A., & Shimomura, Y. 2018. Ca^{2+}-dependent inhibition of branched-chain α-ketoacid dehydrogenase kinase by thiamine pyrophosphate. Biochemical and Biophysical Research communications 504: 916–920.

Ortigoza-Escobar, J. D., Alfadhel, M., Molero-Luis, M., Darin, N., Spiegel, R., de Coo, I. F., Gerards, M., Taylor, R. W., Artuch, R., Nashabat, M., Rodríguez-Pombo, P., Tabarki, B., Pérez-Dueñas, B., & Thiamine Deficiency Study Group. 2017. Thiamine deficiency in childhood with attention to genetic causes: Survival and outcome predictors. Annals of Neurology 82: 317–330.

Ortigoza-Escobar, J. D., Molero-Luis, M., Arias, A., Martí-Sánchez, L., Rodriguez-Pombo, P., Artuch, R., & Pérez-Dueñas, B. 2016. Treatment of genetic defects of thiamine transport and metabolism. Expert Review of Neurotherapeutics 16: 755–763.

Ozand, P. T., Gascon, G. G., Al Essa, M., Joshi, S., Al Jishi, E., Bakheet, S., Al Watban, J., Al-Kawi, M. Z., & Dabbagh, O. 1998. Biotin-responsive basal ganglia disease: a novel entity. Brain : A Journal of Neurology 121: 1267–1279.

Panic, V., Pearson, S., Banks, J., Tippetts, T. S., Velasco-Silva, J. N., Lee, S., Simcox, J., Geoghegan, G., Bensard, C. L., van Ry, T., Holland, W. L., Summers, S. A., Cox, J., Ducker, G. S., Rutter, J., & Villanueva, C. J. 2020. Mitochondrial pyruvate carrier is required for optimal brown fat thermogenesis. eLife 9: e52558.

Pei, Z., Fraisl, P., Berger, J., Jia, Z., Forss-Petter, S., & Watkins, P. A. 2004. Mouse very long-chain Acyl-CoA synthetase 3/fatty acid transport protein 3 catalyzes fatty acid activation but not fatty acid transport in MA-10 cells. The Journal of Biological Chemistry 279: 54454–54462.

Perdikari, A., Leparc, G. G., Balaz, M., Pires, N. D., Lidell, M. E., Sun, W., Fernandez-Albert, F., Müller, S., Akchiche, N., Dong, H., Balazova, L., Opitz, L., Röder, E., Klein, H., Stefanicka, P., Varga, L., Nuutila, P., Virtanen, K. A., Niemi, T., Taittonen, M., … Wolfrum, C. 2018. BATLAS: deconvoluting brown adipose tissue. Cell Reports 25: 784–797.

Pereira, M. J., Andersson-Assarsson, J. C., Jacobson, P., Kamble, P., Taube, M., Sjöholm, K., Carlsson, L., & Svensson, P. A. 2021. Human adipose tissue gene expression of solute carrier family 19 member 3 (SLC19A3); relation to obesity and weight-loss. Obesity Science & Practice 8: 21–31.

Perkins, C. P., Mar, V., Shutter, J. R., del Castillo, J., Danilenko, D. M., Medlock, E. S., Ponting, I. L., Graham, M., Stark, K. L., Zuo, Y., Cunningham, J. M., & Bosselman, R. A. 1997. Anemia and perinatal death result from loss of the murine ecotropic retrovirus receptor mCAT-1. Genes & Development 11: 914–925.

Peterson, L. A., Cheskin, L. J., Furtado, M., Papas, K., Schweitzer, M. A., Magnuson, T. H., & Steele, K. E. 2016. Malnutrition in bariatric surgery candidates: multiple micronutrient deficiencies prior to surgery. Obesity Surgery 26: 833–838.

Purcell, S. H., Aerni-Flessner, L. B., Willcockson, A. R., Diggs-Andrews, K. A., Fisher, S. J., & Moley, K. H. 2011. Improved insulin sensitivity by GLUT12 overexpression in mice. Diabetes, 60: 1478–1482.

Puxty, J. A., Haskew, A. E., Ratcliffe, J. G., & McMurray, J. 1985. Changes in erythrocyte transketolase activity and the thiamine pyrophosphate effect during storage of blood. Annals of Clinical Biochemistry 22: 423–427.

Rahbani, J. F., Roesler, A., Hussain, M. F., Samborska, B., Dykstra, C. B., Tsai, L., Jedrychowski, M. P., Vergnes, L., Reue, K., Spiegelman, B. M., & Kazak, L. 2021. Creatine kinase B controls futile creatine cycling in thermogenic fat. Nature 590: 480–485.

Reidling, J. C., Lambrecht, N., Kassir, M., & Said, H. M. 2010. Impaired intestinal vitamin B1 (thiamin) uptake in thiamin transporter-2-deficient mice. Gastroenterology 138: 1802–1809.

Rosenbaum, M., & Leibel, R. L. 2010. Adaptive thermogenesis in humans. International Journal of Obesity 34: S47–S55.

Rosenberg, D., Artoul, S., Segal, A. C., Kolodney, G., Radzishevsky, I., Dikopoltsev, E., Foltyn, V. N., Inoue, R., Mori, H., Billard, J. M., & Wolosker, H. 2013. Neuronal D-serine and glycine release via the Asc-1 transporter regulates NMDA receptor-dependent synaptic activity. The Journal of Neuroscience 33: 3533–3544.

Ruas, J. S., Siqueira-Santos, E. S., Amigo, I., Rodrigues-Silva, E., Kowaltowski, A. J., & Castilho, R. F. 2016. Underestimation of the maximal capacity of the mitochondrial electron transport system in oligomycin-treated cells. PloS one 11: e0150967.

Rutter, A. R., Fradley, R. L., Garrett, E. M., Chapman, K. L., Lawrence, J. M., Rosahl, T. W., & Patel, S. 2007. Evidence from gene knockout studies implicates Asc-1 as the primary transporter mediating d-serine reuptake in the mouse CNS. The European Journal of Neuroscience 25: 1757–1766.

Said, H. M., Balamurugan, K., Subramanian, V. S., & Marchant, J. S. 2004. Expression and functional contribution of hTHTR-2 in thiamin absorption in human intestine. American journal of physiology. Gastrointestinal and Liver Physiology 286: G491–G498.

Saito, N., Kimura, M., Kuchiba, A., & Itokawa, Y. 1987. Blood thiamine levels in outpatients with diabetes mellitus. Journal of Nutritional Science and Vitaminology 33: 421–430.

Sakers, A., De Siqueira, M. K., Seale, P., & Villanueva, C. J. 2022. Adipose-tissue plasticity in health and disease. Cell 185: 419–446.

Salisbury, E. A., Lazard, Z. W., Ubogu, E. E., Davis, A. R., & Olmsted-Davis, E. A. 2012. Transient brown adipocyte-like cells derive from peripheral nerve progenitors in response to bone morphogenetic protein 2. Stem Cells Translational Medicine 1: 874–885.

Scharfe, C., Hauschild, M., Klopstock, T., Janssen, A. J., Heidemann, P. H., Meitinger, T., & Jaksch, M. 2000. A novel mutation in the thiamine responsive megaloblastic anaemia gene SLC19A2 in a patient with deficiency of respiratory chain complex I. Journal of Medical Genetics 37: 669–673.

Seale, P., Kajimura, S., Yang, W., Chin, S., Rohas, L. M., Uldry, M., Tavernier, G., Langin, D., & Spiegelman, B. M. 2007. Transcriptional control of brown fat determination by PRDM16. Cell Metabolism 6: 38–54.

Seiler, S. E., Xu, D., Ho, J. P., Lo, K. A., Buehrer, B. M., Ludlow, Y. J., Kovalik, J. P., & Sun, L. 2015. Characterization of a primary brown adipocyte culture system derived from human fetal interscapular fat. Adipocyte 4: 303–310.

Sharp, L. Z., Shinoda, K., Ohno, H., Scheel, D. W., Tomoda, E., Ruiz, L., Hu, H., Wang, L., Pavlova, Z., Gilsanz, V., & Kajimura, S. 2012. Human BAT possesses molecular signatures that resemble beige/brite cells. PloS One 7: e49452.

Shi, S. Y., Zhang, W., Luk, C. T., Sivasubramaniyam, T., Brunt, J. J., Schroer, S. A., Desai, H. R., Majerski, A., & Woo, M. 2016. JAK2 promotes brown adipose tissue function and is required for diet- and cold-induced thermogenesis in mice. Diabetologia 59: 187–196.

Shinoda, K., Luijten, I. H., Hasegawa, Y., Hong, H., Sonne, S. B., Kim, M., Xue, R., Chondronikola, M., Cypess, A. M., Tseng, Y. H., Nedergaard, J., Sidossis, L. S., & Kajimura, S. 2015. Genetic and functional characterization of clonally derived adult human brown adipocytes. Nature Medicine 21: 389–394.

Singh, A. M., Zhang, L., Avery, J., Yin, A., Du, Y., Wang, H., Li, Z., Fu, H., Yin, H., & Dalton, S. 2020. Human beige adipocytes for drug discovery and cell therapy in metabolic diseases. Nature Communications 11: 2758.

Sperandeo, M. P., Borsani, G., Incerti, B., Zollo, M., Rossi, E., Zuffardi, O., Castaldo, P., Taglialatela, M., Andria, G., & Sebastio, G. 1998. The gene encoding a cationic amino acid transporter (SLC7A4) maps to the region deleted in the velocardiofacial syndrome. Genomics 49: 230–236.

Sun, Y., Rahbani, J. F., Jedrychowski, M. P., Riley, C. L., Vidoni, S., Bogoslavski, D., Hu, B., Dumesic, P. A., Zeng, X., Wang, A. B., Knudsen, N. H., Kim, C. R., Marasciullo, A., Millán, J.

L., Chouchani, E. T., Kazak, L., & Spiegelman, B. M. 2021. Mitochondrial TNAP controls thermogenesis by hydrolysis of phosphocreatine. Nature 593: 580–585.

Suwandhi, L., Altun, I., Karlina, R., Miok, V., Wiedemann, T., Fischer, D., Walzthoeni, T., Lindner, C., Böttcher, A., Heinzmann, S. S., Israel, A., Khalil, A., Braun, A., Pramme-Steinwachs, I., Burtscher, I., Schmitt-Kopplin, P., Heinig, M., Elsner, M., Lickert, H., Theis, F. J., … Ussar, S. 2021. Asc-1 regulates white versus beige adipocyte fate in a subcutaneous stromal cell population. Nature Communications 12: 1588.

Svensson, P. A., Jernås, M., Sjöholm, K., Hoffmann, J. M., Nilsson, B. E., Hansson, M., & Carlsson, L. M. 2011. Gene expression in human brown adipose tissue. International Journal of Molecular Medicine 27: 227–232.

Talwar, D., Davidson, H., Cooney, J., & St JO'Reilly, D. 2000. Vitamin B(1) status assessed by direct measurement of thiamin pyrophosphate in erythrocytes or whole blood by HPLC: comparison with erythrocyte transketolase activation assay. Clinical Chemistry 46: 704–710.

Tanaka, T., Kono, T., Terasaki, F., Yasui, K., Soyama, A., Otsuka, K., Fujita, S., Yamane, K., Manabe, M., Usui, K., & Kohda, Y. 2010. Thiamine prevents obesity and obesity-associated metabolic disorders in OLETF rats. Journal of Nutritional Science and Vitaminology 56: 335–346.

Tanev, K. S., Roether, M., & Yang, C. 2008. Alcohol dementia and thermal dysregulation: a case report and review of the literature. American Journal of Alzheimer's Disease and Other Dementias 23: 563–570.

Thornalley, P. J., Babaei-Jadidi, R., Al Ali, H., Rabbani, N., Antonysunil, A., Larkin, J., Ahmed, A., Rayman, G., & Bodmer, C. W. 2007. g. Diabetologia 50: 2164–2170.

Thurnham, D.I. 2013. Thiamin: physiology. Encycl. Hum. Nutrition 4: 274–279

Tittmann K. 2009. Thiamin diphosphate in biological chemistry: applications in biocatalysis, coenzyme analogues as mechanistic probes and natural derivatives of thiamin. The FEBS journal, 276(11), 2893.

Tóth, B. B., Arianti, R., Shaw, A., Vámos, A., Veréb, Z., Póliska, S., Győry, F., Bacso, Z., Fésüs, L., & Kristóf, E. 2020. FTO Intronic SNP Strongly Influences Human Neck Adipocyte Browning Determined by Tissue and PPARγ Specific Regulation: A Transcriptome Analysis. Cells 9: 987.

Townsend, K. L., & Tseng, Y. H. 2014. Brown fat fuel utilization and thermogenesis. Trends in Endocrinology and Metabolism: TEM 25: 168–177.

Tseng, Y. H., Kokkotou, E., Schulz, T. J., Huang, T. L., Winnay, J. N., Taniguchi, C. M., Tran, T. T., Suzuki, R., Espinoza, D. O., Yamamoto, Y., Ahrens, M. J., Dudley, A. T., Norris, A. W., Kulkarni, R. N., & Kahn, C. R. 2008. New role of bone morphogenetic protein 7 in brown adipogenesis and energy expenditure. Nature 454: 1000–1004.

Tvrdik, P., Asadi, A., Kozak, L. P., Nedergaard, J., Cannon, B., & Jacobsson, A. 1997. Cig30, a mouse member of a novel membrane protein gene family, is involved in the recruitment of brown adipose tissue. The Journal of Biological Chemistry 272: 31738–31746.

Ukropec, J., Anunciado, R. P., Ravussin, Y., Hulver, M. W., & Kozak, L. P. 2006. UCP1-independent thermogenesis in white adipose tissue of cold-acclimated Ucp1-/- mice. The Journal of Biological Chemistry 281: 31894–31908.

Ussar, S., Lee, K. Y., Dankel, S. N., Boucher, J., Haering, M. F., Kleinridders, A., Thomou, T., Xue, R., Macotela, Y., Cypess, A. M., Tseng, Y. H., Mellgren, G., & Kahn, C. R. 2014. ASC-1, PAT2, and P2RX5 are cell surface markers for white, beige, and brown adipocytes. Science Translational Medicine 6: 247ra103.

van Marken Lichtenbelt, W. D., & Schrauwen, P. 2011. Implications of nonshivering thermogenesis for energy balance regulation in humans. American Journal of Physiology 301: R285–R296.

Verrey, F., Closs, E. I., Wagner, C. A., Palacin, M., Endou, H., & Kanai, Y. 2004. CATs and HATs: the SLC7 family of amino acid transporters. Pflugers Archiv : European Journal of Physiology 447: 532–542.

Villarroya, F., Peyrou, M., & Giralt, M. 2017. Transcriptional regulation of the uncoupling protein-1 gene. Biochimie 134: 86–92.

Villarroya, F., Peyrou, M., & Giralt, M. 2017. Transcriptional regulation of the uncoupling protein-1 gene. Biochimie 134: 86–92.

Virtanen, K. A., Lidell, M. E., Orava, J., Heglind, M., Westergren, R., Niemi, T., Taittonen, M., Laine, J., Savisto, N. J., Enerbäck, S., & Nuutila, P. 2009. Functional brown adipose tissue in healthy adults. The New England Journal of Medicine 360: 1518–1525.

Wade, G., McGahee, A., Ntambi, J. M., & Simcox, J. 2021. Lipid transport in brown adipocyte thermogenesis. Frontiers in Physiology 12: 787535.

Waldén, T. B., Hansen, I. R., Timmons, J. A., Cannon, B., & Nedergaard, J. 2012. Recruited vs. nonrecruited molecular signatures of brown, "brite," and white adipose tissues. American journal of physiology. Endocrinology and Metabolism 302: E19–E31.

Wang, W., Kissig, M., Rajakumari, S., Huang, L., Lim, H. W., Won, K. J., & Seale, P. 2014. Ebf2 is a selective marker of brown and beige adipogenic precursor cells. Proceedings of the National Academy of Sciences of the United States of America 111: 14466–14471.

Weir, G., Ramage, L. E., Akyol, M., Rhodes, J. K., Kyle, C. J., Fletcher, A. M., Craven, T. H., Wakelin, S. J., Drake, A. J., Gregoriades, M. L., Ashton, C., Weir, N., van Beek, E., Karpe, F., Walker, B. R., & Stimson, R. H. 2018. Substantial Metabolic Activity of Human Brown Adipose Tissue during Warm Conditions and Cold-Induced Lipolysis of Local Triglycerides. Cell Metabolism 27: 1348–1355.e4.

Whitfield, K. C., Bourassa, M. W., Adamolekun, B., Bergeron, G., Bettendorff, L., Brown, K. H., Cox, L., Fattal-Valevski, A., Fischer, P. R., Frank, E. L., Hiffler, L., Hlaing, L. M., Jefferds, M. E., Kapner, H., Kounnavong, S., Mousavi, M., Roth, D. E., Tsaloglou, M. N., Wieringa, F., & Combs, G. F., Jr. 2018. Thiamine deficiency disorders: diagnosis, prevalence, and a roadmap for global control programs. Annals of the New York Academy of Sciences 1430: 3–43.

World Health Organization. 2021. Obesity and overweight. www.who.int/health-topics/obesity

Wu, J., Boström, P., Sparks, L. M., Ye, L., Choi, J. H., Giang, A. H., Khandekar, M., Virtanen, K. A., Nuutila, P., Schaart, G., Huang, K., Tu, H., van Marken Lichtenbelt, W. D., Hoeks, J., Enerbäck, S., Schrauwen, P., & Spiegelman, B. M. 2012. Beige adipocytes are a distinct type of thermogenic fat cell in mouse and human. Cell 150: 366–376.

Wu, Q., Kazantzis, M., Doege, H., Ortegon, A. M., Tsang, B., Falcon, A., & Stahl, A. 2006. Fatty acid transport protein 1 is required for nonshivering thermogenesis in brown adipose tissue. Diabetes 55: 3229–3237.

Wu, Y., Dong, Y., Atefi, M., Liu, Y., Elshimali, Y., & Vadgama, J. V. 2016. Lactate, a neglected factor for diabetes and cancer interaction. Mediators of Inflammation 2016: 6456018.

Xian, X., Liao, L., Shu, W., Li, H., Qin, Y., Yan, J., Luo, J., & Lin, F. Q. 2018. A Novel Mutation of SLC19A2 in a Chinese Zhuang Ethnic Family with Thiamine-Responsive Megaloblastic Anemia. Cellular Physiology and Biochemistry : International Journal of Experimental Cellular Physiology, Biochemistry, and Pharmacology 47: 1989–1997.

Yan, R., Zhao, X., Lei, J., & Zhou, Q. 2019. Structure of the human LAT1-4F2hc heteromeric amino acid transporter complex. Nature 568: 127–130.

Yang, Q., Graham, T. E., Mody, N., Preitner, F., Peroni, O. D., Zabolotny, J. M., Kotani, K., Quadro, L., & Kahn, B. B. 2005. Serum retinol binding protein 4 contributes to insulin resistance in obesity and type 2 diabetes. Nature 436: 356–362.

Yoneshiro, T., Wang, Q., Tajima, K., Matsushita, M., Maki, H., Igarashi, K., Dai, Z., White, P. J., McGarrah, R. W., Ilkayeva, O. R., Deleye, Y., Oguri, Y., Kuroda, M., Ikeda, K., Li, H., Ueno, A., Ohishi, M., Ishikawa, T., Kim, K., Chen, Y., Sponton, C. H., Pradhan, R. N., Majd, H., Greiner, V. J., Yoneshiro, M., Brown, Z., Chondronikola, M., Takahashi, H., Goto, T., Kawada, T., Sidossis, L., Szoka, F. C., McManus, M. T., Saito, M., Soga, T., Kajimura, S. 2019. BCAA catabolism in brown fat controls energy homeostasis through SLC25A44. Nature 572: 614–619.

Zachar, Z., Marecek, J., Maturo, C., Gupta, S., Stuart, S. D., Howell, K., Schauble, A., Lem, J., Piramzadian, A., Karnik, S., Lee, K., Rodriguez, R., Shorr, R., & Bingham, P. M. 2011. Non-redox-active lipoate derivates disrupt cancer cell mitochondrial metabolism and are potent anticancer agents in vivo. Journal of Molecular Medicine 89: 1137–1148.

Zhang, Q., Zhang, Y., Diamond, S., Boer, J., Harris, J. J., Li, Y., Rupar, M., Behshad, E., Gardiner, C., Collier, P., Liu, P., Burn, T., Wynn, R., Hollis, G., & Yeleswaram, S. 2014. The Janus kinase 2 inhibitor fedratinib inhibits thiamine uptake: a putative mechanism for the onset of Wernicke's encephalopathy. Drug metabolism and disposition: the biological fate of chemicals, 42(10), 1656–1662.

Zhang, Y., Zhang, Y., Sun, K., Meng, Z., & Chen, L. 2019. The SLC transporter in nutrient and metabolic sensing, regulation, and drug development. Journal of Molecular Cell Biology 11: 1–13.

Zhou, X., He, L., Wu, C., Zhang, Y., Wu, X., & Yin, Y. 2017. Serine alleviates oxidative stress via supporting glutathione synthesis and methionine cycle in mice. Molecular Nutrition & Food Research 61: 10.1002/mnfr.201700262.

11. Acknowledgements

I would like to express my sincere gratitude to my supervisor, Prof. Dr. László Fésüs for the excellent and extraordinary training, support (both mentally and financially in regards of science), motivation to excell the soft skills, scientific discussions (mainly during the journal club and our meetings), and exceptional inspiration during my PhD study. I am forever thankful for the opportunity to join his research group and learn many things throughout my PhD study. It is an honor to me to work under his supervision. I want to thank him for being a very reliable supervisor and for the very warm welcome since my first day in Debrecen.

I also would like to thank my senior colleague and tutor, Dr. Endre Kristóf for the countless help, constructive advice, and scientific discussions throughout my PhD. I got a lot of useful inputs from him thus the research projects can be performed efficiently. I want to thank him for being a dependable senior colleague and teaching me many useful techniques.

Many thanks to my colleague and best friend, Boglárka Ágnes Vinnai for helping me to perform gene expression analysis and cell culture thus I can finish our projects more efficiently. Thank you for being a very good tandem of me in the lab.

I am especially grateful to my colleague, best friend, and big brother, Dr. Károly Jambrovics for his helps and companion during my PhD. He teaches and introduces many techniques to me, both manual lab works and data analysis. I am thankful for our unofficial scientific discussion during weekend in our regular coffee shop.

An exceptional gratitude for Jennifer Nagy who provided a great assistance throughout my PhD study. I could perform all of the experiments because she prepared all the critical components. Thank you for being a very reliable person in our lab.

Many thanks to all of my PhD fellows, Dr. Kinga Fedor-Lénárt, Dr. Zsuzsa Csoban-Szabó, Dr. Abhirup Shaw, Attila Vámos, and Bianka Csaholczi for a friendly and warm working atmosphere in our lab. All of you made my PhD life in a foreign country much easier and more bearable.

I also want to thank Prof. Dr. József Tőzsér, current Head of the Department of Biochemistry and Molecular Biology for the opportunity to work in a this institute.

Special thanks to Dr. Ferenc Győry and the surgery group at the Auguszta Surgery Center of the University of Debrecen, Faculty of Medicine, for providing human neck tissue samples. Many thanks to Dr. Szilárd Póliska for the help in RNA-Sequencing analysis. Thanks to our collaborators from University Medical Center Ulm, Germany: Pamela Fischer-Posovszky and Martin Wabitsch for providing SGBS cell line, also to Dr. Éva Csősz from Proteomic Core Centre Facility, University of Debrecen for metabolomics analysis.

Many thanks to Gyula Ujlaki for our fruitful discussions from cellular to universal level and encouragement throughout my PhD study.

Special thanks to Dr. Abdelmalek Taoutioui for the personal support, motivation, and inter-dicipline scientific discussion. I am grateful for our special friendship.

To Indonesian and Malaysian students in Debrecen, thank you for the friendship and warm atmosphere during our gathering thus Debrecen feels like home.

To my best friends: Nikita, Luke Sekar Andari, Reviona Dwian Rahayu, Agci Hikmawati, Fini Anggraini, Burhannudin, M. Ikhsan, and Reyhan Bagaskara, thank you for our long-last beautiful friendship and for always having my back during my difficult times.

Lastly, but this is the most important part of the acknowledgements, I would like to thank my parents, Mr. Markoriansyah and Mrs. Hoziah, for giving me all the best things in this world, giving me wings to fly high, and encouraging me to conquer the difficult times. To my sisters and their husbands, Siskha Jayanti, Indah Dwi Julianti, and Rhela Riliziah; Firmansyah Putra, Rio Adi Saputra, and Muhammad Zulivan, thank you for believing in me and bringing joys into my life. To my fairy-god parents, Mr. Djamatullah and Mrs. Feri Wijayanti, and sisters Ghalda Anisah and Mulia Nur Alisya, thank you for always having my back and caring about me.

My PhD study was supported by Hungarian Government through Stipendium Hungaricum program. I was also supported by Indonesian Education Scholarship (LPDP Indonesia) for completing my dissertation. This research was funded by the European Union and the European Regional Development Fund (GINOP-2.3.2-15-2016-00006) and the National Research, Development and Innovation Office (NKFIH-FK131424 and K129139) of Hungary.

12. Publications and Attended Conference

UNIVERSITY of DEBRECEN

UNIVERSITY AND NATIONAL LIBRARY
UNIVERSITY OF DEBRECEN
H-4002 Egyetem tér 1, Debrecen
Phone: +3652/410-443, email: publikaciok@lib.unideb.hu

Registry number: DEENK/229/2022.PL
Subject: PhD Publication List

Candidate: Rini Arianti
Doctoral School: Doctoral School of Molecular Cellular and Immune Biology

List of publications related to the dissertation

1. **Arianti, R.**, Vinnai, B. Á., Bartáné Tóth, B., Shaw, A., Csősz, É., Vámos, A., Győry, F., Fischer-Posovszky, P., Wabitsch, M., Kristóf, E., Fésüs, L.: ASC-1 transporter-dependent amino acid uptake is required for the efficient thermogenic response of human adipocytes to adrenergic stimulation.
   FEBS Lett. 595 (16), 2085-2098, 2021.
   DOI: http://dx.doi.org/10.1002/1873-3468.14155
   IF: 4.124 (2020)
2. Bartáné Tóth, B., **Arianti, R.**, Shaw, A., Vámos, A., Veréb, Z., Póliska, S., Győry, F., Bacsó, Z., Fésüs, L., Kristóf, E.: FTO intronic SNP strongly influences human neck adipocyte browning determined by tissue and PPARγ specific regulation: a transcriptome analysis.
   Cells. 9 (4), E987, 2020.
   DOI: https://doi.org/10.1101/2020.02.21.959593
   IF: 6.6

List of other publications

3. Shaw, A., Bartáné Tóth, B., **Arianti, R.**, Csomós, I., Póliska, S., Vámos, A., Bacsó, Z., Győry, F., Fésüs, L., Kristóf, E.: BMP7 increases UCP1-dependent and independent thermogenesis with a unique gene expression program in human neck area derived adipocytes.
   Pharmaceuticals (Basel). 14 (11), 1-21, 2021.
   DOI: http://dx.doi.org/10.3390/ph14111078
   IF: 5.863 (2020)
4. **Arianti, R.**, Ariani, N. L., Muhammad, A. A., Sadewa, A. H., Farmawati, A., Sunarti, Hastuti, P., Kristóf, E.: Influence of Single Nucleotide Polymorphism of ENPP1 and ADIPOQ on Insulin Resistance and Obesity: a Case-Control Study in a Javanese Population.
   Life (Basel). 11 (6), 552-, 2021.
   DOI: http://dx.doi.org/10.3390/life11060552
   IF: 3.817 (2020)

UNIVERSITY of DEBRECEN

UNIVERSITY AND NATIONAL LIBRARY
UNIVERSITY OF DEBRECEN
H-4002 Egyetem tér 1, Debrecen
Phone: +3652/410-443, email: publikaciok@lib.unideb.hu

5. Shaw, A., Bartáné Tóth, B., Király, R., **Arianti, R.**, Csomós, I., Póliska, S., Vámos, A., Korponay-Szabó, I., Bacsó, Z., Győry, F., Fésüs, L., Kristóf, E.: Irisin stimulates the release of CXCL1 from differentiating human subcutaneous and deep-neck derived adipocytes via upregulation of NF[kappa]B pathway.
Front. Cell. Dev. Biol. 9, 1-19, 2021.
DOI: http://dx.doi.org/10.3389/fcell.2021.737872
IF: 6.684 (2020)

Total IF of journals (all publications): 27,088
Total IF of journals (publications related to the dissertation): 10,724

The Candidate's publication data submitted to the iDEa Tudóstér have been validated by DEENK on the basis of the Journal Citation Report (Impact Factor) database.

28 April, 2022

DEBRECENI EGYETEM
Egyetemi és Nemzeti Könyvtár

Conferences

Oral presentations:

K121Q polymorphism of ectonucleotide pyrophosphatase phosphodiesterase 1 increase the risk of insulin resistance in Javanese obese adults (FEBS Advance Course: can we infer phenotype from protein variant analysis?, 2018, Bologna)

Rini Arianti, Beáta Tóth, Szilárd Poliska, Ferenc Győry, Endre Kristóf, and László Fésüs. Identification of unique molecular signature of browning in human primary adipocytes from deep neck and subcutaneous neck (12th Molecular, Cell, and Immune Biology Winter Symposium, 2019, Debrecen)

Rini Arianti, Beáta Tóth, Szilárd Poliska, Ferenc Győry, Endre Kristóf, and László Fésüs. Potential significance of cell membrane SLC transporter in human adipocytes browning (13th Molecular, Cell, and Immune Biology Winter Symposium, 2020, Debrecen)

Rini Arianti, Boglarka Ágnes Vinnai, Ferenc Győry, Endre Kristóf, and László Fésüs. Thiamine enhances thermogenic activation in human neck adipocytes (14th Molecular, Cell, and Immune Biology Winter Symposium, 2021, Debrecen)

Rini Arianti, Boglarka Ágnes Vinnai, Szilárd Poliska, Ferenc Győry, Endre Kristóf, and László Fésüs. High level of thiamine is required for efficient thermogenesis in human neck adipocytes (15th Molecular, Cell, and Immune Biology Winter Symposium, 2022, Debrecen)

Poster presentation

Rini Arianti, Beáta Bartane Toth, Abhirup Shaw, Attila Vamos, Ferenc Győry, Szilárd Póliska, Endre Kristóf, László Fésüs. Comparison of gene expression profiles of deep neck and subcutaneous human adipocytes to investigate thermogenic potential (FEBS3+ Meeting: From Molecules to Living Systems, 2018, Balaton, Hungary)

Rini Arianti, Beáta Bartane Toth, Abhirup Shaw, Attila Vamos, Ferenc Győry, Szilárd Póliska, Endre Kristóf, László Fésüs. Identification of unique molecular signature of browning in human primary adipocytes from subcutaneous and deep neck fat (The 44th FEBS Congress, 2019, Krakow, Poland)

Rini Arianti, Boglarka Ágnes Vinnai, Beata B Toth, Abhirup Shaw, Éva Csősz, Attila Vamos Ferenc Győry, Pamela Fischer-Posovszky, Martin Wabitsch, Endre Kristóf, and László Fésüs. ASC-1 transporter-dependent amino acid uptake is required for the efficient thermogenic response of human adipocytes to adrenergic stimulation (Hungarian Molecular Life Science Conference, 2021, Eger, Hungary)

Rini Arianti, Beáta Tóth, Szilárd Poliska, Ferenc Győry, Endre Kristóf, and László Fésüs. Gene expression profile of mitochondrial protein in thermogenic human adipocytes is determined by anatomical origin, brown differentiation and the FTO obesity allele (Crosstalk between nucleus and mitochondria in human disease – IUBMB Focused Meeting/FEBS Workshop, 2022, Seville, Spain)